UC Berkeley
UC Berkeley Electronic Theses and Dissertations

Title
TLR9 Immune Evasion by Murine Gammaherpesvirus 68

Permalink
https://escholarship.org/uc/item/5pw583h8

Author
Pezda, Andrea Christiane

Publication Date
2010

Peer reviewed|Thesis/dissertation

eScholarship.org Powered by the California Digital Library
University of California

TLR9 Immune Evasion by Murine Gammaherpesvirus 68

By

Andrea Christiane Pezda

A dissertation submitted in partial satisfaction of the

requirements for the degree of

Doctor of Philosophy

in

Molecular and Cell Biology

in the

Graduate Division

of the

University of California Berkeley

Committee in charge:

Professor Laurent Coscoy, Chair
Professor Gregory Barton
Professor Daniel Portnoy
Professor Britt Glaunsinger

Fall 2010

TLR9 Immune Evasion by Murine Gammaherpesvirus 68

Copyright 2010

by

Andrea Christiane Pezda

Abstract

TLR9 Immune Evasion by Murine Gammaherpesvirus 68

by

Andrea Christiane Pezda

Doctor of Philosophy in Molecular and Cell Biology

University of California Berkeley

Professor Laurent Coscoy, Chair

Multiple receptors within the innate immune system have evolved to recognize nucleic acids as signatures of viral infection. It is thought that this specificity is essential for viral detection, as viruses often lack other invariant features that can serve as suitable targets for innate receptors. One such innate receptor, Toll-like receptor 9 (TLR9) has been implicated in the detection of many double-stranded DNA viruses. Here, I investigate the detection of murine herpesvirus 68 (MHV68) by TLR9. I find that MHV68 genomic DNA poorly activates TLR9 compared to murine cytomegalovirus (MCMV), a very potent inducer of innate responses. Genome-wide analysis of the number of stimulatory versus non-stimulatory CpG motifs present in the genome of each virus reveals that the MHV68 genome contains only a fraction of the number of immunostimulatory motifs present in MCMV. Interestingly, MHV68 appears to have selectively suppressed the number of stimulatory motifs through cytosine to thymine conversion. These data suggest that certain viruses may have evolved and modified their genomic content to avoid recognition by nucleic acid-sensing receptors of the innate immune system. In order to enhance TLR9-mediated recognition, 54 highly stimulatory CpG or non-stimulatory GpC motifs were inserted into the MHV68 genome. Surprisingly, while the stimulatory CpG motifs by themselves were able to stimulate TLR9, no increased stimulation was observed when the motifs were presented within the context of the MHV68 genome compared to its wildtype or GpC motif-containing counterparts. Furthermore, I show that microfluidic-based protein – DNA interaction studies can be used to gain better understanding of the DNA sequence motifs that interact with TLR9.

TABLE OF CONTENTS

Abstract **1**
Table of Contents ..... **i**
List of Figures and Tables ..... **iii**
Abbreviations ..... **v**
Acknowledgements ..... **vii**

CHAPTER 1 ..... **1**

Introduction **2**
PATTERN RECOGNITION BY THE INNATE IMMUNE SYSTEM 2
Viral Recognition by Cytosolic Receptors *2*
Viral Recognition by Toll-like Receptors *3*
TLR9 BIOLOGY 4
TLR9 Ligands *4*
TLR9 Signaling *5*
HERPESVIRUSES 6
Role of TLR9 in the Recognition of Herpesviruses *7*

CHAPTER 2 ..... **8**

Activation of Innate Immune Responses by MHV68 ..... **9**
INTRODUCTION 9
MATERIALS AND METHODS 11
RESULTS 13
MHV68 is a poor inducer of IFN-I and IL-12p40 in vivo *13*
Conventional DCs lytically infected with MHV68 suppress TLR-induced cytokine production *15*
MHV68 ORF45 interferes with IFN-I induction in vitro *19*
MHV68 neither replicates nor suppresses TLR signaling in pDCs *21*
DISCUSSION 26

CHAPTER 3 ..... **28**

Suppression of TLR9-Immunostimulatory Motifs in MHV68 ..... **29**
INTRODUCTION 29
MATERIALS AND METHODS 30
RESULTS 32
The MHV68 genome poorly activates TLR9 ..... *32*
The MHV68 genome has few TLR9 stimulatory motifs *34*
Selective loss of stimulatory sequences in the MHV68 genome by cytosine to thymine conversion *38*
DISCUSSION 40

CHAPTER 4 ..... **43**

Generation and Characterization of a CpG-Enriched MHV68 Mutant **44**
INTRODUCTION 44

MATERIALS AND METHODS 46
RESULTS 49
Generation of a Stimulatory CpG and a Non-stimulatory GpC Repeat ... 49
A CpG enriched MHV68 mutant does not increase innate immune recognition 52
DISCUSSION 57
SUPPLEMENTARY PROTOCOL 59
Overview of Thymidylate synthase A (thyA)-mediated BAC mutagenesis 59
Generation of mCherry-ORF45 MHV68 62
Generation of CpG MHV68 and GpC MHV68 65
Wong et al. thyA-mediated BAC mutagenesis protocol 67

CHAPTER 5 72

Characterizing DNA Motifs that Interact with TLR9 73
INTRODUCTION 73
MATERIALS AND METHODS 75
RESULTS 77
Optimizing TLR9 – CpG ODN binding in vitro 77
Microfluidic set up to determine all DNA motifs recognized by TLR9 82
DISCUSSION 88

REFERENCES 90

List of Figures and Tables

CHAPTER 1 1

Figure 1-1: Overview of TLR9-mediated signaling pathway 6
Table 1: Human and Mouse Herpesviruses 7

CHAPTER 2 8

Figure 2-1: MHV68 is a poor inducer of innate cytokines *in vivo* 14
Figure 2-2: IL-12 production by GMCSF-DCs following infection with MHV68 17
Figure 2-3: MHV68 suppresses TLR signaling in conventional DCs 18
Figure 2-4: Suppression of IFN-I induction by MHV68 ORF45 20
Figure 2-5: MHV68 does not replicate well in plasmacytoid DCs 23
Figure 2-6: IFN-I production in FLT3-Ligand derived DCs following infection with MHV68 24
Figure 2-7: Absence of immunomodulation by MHV68 in plasmacytoid DCs 25

CHAPTER 3 28

Figure 3-1: MHV68 genomic DNA stimulates TLR9N4C poorly 33
Table 2: The MHV68 genome is methylated only during latency. 33
Figure 3-2: Stimulation of TLR9N4C by DNA ODN containing the Pur-Pur-C-G-Pyr-Pyr consensus motif 35
Figure 3-3: Suppression of stimulatory CpG motifs in the MHV68 and MCMV genomes 36
Figure 3-4: Deamination of stimulatory CpG motifs in MHV68 but not MCMV 38

CHAPTER 4 42

Figure 4-1: Defining the context around the stimulatory 6-mer CpG motifs 49
Figure 4-2: Dose-dependent stimulation of TLR9N4C by 20-mer and 60-mer ODN containing stimulatory CpG or non-stimulatory GpC motifs 49
Figure 4-3: Stimulation of TLR9N4C with 1.4 kb containing 54 stimulatory CpG or non-stimulatory GpC motifs 50
Figure 4-4: Construction of CpG or GpC enriched MHV68 52
Figure 4-5: Stimulation of TLR9N4C with genomic DNA from wildtype, CpG, or GpC MHV68 52
Figure 4-6: Growth curve of wildtype, CpG and GpC MHV68 viruses 53
Figure 4-7: TNFα production by conventional DCs infected with either wildtype, CpG or GpC MHV68 54

Figure 4-8: TNFα production by plasmacytoid DCs infected with either wildtype, CpG or GpC MHV68 55
Figure 4-9: BAC mutagenesis strategy 60
Figure 4-10: Mutagenesis strategy for mCherry-ORF45 MHV68 62
Figure 4-11: Generation of mCherry-ORF45 MHV68 63
Figure 4-12: Generation of CpG or GpC enriched MHV68 65

CHAPTER 5 71

Figure 5-1: TLR9 fusion constructs 78
Figure 5-2: TLR9 – phosphorothioate CpG binding at pH 8 78
Figure 5-3: TLR9 – phosphorothioate CpG binding *in vitro* is optimal at pH 6 79
Figure 5-4: Binding of full length TLR9 to CpG ODN with phosphorothioate or phosphodiester-linked backbones 79
Figure 5-5: Binding of cleaved TLR9 to CpG ODN with phosphorothioate or phosphodiester-linked backbones 80
Figure 5-6: Binding of full length extracellular domain TLR9 fusion constructs to CpG ODN with phosphorothioate or phosphodiester-linked backbones 80
Table 3: Names and sequences of stimulatory, inhibitory, and neutral ODN 81
Figure 5-7: Microfluidic set up 83
Figure 5-8: TLR9 binding to stimulatory, inhibitory, and neutral ODN 84
Figure 5-9: Stimulation of TLR9N4C with stimulatory, inhibitory, or neutral ODN 85
Figure 5-10: Inhibition of TLR9N4C stimulation by inhibitory ODN 86

Abbreviations

AIM2	absent in melanoma 2
CARD	caspase activation and recruitment domains
cDC	conventional DC
DAI/ZBP1	DNA-dependent activator of IFN-regulatory factors/Z-DNA binding protein 1
DC	dendritic cell
EBV	Epstein-Barr Virus
FLT3	*fms*-like tyrosine kinase 3
HCMV	human cytomegalovirus
HSV-1	Herpes Simplex Virus type 1
HSV-2	Herpes Simplex Virus type 2
IFN	interferon
IFN-I	type I IFN
IκB	Inhibitor of NF-κB
IKK-i	inducible IκB kinase
IL	Interleukin
IRAK	interleukin-1 receptor associated kinase
KSHV	Kaposi's sarcoma-associated herpesvirus
LGP2	laboratory of genetics and physiology 2
LRR	leucine-rich repeats
MAVS	mitochondrial antiviral signaling
MCMV	murine cytomegalovirus
MDA5	melanoma differentiation-associated gene 5
MHV68	Murine Gammaherpesvirus 68
MITOMI	mechanically induced trapping of molecular interactions
MOI	multiplicity of infection
MyD88	Myeloid differention factor 88
NF-κB	nuclear factor kappa B
NLR	Nod-like receptors
ODN	oligodeoxynucleotide
ORF	open reading frame
PAMP	pathogen-associated molecular patterns
pDC	plasmacytoid DC
PDMS	polydimethylsiloxane
PFU	plaque-forming units
PRRs	pattern recognition receptors
RIG-I	retinoic acid inducible gene I
RLR	RIG-I-like receptors
TAK1	transforming growth factor-β associated kinase
TANK	TRAF family member-associated NF-κB activator
TBK1	TANK-binding kinase 1
thyA	thymidylate synthase A

TIR	Toll/interleukin-1 receptor homology domain
TLRs	Toll-like receptors
TNF	Tumor necrosis factor
TNFR	TNF receptor
TRAF	tumor necrosis factor receptor-associated factor
TRIF	TIR-domain-containing adapter inducing IFNβ

Acknowledgements

First and foremost, I am grateful to my advisor, Laurent Coscoy, who gave me the opportunity to explore my interest in virology and host-pathogen interactions in his lab. The work presented in this thesis would not have been possible without his encouragement and support. I would also like to thank the members of my thesis committee, Dan Portnoy, Greg Barton and Britt Glaunsinger, for their continued guidance and advice throughout my years at Berkeley. Last but not least, thank you to Maria, Veronica, Damian, Elena, Brian, Ken, Clarisse, Nadine, Mark, Felix, Adriana and Zoe. I am grateful for the wonderful work environment you have provided throughout my PhD.

Research by the following people has directly contributed to or is included in this thesis: Felix Kellndorfer, Mark Luskus, Adriana Lippy, and Polly Fordyce.

CHAPTER 1

Introduction

Chapter 1:

Introduction

Pattern Recognition by the Innate Immune System

The innate immune response represents the first line of defense against pathogens. The activation of this response relies on the efficient recognition of conserved features of pathogens by a variety of innate immune receptors referred to as pattern recognition receptors (PRRs). Four families of PRRs are currently known, including Toll-like receptors (TLRs), retinoic acid inducible gene I (RIG-I)-like receptors (RLRs), Nod-like receptors (NLRs), and HIN-200 family members (1, 2). PRRs link the recognition of viral and microbial ligands to activation of both the innate and adaptive immune system, thereby playing a vital role in the host response to infection (3, 4). Microbial ligands recognized by TLRs 1/2, 2/6, 4, and 5 represent biochemical products that are present in pathogens but absent from the host (e.g., Lipopolysaccharide (LPS), peptidoglycan, β-glucans) (5). Viruses, however, because they replicate within our own cells, often lack the unique biochemical products that are typically targeted by these TLRs. Instead, the innate immune system uses the recognition of nucleic acids as one indicator of viral infection (6, 7). Distinct pathways recognizing viral nucleic acid have evolved in mammals. TLR3, TLR7, TLR8, and TLR9 detect various forms of viral nucleic acid in endosomal compartments (8). The DExD/H box helicases retinoic acid inducible gene I (RIG-I), melanoma differentiation-associated gene 5 (MDA-5), and laboratory of genetics and physiology 2 (LGP2) recognize viral RNA in the cytoplasm (8), while cytosolic DNA is sensed by receptors like DNA-dependent activator of IFN-regulatory factors/Z-DNA binding protein 1 (DAI/ZBP1) (9, 10), absent in melanoma 2 (AIM2) (11), RNA Polymerase III (which generates an RNA intermediate that is sensed through RIG-I) (12, 13) as well as other as yet unidentified receptors. These pathways all lead to induction of type I interferon (IFN-I) and/or inflammatory cytokines, yet their signal transduction pathways and their roles in antiviral immunity appear distinct (14, 15). The features of nucleic acid that are recognized vary for each receptor, and in some cases the precise sequence motifs or structural elements remain poorly defined. In recent years various strategies by which viruses modulate innate immune responses have been identified (16).

Viral Recognition by Cytosolic Receptors

RLRs and NLRs are among the PRRs that sense viral nucleic acids in the cytosol. The two RLRs RIG-I and MDA5 sense RNA viruses in conventional dendritic cells (cDCs), macrophages and fibroblasts. Both contain N-terminal tandem caspase activation and recruitment domains (CARDs) followed by an

RNA helicase domain (17). Interaction of the RLR CARD with that of the mitochondrial antiviral signaling (MAVS) protein (18-21) leads to downstream activation of TANK-binding kinase 1 (TBK1) and inducible inhibitor of nuclear factor-κB (IκB) kinase (IKK-i), resulting in the phosphorylation and translocation of Interferon-regulatory factor 3 (IRF3) into the nucleus and subsequent expression of IFNβ (22). The third member of this family, LGP2, lacks the CARD and may positively regulate RIG-I and MDA5-mediated antiviral responses (23). The ligand recognized by RIG-I is blunt-ended 5' triphosphate dsRNA at least 20 bp in length (24), and this receptor recognizes RNA viruses including influenza virus, vesicular stomatitis virus, and Japanese encephalitis virus (25). MDA5, on the other hand, binds long dsRNA molecules forming branched structures containing both ssRNA and dsRNA and has been implicated in picorna virus infections (25, 26).

Introduction of viral or bacterial DNA into the cytosol also triggers a potent innate immune response, however, many of the relevant receptors are still unknown (27-29). Two recent studies elucidated a role for RNA Polymerase III in the sensing of AT-rich DNA, through the generation of an RNA intermediate detected by RIG-I (12, 13). In addition, Takaoka *et al*. identified a previously known DNA binding protein, DAI/ZBP1, as a potential cytosolic DNA sensor (9). Indeed, DAI has since been linked to recognition of human cytomegalovirus (HCMV) (30). However, another study failed to observe a role of DAI in cytosolic DNA sensing (31). The NLR family member AIM2 was shown to respond to cytosolic DNA and Vaccinia virus, leading to inflammasome-dependent caspase 1 activation and production of proinflammatory interleukin-1β (IL-1β) (11, 32, 33).

Viral Recognition by Toll-like Receptors

Toll-like receptors are a crucial component of the innate immune system in the defense against viruses. While bacteria provide pathogen-associated molecular patterns (PAMPs) such as LPS, flagellin or components of the bacterial cell wall, which are recognized by TLRs located on the cell surface (5), the innate immune system uses the recognition of viral nucleic acids as an indicator of viral infection (6, 7). Nucleic acid-sensing TLRs comprised of TLR3, 7, 8, and 9 are located within endosomes and lysosomes. TLR3, which is widely expressed though mainly functions in cDCs (34), recognizes dsRNA and mice deficient in this receptor are susceptible to infection with West Nile virus (35) and influenza virus (36). It also differs from the other nucleic acid sensing TLRs in that it signals through the adapter Toll/interleukin-1 receptor homology (TIR) domain-containing adapter inducing IFNβ (TRIF) (37, 38), while Myeloid differentiation factor 88 (MyD88) is the adapter interacting with the TIR domains of TLR7, 8 and 9 (8). TLR7 detects single-stranded RNA molecules, and has been shown to be important for orthomyxovirus infection. TLR8 has also been implicated in the recognition of viral RNA; however, its precise function is still unclear. TLR9 is the only TLR to recognize DNA. In particular, unmethylated

single stranded DNA containing a CpG motif mediates TLR9 activation (39). The receptor has been implicated in the recognition of a wide range of DNA viruses, including poxviruses (40), adenoviruses (41) and herpesviruses (42-49). TLR7 and 9 are particularly important in the innate immune response against viruses, as they are the only PRRs expressed in plasmacytoid DCs (pDCs), which produce large amounts of IFN-I in response to nucleic acid recognition (50).

In addition to nucleic acid-sensing TLRs that a located in an endosomal compartment, surface TLRs have also recently been linked to viral recognition. TLR2, which was initially found to recognize microbial lipopeptides, has since been shown to play a role in various viral infections including those with Herpes simplex viruses types 1 and 2 (51, 52), Varicella-zoster virus (53, 54), Human Cytomegalovirus (55, 56), murine cytomegalovirus (MCMV) (57), vaccinia virus (58, 59), measles virus (60), hepatitis C virus (61) and lymphocytic choriomeningitis virus (62). Furthermore, TLR4, which responds to bacterial LPS, also mediates responses to respiratory syncytial virus and murine retroviruses (63, 64).

TLR9 Biology

The TLR9 protein consists of an N-terminal portion containing 26 leucine-rich repeats (LRRs), followed by a transmembrane and a cytoplasmic TIR domain (65). To encounter its cognate ligand and induce a downstream signal transduction cascade TLR9 needs to be transported from the endoplasmic reticulum to an endolysosomal compartment in a process that requires the multi-pass transmembrane protein UNC-93B (66-69). The receptor undergoes a proteolytic cleavage event within or distal to LRR 14, removing approximately half of the extracellular domain (68, 70). Ligand binding occurs within the LRRs and requires endosomal acidification (71, 72). It induces a membrane-proximal conformational change believed to be important for subsequent adapter recruitment and activation (70, 73). The localization of TLR9 in endolysosomes, vesicles normally devoid of self-nucleic acid but where viruses are degraded upon phagocytosis, is believed to account in part for how this receptor discriminates between self and viral DNA (74).

TLR9 Ligands

The ligands for TLR9 are CpG oligodeoxynucleotide (ODN), bacterial and viral DNA (65). Two subtypes of CpG ODN exist, B/K-type and A/D-type. The former have a phosphorothioate-linked backbone and induce DC maturation and B cell proliferation. In contrast, A/D-type CpG ODN carry the CpG motif within a phosphodiester-linked sequence, but are flanked with phosphorothioate-modified poly G stretches on either end. Stimulation with these ODN induces IFN-I in pDCs (75). TLR9 was also reported to be activated by ODN containing nucleotide derivatives, the phosphorothioate backbone along with a bicyclic heterobase

structure, or the DNA sugar backbone alone (80-83). In the latter case, addition of bases increased TLR9-mediated stimulation. A phosphorothioate backbone by itself inhibited TLR9 activation, but was converted to an agonist with the addition of CpG motifs (80). Previous studies have reported TLR9 to play a role in the response against several bacteria including *Mycobacterium tuberculosis*, *Brucella*, and *Streptococcus pneumonia* (76-78). Viral DNA may also contain unmethylated CpG motif and thus present a ligand for TLR9. Viral families whose members have previously been shown to be recognized by TLR9 include herpesviruses (42-49), poxviruses (40), adenoviruses (41), and most recently Torquetenoviruses (79). However, that the ligands recognized in viral DNA are indeed CpG motifs remains to be shown. In addition to DNA, TLR9 has also been shown to recognize the malarial heme-detoxification byproduct, hemozoin (84, 85). Despite the wealth of research into TLR9 – ligand interactions, the nature of the DNA sequence motifs that are recognized by and stimulate or inhibit TLR9 in the context of a natural infection are still poorly understood.

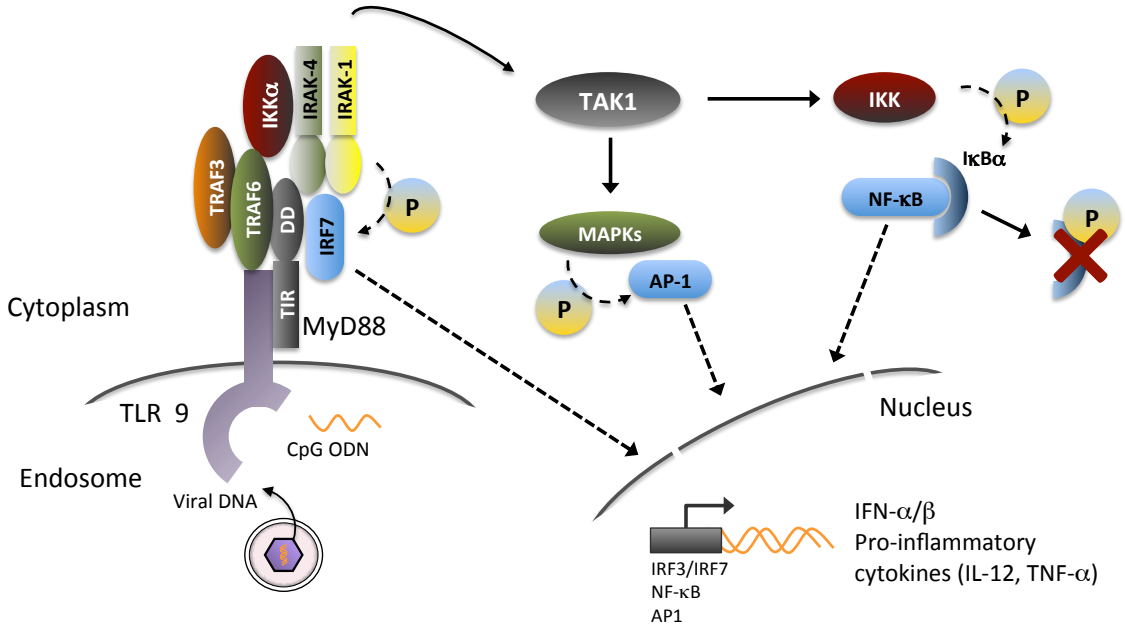
TLR9 Signaling

In the mouse TLR9 is expressed in various cell types including macrophages, B cells, cDCs and pDCs, whereas TLR9 is only expressed in B cells and pDCs in humans (86). Generally, activation of TLR9 in macrophages and cDCs leads to the expression of proinflammatory cytokines. Upon ligand binding, the TIR domain of TLR9 interacts with the TIR domain and death domain-containing adapter MyD88 (87). The latter interacts with interleukin-1 receptor associated kinase-1 (IRAK-1) and IRAK-4 through its death domain. Both kinases are required for TLR9-mediated cytokine production (88). IRAK-4 phosphorylates IRAK-1, which in turn upregulates its kinase activity and recruits tumor necrosis factor associated factor 6 (TRAF6). TRAF6 is an E3 ubiquitin ligase, which mediates activation of transforming growth factor-β associated kinase (TAK1) (89). TAK1 phosphorylates IKK, which in turn phosphorylates IκB causing its dissociation from the transcription factor nuclear factor kappa B (NF-κB), the latter of which then translocates into the nucleus (90). TAK1 is also required for activation of mitogen-activated protein kinases, which cause the downstream phosphorylation and nuclear translocation of the transcription factor AP-1 (91, 92). Both NF-κB and AP-1 act to induce transcription of proinflammatory cytokine genes such as Tumor necrosis factor α (TNFα), IL-6, and IL-12 (Fig 1-1). A third transcription factor required for the expression of these cytokines is IRF5, which directly interacts with MyD88 and translocates to the nucleus upon TLR9 activation (93).

In addition to the expression of proinflammatory cytokines, activation of TLR9 also leads to the expression of IFN-I. In cDCs IFNβ expression is mediated by the transcription factor IRF1 (94). However, robust expression of IFNα is only observed in pDCs. This is in part mediated by the transcription factor IRF7, which is highly expressed in pDCs but not other cells types (95). In these cells MyD88,

IRAK-1, IRAK-4 and TRAF6 from a large complex in which IRF7 directly interacts with MyD88 (96). IRF7 phosphorylation prior to its nuclear translocation is likely mediated by IRAK-1 (65). In addition, IKKα may also phosphorylate IRF7, as the IFN-α response in IKKα-deficient pDCs is diminished in response to TLR9 stimulation (97).

Figure 1-1: Overview of TLR9-mediated signaling pathway



TLR9 recognizes its ligands in an endosomal compartment. Upon ligand binding the cytoplasmic TIR domain of TLR9 recruits the adapter MyD88 and other molecules to a signaling complex. Upon activation the transcription factors IRF7, AP-1 and NF-κB translocate to the nucleus to initiate transcription of IFN-I and proinflammatory cytokines.

Herpesviruses

The *Herpesviridae* is a family of large, dsDNA viruses with linear genomes ranging from 120 to 230 kb in size and encoding 80 to 200 open reading frames (ORFs). Virions are enveloped and the viral genomic DNA is contained within a capsid, which is surrounded by an amorphous protein layer called the tegument. They comprise three subfamilies designated *Alphaherpesvirinae*, *Betaherpesvirinae* and *Gammaherpesvirinae*. The most prominent human and mouse herpesviruses of each subfamily are shown in Table 1 below.

Table 1: Human and Mouse Herpesviruses

Alphaherpesviruses	
HSV 1 / HHV 1	Herpes Simplex Virus type 1
HSV 2 / HHV 2	Herpes Simplex Virus type 2
VZV / HHV 3	Varicella Zoster Virus
Betaherpesviruses	
HCMV / HHV 5	Human Cytomegalovirus
HHV 6	Human Herpesvirus 6
HHV 7	Human Herpesvirus 7
MCMV	Murine Cytomegalovirus
Gammaherpesviruses	
EBV / HHV 4	Epstein-Barr Virus
HHV 8 / KSHV	Kaposi's sarcoma-associated herpesvirus
MHV68	Murine Gammaherpesvirus 68

HHV Human Herpesvirus

Role of TLR9 in the Recognition of Herpesviruses

An essential role for TLR9 has been demonstrated in the response to alphaherpesviruses (HSV-1 and HSV-2) (42, 44, 47, 98) and betaherpesviruses (MCMV) (43, 45, 46, 48). Cells from TLR9-deficient mice are impaired in their ability to recognize these viruses, and TLR9-deficient mice are highly susceptible to MCMV infection (43, 45, 46). The importance of TLR9 in controlling gammaherpesvirus infection is less evident. In two recent studies with murine gammaherpesvirus 68 (MHV68), a mouse model for gammaherpesvirus infection, no acute replication defect was observed in MyD88$^{-/-}$ or TLR9$^{-/-}$ mice following intranasal infection (99, 100). However, viral titers in TLR9$^{-/-}$ mice were significantly increased after intraperitoneal infection with MHV68. In TLR9$^{-/-}$ but not MyD88$^{-/-}$ mice, latent viral load was also only increased upon intraperitoneal but unaffected following intranasal infection (99, 100). Surprisingly, latency establishment was reduced in MyD88$^{-/-}$ mice following intranasal infection, suggesting that TLR signaling is important rather than detrimental for these events (100).

CHAPTER 2

Activation of Innate Immune Responses by MHV68

Chapter 2:

Activation of Innate Immune Responses by MHV68

Introduction

The innate immune response represents the first line of defense against pathogens. The activation of this response relies on the efficient recognition of conserved features of pathogens by a variety of innate immune receptors referred to as PRRs. Four families of PRRs are currently known, including TLRs, RLRs, NLRs, and HIN-200 family members (1, 2). PRRs link the recognition of viral and microbial ligands to activation of both the innate and adaptive immune system, thereby playing a vital role in the host response to infection (3, 4). Microbial ligands recognized by TLRs 1/2, 2/6, 4, and 5 represent biochemical products that are present in pathogens but absent from the host (e.g., LPS, peptidoglycan, β-glucans) (5). Viruses, however, because they replicate within our own cells, often lack the unique biochemical products that are typically targeted by these TLRs. Instead, the innate immune system uses the recognition of nucleic acids as one indicator of viral infection (6, 7). Distinct pathways recognizing viral nucleic acid have evolved in mammals. TLR3, TLR7, TLR8, and TLR9 detect various forms of viral nucleic acid in endosomal compartments (8). The DExD/H box helicases RIG-I, MDA-5, and LGP2 recognize viral RNA in the cytoplasm (8), while cytosolic DNA is sensed by receptors like DAI/ZBP1 (9, 10), AIM2 (11), RNA Polymerase III (which generates an RNA intermediate that is sensed through RIG-I) (12, 13) as well as other as yet unidentified receptors. These pathways all lead to induction of IFN-I and/or inflammatory cytokines, yet their signal transduction pathways and their roles in antiviral immunity appear distinct (14, 15). The features of nucleic acid that are recognized vary for each receptor, and in some cases the precise sequence motifs or structural elements remain poorly defined. In recent years various strategies by which viruses modulate innate immune responses have been identified (16).

An understanding of innate responses to MHV68 is complicated by conflicting data from *in vitro* DC infection studies. In general, MHV68 only infects immature DCs, the majority of which become latently-infected (101, 102). Furthermore, granulocyte macrophage colony-stimulating factor (GM-CSF)-derived DCs, a homogeneous population with mostly $CD11c^+$ $CD11b^+$ cDCs (103), respond poorly when exposed to MHV68 as evident by the lack of cytokine secretion or up-regulation of cell surface activation markers such as CD86 or major histocompatibility molecules (101, 102, 104, 105). Whether this is a result of an active immune evasion mechanism is still unclear. Previous studies have not distinguished between uninfected, lytically-infected, or latently-infected DCs when assessing whether or not MHV68 can prevent activation of infected cDCs after stimulation with TLR ligands (101, 104, 105). Interestingly, *fms*-like tyrosine

kinase 3 (FLT3)-Ligand-derived DCs, which are a heterogeneous population comprised of 70-80% $CD11c^+$ $CD11b^+$ cDCs and 20-30% $CD11c^+$ $B220^+$ pDCs (103), become activated when infected with MHV68, though IFN-I production is undetectable (105). The authors conclude that MHV68-induced activation of cDCs requires the presence of pDCs and that the virus does not actively prevent activation of either pDCs or cDCs when stimulated with exogenous TLR ligands. The inability to detect IFN-I upon MHV68 infection *in vitro* or *in vivo* is particularly surprising given the fact that $IFNR^{-/-}$ mice are highly susceptible to infection with MHV68 (106, 107).

Here I show that MHV68 elicits poor cytokine responses upon infection of cDCs and pDC. The former but not the latter were lytically infected with MHV68. Similarly, in cDCs but not pDCs cytokine responses diminished in MHV68-infected cells that were treated with exogenous TLR ligands compared with cells that were treated with ligands alone. My observations suggest that poor recognition and active immune evasion mechanisms contribute to the poor cytokine responses elicited by MHV68.

Materials and Methods

Mice and Viruses

C57BL/6 mice were obtained from the Jackson Laboratory (Bar Harbor, Maine). Experiments were conducted with 6 to 12 week old mice in accordance with institutional guidelines for animal care and use. MHV68 was obtained from the ATCC (VR-1465) and propagated on BHK-21 cells. Viral titers were determined in a standard plaque assay on NIH 3T3 cells. Smith strain MCMV (MW97.01) was obtained from Dr. David Raulet and was first described by Wagner and colleagues (108). MCMV was propagated and titered on NIH 3T3 cells. Viral titers reflect the titer of the stock at the time of the infection (i.e. after freeze-thawing). Virus containing supernatants were cleared of cellular debris by low speed centrifugation for 20 min. Virus was subsequently concentrated by centrifugation at 24,000 × g for 2 hrs and purified over a 30% sucrose cushion by centrifugation at 85,000 × g. Pelleted virus was resuspended in PBS and stored at -80 ºC. BHK-21 and NIH 3T3 cells were grown in DMEM supplemented with 10% FBS and 100 Units/ml penicillin and 100 μg/ml streptomycin. Mice were injected intraperitoneally with MHV68 or MCMV (2×10^6 plaque-forming units (PFU) per mouse) in 200 μl volumes and sera collected at the indicated time points.

Isolation and Culture of DC

Bone marrow cells were isolated from the femurs and tibiae of C57BL/6 or MyD88$^{-/-}$ mice and red blood cells were removed by ammonium chloride lysis. To derive cDCs, bone marrow cells were plated into 24-well plates at 7×10^5 cells per well in RPMI 1640 medium supplemented with 10% FBS, 100 Units/ml Penicillin, 100 μg/ml Streptomycin, 100 μM MEM non-essential amino acids, 1 mM sodium pyruvate, 2 mM L-glutamine, 50 μM 2-mercaptoethanol, and GM-CSF for 7 days. Cells were fed every other day by adding 50% fresh medium containing GM-CSF. By day 7, cultures contained 70-80% CD11c$^+$ CD11b$^+$ conventional DCs (data not shown). To derive pDCs, bone marrow cells were plated into 24-well plates at 1×10^6 cells per well in RPMI 1640 medium supplemented with 10 % FBS, 100 Units/ml Penicillin, 100 μg/ml Streptomycin, 100 μM MEM non-essential amino acids, 1 mM sodium pyruvate, 2 mM L-glutamine, 50 μM 2-mercaptoethanol, and 25 ng/ml recombinant mouse FLT3-Ligand (R&D) for 8 days. Cells were fed on day 4 by adding 50% fresh medium containing FLT3-Ligand. By day 8, cultures contained 20-30% CD11c$^+$ B220$^+$ positive plasmacytoid DCs and 70-80% CD11c$^+$ and CD11b$^+$ conventional DCs (data not shown). GM-CSF-DCs and FLT3-Ligand-DCs were plated into 96-well plates at 1×10^5 cells per well and infected with MCMV or MHV68 at the indicated multiplicities of infection (MOIs) and treated with phosphorothioate-linked B/K-type CpG ODN (5'- TCCATGACGTTCCTGACGTT-3') at 1 μM 2 hours post infection.

Flow Cytometry

GM-CSF-DCs and FLT3-Ligand-DCs were plated into 24-well plates at 5×10^5 or 3×10^5 cells per well, respectively. DCs were infected with MHV68 at the indicated MOIs or MCMV at MOI 1 for 2 hours, and treated with TLR ligands (1μg/ml LPS, 1μM phosphorothioate B/K-type CpG ODN 5'-TCCATGACGTTCCTGACGTT-3'; 2μg/ml R848) 2 hours post infection. Intracellular cytokine staining was performed using the BD Cytofix/Cytoperm™ Fixation/Permeabilization Solution Kit with BD GolgiPlug™ according to manufacturer's instructions. Antibodies were obtained from BD Biosciences (CD11c clone HL3, CD11b clone M1/70, IL-12(p40/p70) clone C15.6) and eBioscience (TNFα clone Mab11, B220 clone RA3-6B2). Data were collected on a LSR II flow cytometer (BD Biosciences) and analyzed using FloJo software (TreeStar).

ELISA and ISRE Bioassay

IL-12p40 levels in sera and culture supernatants were measured by sandwich ELISA using anti-IL-12p40 antibodies from eBioscience. Briefly, Nunc-Immuno 96-well plates (Fisher Cat # 12-565-136) were coated with anti-mouse IL-12/IL-23p40 antibody (eBioscience Cat # 14-7125), incubated with supernatants or mouse recombinant IL-12p70 (eBioscience Cat # 14-8121) as standard. Complexes were captured with biotinlylated anti-mouse IL-12/IL-23p40 antibody (eBioscience Cat # 13-7123) and detected using Alkaline Phosphatase-conjugated Streptavidin (BD Biosciences Cat # 554065) and p-Nitrophenyl phosphate (Sigma Cat # N2770).

IFN-I was measured by bioassay using ISRE cells (109) or by IFNα ELISA. For the ELISA, Nunc-Immuno 96-well plates (Fisher Cat # 12-565-136) were coated with monoclonal rat anti-mouse IFNα antibody (HyCult Biotech Cat # HM1001), incubated with supernatants or murine IFNα (HyCult Biotech Cat # HC1040) as standard. Complexes were captured with polyclonal rabbit anti-mouse IFNα antibody (PBL Cat # 32100-1) and detected using Peroxidase-conjugated $F(ab')_2$ donkey anti-rabbit IgG (Jackson Immunoresearch Cat # 711-036-152) and o-Phenylenediamine dihydrochloride (Sigma Cat # P3804).

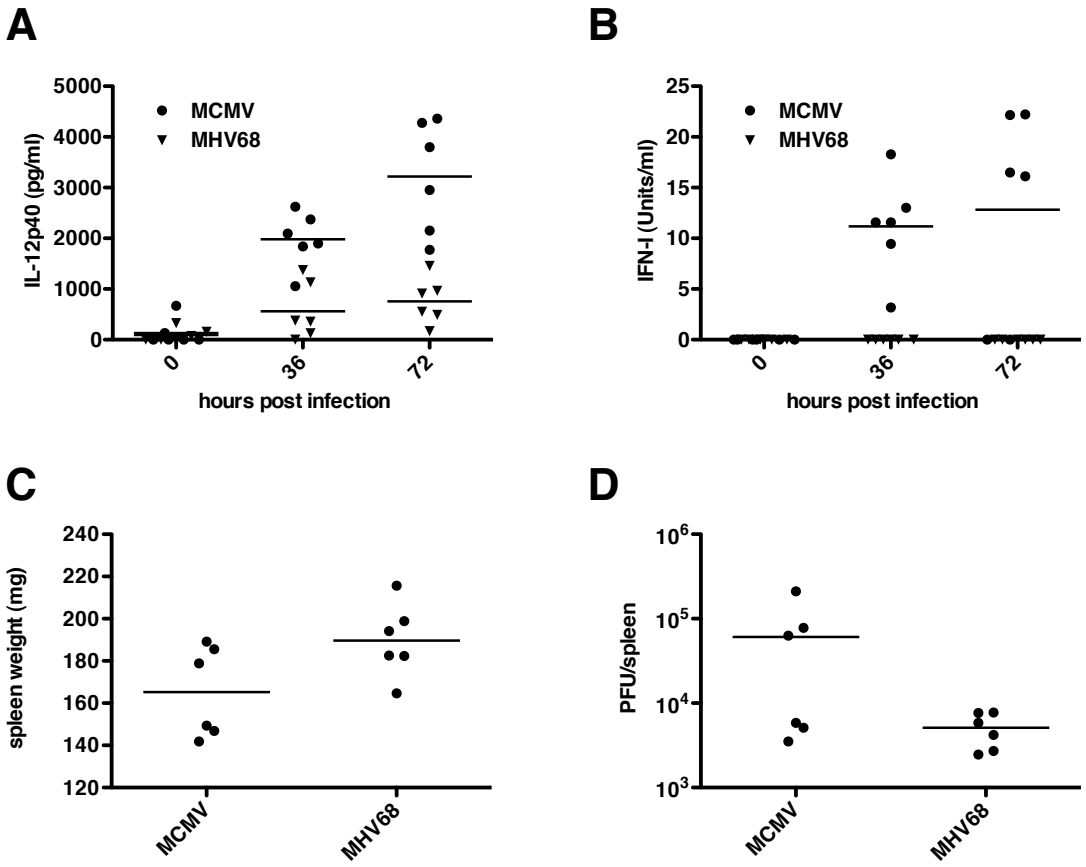
For the bioassay ISRE cells were plated in 96-well plates at 5×10^4 cells per well. Mouse sera diluted in 1% BSA/PBS or culture supernatants were incubated with ISRE cells the following day for 6 to 8 hours. Cells were lysed in 1x Passive Lysis Buffer (Promega) and luciferase activity measured using an LMAX II^{384} luminometer (Molecular Devices).

Results

MHV68 is a poor inducer of IFN-I and IL-12p40 in vivo

DCs are some of the most prolific producers of IFN-I and IL-12 during the innate immune response and thus play a critical role in controlling virus replication as well as in shaping the adaptive antiviral immune response. Given the lack of DC activation and cytokine secretion previously reported *in vitro* and *in vivo* (101, 104, 105) I wanted to compare systemic cytokine responses to MHV68 with those to MCMV, a betaherpesvirus that elicits a robust innate immune response (46). C57BL/6 mice were infected intraperitoneally with 2×10^6 pfu of cell culture-derived MCMV or MHV68. Serum levels of IL-12 and IFN-I were measured prior to, as well as 36 and 72 hours post infection. Spleen weight and splenic viral titers were also measured 72 hours post infection. As shown in Figure 2-1, both cytokines were readily detectable in the sera of MCMV-infected mice. By contrast, IL-12 levels in the sera of MHV68-infected mice barely increased throughout the course of infection (Fig 2-1A), and IFN-I was below the limit of detection in our bioassay (Fig 2-1B). This is in accordance with Weslow-Schmidt *et al.*, who were unable to detect IFN-I locally in broncho-alveolar lavage fluid following intranasal infection with MHV68 (105). Importantly, IFN-I might still be secreted locally, at low levels, since mice lacking the IFN-I receptor are highly susceptible to MHV68 (106, 107). Despite these differences in serum cytokines, spleens from mice infected with either virus were similarly enlarged (Fig 2-1C). In contrast, MCMV replicated to higher splenic viral titers 72 hours post infection compared to MHV68 (Fig 2-1D). Differences in life cycle, tropism, and pathogenesis of these two viruses likely account for this observation.

Figure 2-1: MHV68 is a poor inducer of innate cytokines *in vivo*



(A, B) C57BL/6 mice were infected i.p. with 2×10^6 PFU of either MCMV or MHV68 (n=6). Sera were obtained prior to infection as well as 36 and 72 hours post infection. Serum levels of IL-12p40 (A) and IFN-I (B) were determined by ELISA or ISRE bioassay, respectively. The detection limits are 160 pg/ml for the IL-12p40 ELISA and 0.16 Units/ml in the ISRE bioassay. (C) Spleen weights. (D) Splenic titers of MCMV and MHV68 infected mice.

Conventional DCs lytically infected with MHV68 suppress TLR-induced cytokine production

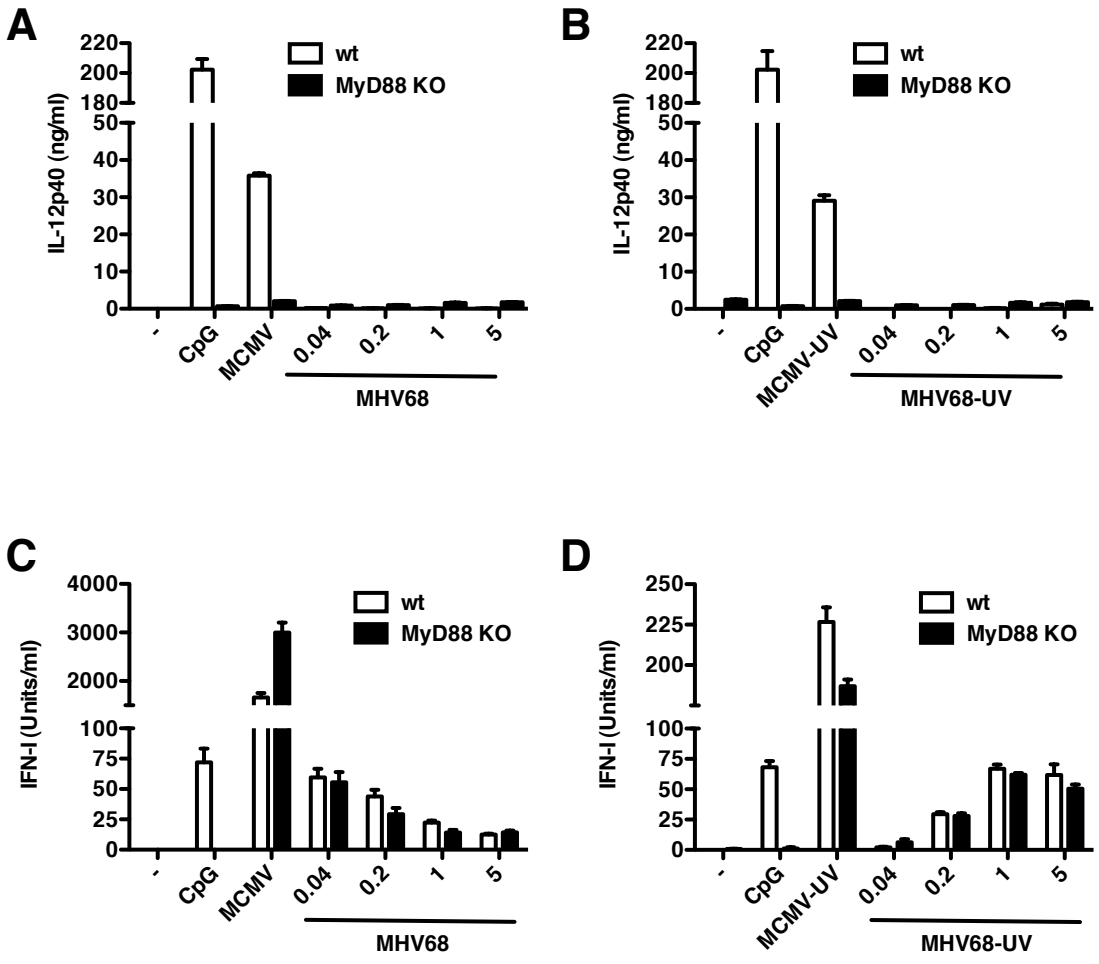
This apparent lack of activation *in vivo* was surprising as a previous study suggested that in the presence of pDCs, MHV68 can activate DCs and thus potentially initiate innate cytokine responses (105). I therefore decided to re-examine DC infections *in vitro*. Bone marrow cells were cultured in the presence of GM-CSF for 7 days to drive differentiation into cDCs ($CD11c^+$, $CD11b^+$). Both MCMV and MHV68 have previously been shown to replicate in cDCs with generation times greater than 24 hours (104, 110). I therefore chose to measure IL-12 and IFN-I production in cDCs at 18 to 20 hours post infection, before progeny virions were released. As expected, MHV68 did not induce IL-12, while it was readily secreted upon stimulation with B/K-type CpG ODN or infection with MCMV (Fig 2-2A). Infection with UV-irradiated virus did not lead to greater IL-12 secretion (Fig 2-2B). Importantly, the lack of IL-12 production by $MyD88^{-/-}$ cells (and MyD88/TRIF DKO cells, data not shown) confirms that IL-12 in cDCs is produced in a TLR-dependent manner, suggesting that MHV68 may be able to inhibit TLR responses and/or is not recognized efficiently. Similarly to Weslow-Schmidt *et al*., I was able to detect low levels of IFN-I in MHV68-infected cultures, albeit lower by at least one order of magnitude compared to MCMV-infected cultures when DCs were infected with live virus (Fig 2-2C) and at least 3-fold lower when DCs were infected with UV-irradiated virus (Fig 2-2D). IFN-I production was not dependent on MyD88 (or TRIF, data not shown), suggesting that in cDCs intracellular nucleic acid sensors recognize MHV68. Activation of cytosolic nucleic acid sensors has been demonstrated to lead to IFN-I production in cDCs, while IFN-I production in response to TLR stimulation is predominantly restricted to pDCs (111).

A recent study by Smith *et al*. utilized a fluorescently-tagged MHV68 in which the endogenous gM protein is tagged with eGFP on its C-terminus to detect lytically-infected cDCs, which are marked by high GFP expression (102). I decided to use MHV68 gM-eGFP to address the question of whether MHV68 inhibits activation of cDCs when exogenously stimulated with TLR ligands. GM-CSF-derived cDCs where infected or not with MHV68 gM-eGFP for 2 hours. Uninfected and infected cells were then treated or not with either LPS or CpG. Cytokine production in cDCs was assessed by intracellular cytokine staining for IL-12 18 hours post infection. As in Figure 2-2, neither lytically (GFP positive), nor latently, or uninfected cDCs (GFP negative) lead to observable cytokine production (Fig 2-3B, bottom left). However, when infected cells were treated with LPS or CpG only GFP-negative cells produced IL-12, while lytically-infected (GFP+) cells did not (Fig 2-3B) suggesting that lytically-infected cells may inhibit DC activation. I was also able to observe inhibition of IL-12 induction in supernatants derived from infected cells that were treated with TLR ligands. Figures 2-3C and D show that the more cells were infected, the less IL-12 was produced when infected cells were treated with TLR ligands. Furthermore, cells

infected with UV-irradiated MHV68 and subsequently treated with TLR ligands showed less of a decrease in IL-12 secretion compared to cells infected with live virus (Fig 2-3E vs. D). UV irradiation damages the viral DNA, thus impairing expression of viral genes that could interfere with TLR signaling.

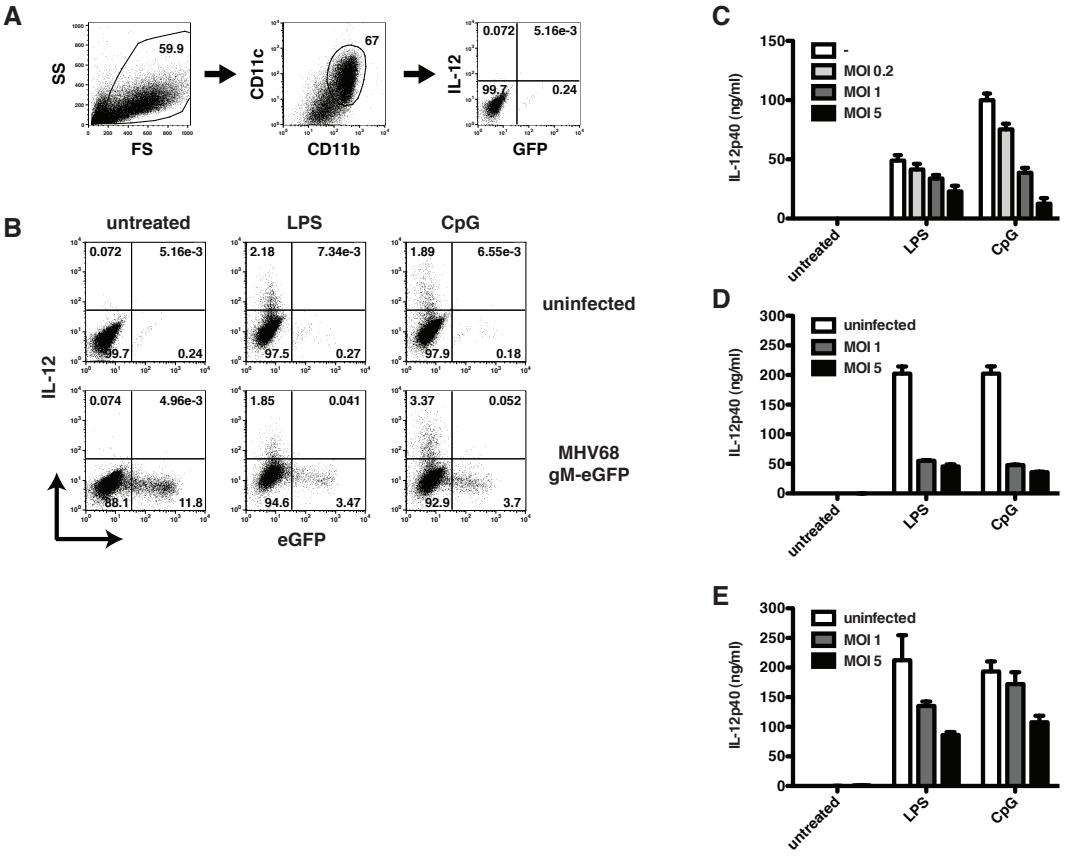
Interestingly, I did observe about a three-fold drop in lytic infection when cells were treated with TLR ligands (Fig 2-3B, bottom middle and right). I speculate that in those cells in which lytic infection was not yet fully established when TLR ligands were added, the resulting DC activation and maturation halted progression to lytic infection, which may then have entered latency or been aborted altogether. Additionally, since MHV68 infects immature, but not mature DCs (101, 102), lytic infections that have not yet been initiated within the 2-hour window may have been prevented by the process of DC activation and maturation initiated upon TLR ligand addition. Altogether, my data confirm that MHV68 poorly activates cDCs upon infection. I show that lytically-infected cells do not respond to TLR stimulation, suggesting that MHV68 may inhibit activation that lytic infection itself causes in cDCs.

Figure 2-2: IL-12 production by GMCSF-DCs following infection with MHV68



GMCSF-derived DCs from wildtype (white bars) and MyD88$^{-/-}$ (black bars) mice were treated with B/K-type CpG ODN, or infected with live (A, C) or UV-irradiated (B, D) MCMV (MOI 1) or MHV68 (indicated MOIs). Levels of IL-12p40 (A, B) and IFN-I (C, D) secreted into the supernatant were determined 20 hours post infection by ELISA or ISRE bioassay, respectively.

Figure 2-3: MHV68 suppresses TLR signaling in conventional DCs



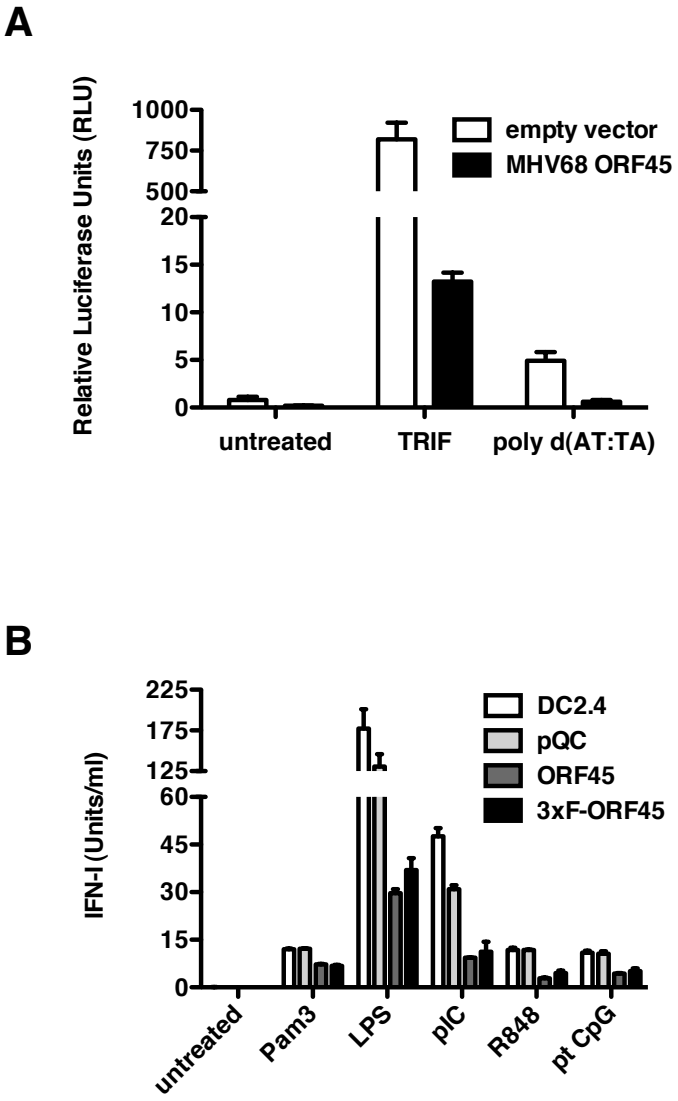
(A, B) GMCSF-derived DCs were infected or not with MHV68 gM-eGFP at MOI 1 for 2 hrs and subsequently treated with LPS or CpG or left untreated. Cytokine production in infected cells was assessed by intracellular cytokine staining for IL-12 (B), data shown is gated on $CD11c^+$, $CD11b^+$ cells (A).

(C-E) GMCSF-derived DCs were infected or not with live (C, D) or UV-irradiated (E) MHV68 at the indicated MOIs for 2 hrs and subsequently treated with LPS or CpG or left untreated. IL-12 secretion into the supernatant was assessed by ELISA for IL12p40.

MHV68 ORF45 interferes with IFN-I induction in vitro

To identify MHV68 gene products important for evasion of the IFN-I response, we devised a screen to test all MHV68 immediate early, early and tegument-encoding genes. L929 fibroblasts carrying an IFN-stimulated response element (ISRE) luciferase reporter construct were stably transfected with each gene and treated with poly d(AT:TA) DNA to stimulate cytosolic DNA sensor(s), subsequent production of IFN-I and transcription from the ISRE luciferase reporter. In this screen MHV68 ORF45 was identified. Its KSHV homologue was previously shown to interfere with IRF7-mediated induction of IFN-I(112). To validate ORF45, 293T cells were transfected with an ISRE-responsive luciferase reporter construct in the presence or absence of ORF45. 20 hours after the initial transfection, cells were also transfected with poly d(AT:TA) DNA to stimulate cytosolic DNA sensors (28). As a positive control, DNA encoding the TLR3 and TLR4 adapter TRIF was co-transfected with or without ORF45. Luciferase activity was measured 8 hours post stimulation. Transfection with poly d(AT:TA) DNA led to an increase in luciferase activity, which was abolished in the presence of ORF45 (Fig 2-4A). Similarly, cells that were co-transfected with TRIF and ORF45 also showed markedly reduced luciferase activity compared to samples in which TRIF alone was present (Fig 2-4). Next, I sought to test whether ORF45 could also reduce IFN-I induction in response to other TLR ligands. To this end, DC2.4 cells, a DC-like cell line(113), were stably expressed ORF45, FLAG-tagged ORF45, or an empty vector control. Stable cell lines were stimulated with various TLR ligands and secretion of IFN-I measured by bioassay. When ORF45 was expressed, IFN-I secretion was uniformly reduced in response to all TLR ligands tested (Fig 2-4B). These results suggest that ORF45 could potentially interfere with the induction of IFN-I *in vivo*.

Figure 2-4: Suppression of IFN-I induction by MHV68 ORF45



(A) 293T cells were transfected with an IFNβ luciferase reporter, empty vector or ORF45 and TRIF as a positive control. 20 hours later indicated samples were transfected with poly d(AT:TA). Luciferase activity was measured 8 hours later. (B) DC2.4 cells untransduced or stably transduced with empty vector, ORF45 or FLAG-tagged ORF45 were treated with either Pam3CSK4 (1 μg/ml), LPS (1 μg/ml), pIC (25 μg/ml), R848 (2 μg/ml), or phosphorothioate B/K-type CpG ODN (1 μM) for 12 hours. IFN-I secreted into the supernatant was measured by bioassay.

MHV68 neither replicates nor suppresses TLR signaling in pDCs

To understand how MHV68 interacts with pDCs, a specialized subset of DCs characterized by their ability to secrete large amount of IFN-I in response to TLR engagement by viral nucleic acid, I first wanted to know whether this cell type supported viral replication. Previous studies with MCMV showed that MCMV does not replicate in pDCs (114, 115). To determine whether this is also the case for MHV68 I infected FLT3-Ligand-DCs with MHV68 gM-eGFP for 24 hours and assessed infection by flow cytometry. MHV68 gM-eGFP marks lytically infected cells as gM-eGFP is only expressed during the lytic replication cycle (102). As expected, 11 % of cDCs ($B220^-$, $CD11b^+$) in FLT3-Ligand-DC cultures were lytically infected, while less than 1 % of pDCs ($CD11b^-$, $B220^+$) supported lytic infection with MHV68 (Fig 2-5). While I did not test this, it is likely that pDCs can be latently infected. Flaño *et al*. were able to detect genome-positive cells in pDC populations isolated from mice 14 days and 3 months post infection. Because we are unable to detect latently-infected pDCs, all subsequent experiments analyze whole populations of infected pDCs or FLT3-Ligand-DCs and will be referred to as MHV68-exposed to indicate this fact.

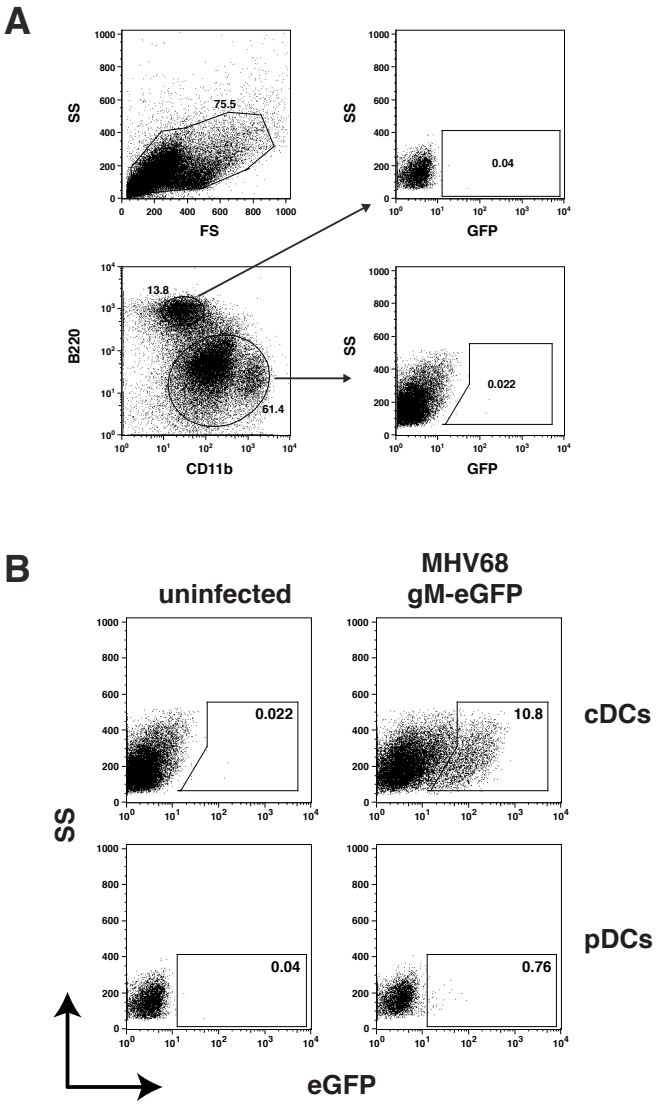
I next sought to re-examine TLR activation by MHV68 in pDCs. FLT3-Ligand-DCs were treated with B/K-type CpG ODN or infected with either MCMV (MOI 1) or MHV68 at the indicated MOIs. Supernatants were recovered 20 hours post infection and IFN-I was measured by bioassay or IFNα ELISA. As before, the production of IFN-I by MHV68 was drastically reduced compared to MCMV (1 to 2 orders of magnitude) (Fig 2-6A and B). Interestingly, the amount of IFN-I produced by MHV68-exposed cells was equal to or less than the amount produced in response to a B/K-type CpG ODN, which has been shown to poorly stimulate IFN-I in pDCs (75). However, unlike in GM-CSF-derived cDCs, IFN-I induction by both viruses was severely diminished in MyD88-deficient cells (20 to 100 fold) and MyD88/TRIF-deficient cells (data not shown), suggesting that in FLT3-Ligand-DCs IFN-I is predominantly produced by the pDC population. The residual IFN-I observed in $MyD88^{-/-}$ FLT3-Ligand-DCs is likely secreted by the cDC population in these cultures owing to activation of cytosolic nucleic acid sensors in these cells (see Fig 2-2C and D). Additionally, infection with UV-irradiated virus further reduced IFN-I secretion from FLT3-Ligand-DCs (Fig 2-6C). My observations indicate that compared with MCMV, MHV68 is a poor inducer of TLR-dependent responses in pDCs.

Next, I wanted to understand whether MHV68-exposed pDCs are able to inhibit TLR stimulation. FLT3-Ligand-DCs were exposed to MHV68 for 2 hours and subsequently treated with R848, a TLR7 ligand, for 7 hours followed by intracellular cytokine staining for TNFα. I found that TNFα production did not diminish in pDCs ($CD11c^+$, $B220^+$) that were exposed to MHV68 and subsequently treated with R848 (Fig 2-7B). I observed similar results in FLT3-Ligand-DCs that were exposed to MHV68 and subsequently treated with LPS, CpG, or R848 or infected with MCMV for 18 hours (Fig 2-7C-E). Unlike the

decrease in IL-12p40 observed in the supernatants from MHV68-infected and TLR ligand-treated cDCs (Fig 2-3), TLR-dependent IFN-I in similarly treated FLT3-Ligand-DC cultures did not diminish. On the contrary, when MHV68-exposed cells were treated with LPS, CpG, or R848 I observed an additive increase in IFN-I production (Fig 2-7C and D). Similar results have been reported previously (104, 105). The additive increase observed after FLT3-Ligand-DCs were exposed to live virus was largely reduced when these cells were exposed to UV-irradiated virus instead. As UV irradiation does alter DNA structurally, these results may be explained simply by the fact that the ligand presented after UV treatment is not efficiently recognized.

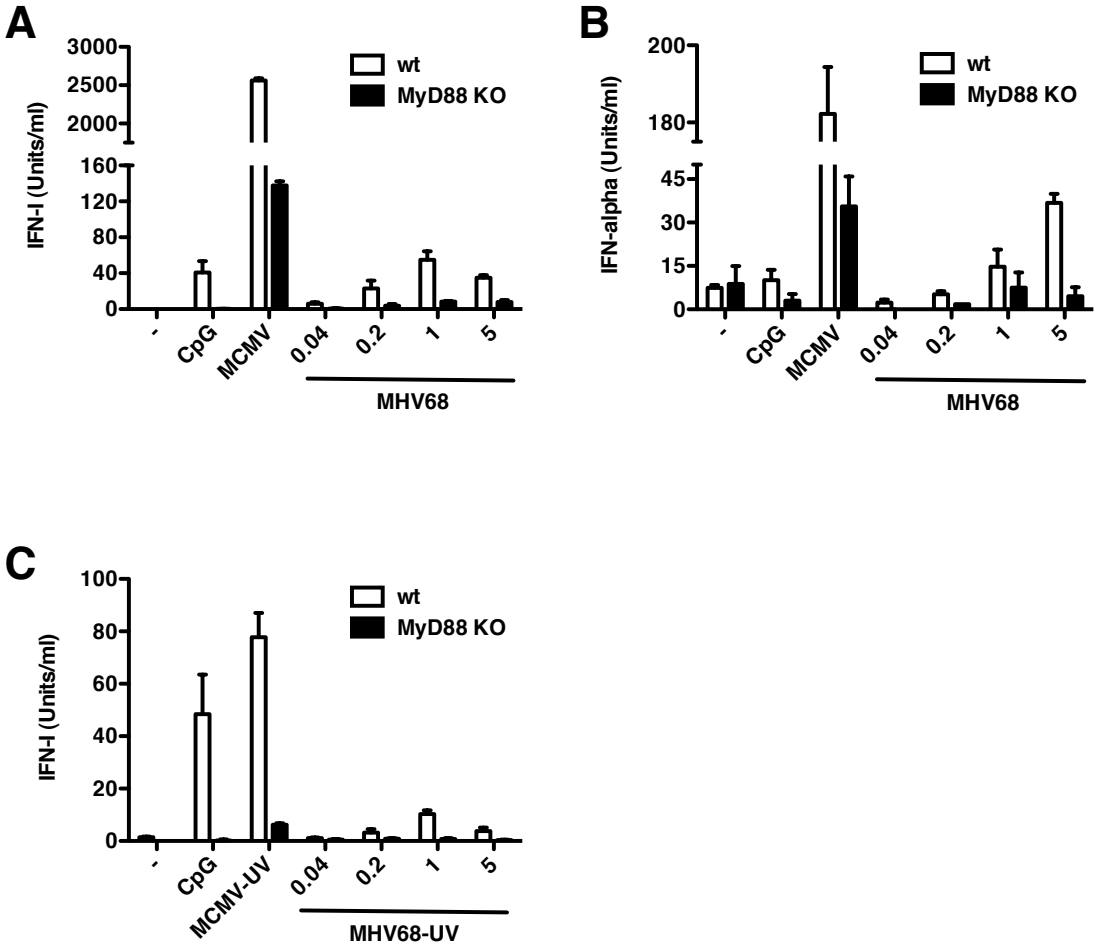
The lack of robust IFN-I secretion by pDCs, a cell type that does not allow replication of MHV68, as well as the absence of inhibition upon exogenous TLR stimulation indicate that MHV68 may not actively interfere with TLR signaling in pDCs. Altogether, my data suggest that MHV68 is not efficiently recognized by TLRs. I predict a lack of recognition by TLR9 in particular, as it is the main Toll-like receptor involved in the recognition of DNA viruses (65, 116).

Figure 2-5: MHV68 does not replicate well in plasmacytoid DCs



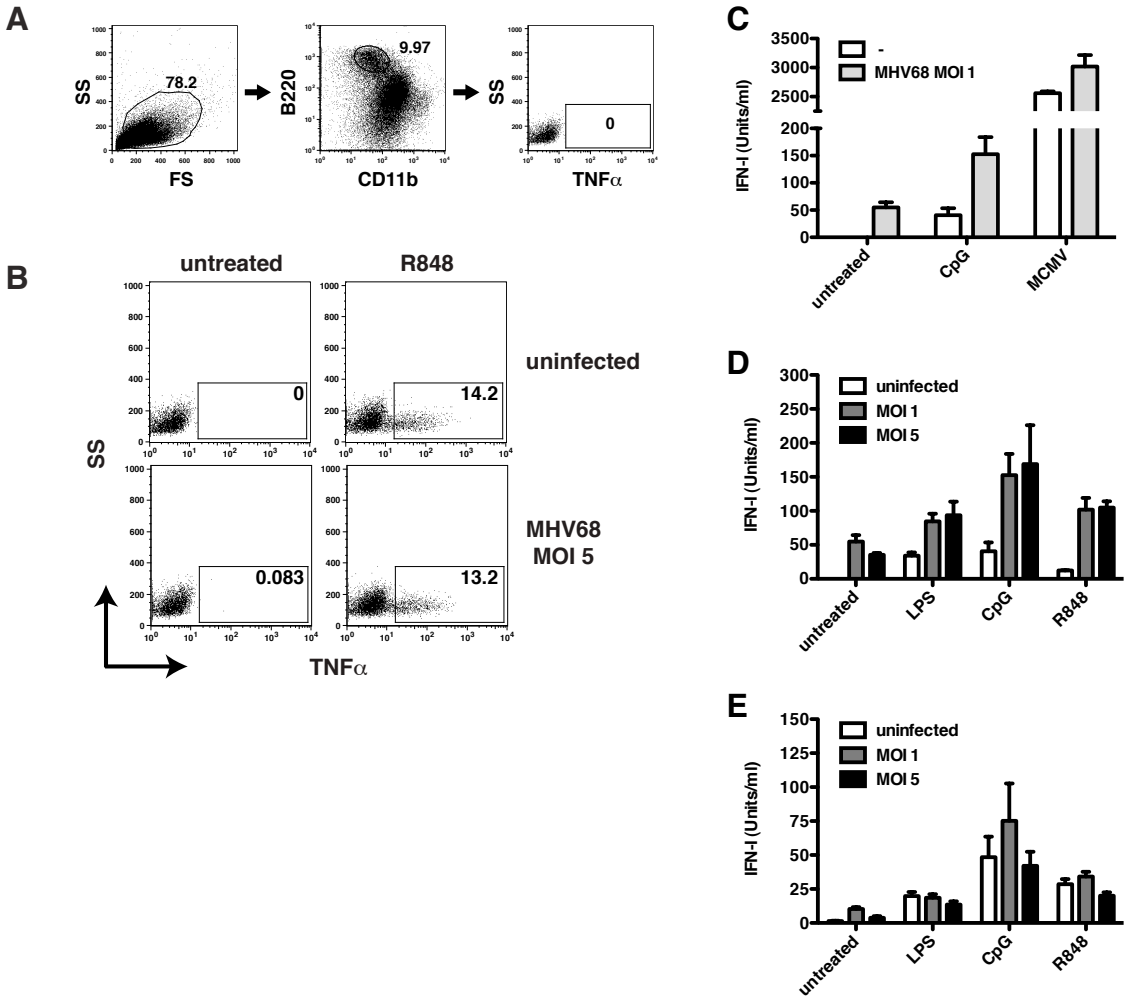
FL-DCs were infected or not with MHV68 gM-eGFP at MOI 1 for 24 hrs. Infection was assessed by flow cytometry (B). Data shown is gated on $B220^-$, $CD11b^+$ (cDCs) or $CD11b^-$, $B220^+$ (pDCs) cells (A).

Figure 2-6: IFN-I production in FLT3-Ligand derived DCs following infection with MHV68



FLT3-Ligand-DCs from wildtype (white bars) and MyD88-/- (black bars) mice were treated with CpG ODN, or infected with live (A, B) or UV-irradiated (C) MCMV (MOI 1) or MHV68 (indicated MOIs). Levels of IFN-I secreted into the supernatant were determined 20 hours post infection by ISRE bioassay (A, C) or IFNα ELISA (B).

Figure 2-7: Absence of immunomodulation by MHV68 in plasmacytoid DCs



(A, B) FLT3-Ligand-DCs were infected or not with MHV68 for 2 hrs and subsequently left untreated or treated with R848. 9 hours post infection TNFα production was assessed by flow cytometry (B). Data shown is gated on $CD11b^-$, $B220^+$ cells (pDCs) (A).
(C-E) FLT3-Ligand-DCs were infected or not with MHV68 for 2 hrs and subsequently left untreated, treated with LPS, CpG or infected with MCMV (MOI 1). Levels of IFN-I secreted into the supernatant were determined 20 hours post infection by ISRE bioassay. (C, D) Live virus. (E) UV-irradiated virus.

Discussion

Together with previous studies, my data furthers our understanding of MHV68-DC interactions and innate immune responses to this gammaherpesvirus. Previous research has shown that MHV68 infects immature, but not mature cDCs and that the majority of cDCs are latently infected (101, 102). Infection of cDCs with MHV68 does not lead to activation and maturation (101, 104, 105). However, whether this is due to an active immune evasion mechanism remains controversial. To address this question, I infected cDCs with MHV68 gM-eGFP, in which high GFP expression is restricted to lytically-infected cells (102), and showed that only lytically-infected cells were able to suppress TLR-mediated cytokine responses (Fig 2-3B). I am unable to distinguish latently-infected from uninfected cells. However, based on Smith *et al*., the majority of cDCs in my cultures should be latently infected (102). The frequency of IL-12 producing, GFP-negative cells, which comprise uninfected as well as latently-infected cells, treated with TLR ligands did not significantly diminish, suggesting that latently-infected cells may not employ an immune evasion strategy. This is not unexpected given the restricted gene expression profile during latency. Interestingly, MHV68-infected cDCs secreted IFN-I, likely due to intracellular nucleic acid sensor recognition of the virus, as this response was entirely MyD88/TRIF-independent (Fig 2-2C and D). This is in agreement with a previous study showing that the 100 bp repeat region of MHV68 induces IFN-I when delivered into the cytosol (117). Furthermore, upon infection with live but not UV-irradiated MHV68 I observed a decrease in the amount of IFN-I secreted as the infectious dose of MHV68 increased (Fig 2-2C and D), suggesting an active mechanism to suppress IFN-I responses could be involved. Although I am not aware of any proteins encoded by herpesviruses that directly prevent TLR activation, some proteins interfere with the IFN-I response. This is the case for three MHV68 gene products, M2, ORF36 and possibly ORF45 (117-119). To what extent these MHV68 gene products contribute to IFN-I suppression during viral infection in cDCs is unknown and in some cases difficult to assess as a number of these genes are also essential for viral replication.

Plasmacytoid DCs are activated following MHV68 infection and are necessary for activation of MHV68-infected cDCs (105). I also observed TLR-dependent IFN-I production in FLT3-Ligand-DCs, which are comprised of cDCs and pDCs, upon MHV68 infection (Fig 2-6A and B). As IFN-I secretion by pDCs but not cDCs is largely TLR-dependent, I speculate that the IFN-I observed in FLT3-Ligand-DCs is produced by activated pDC. However, the amount of IFN-I secreted in response to MHV68 is moderate at best when compared with MCMV (50-fold higher), a very potent inducer of IFN-I (43, 45, 46, 48). This was similarly apparent from my observation that IFN-I produced in response to MHV68 exposure was equally as low as IFN-I produced in response to B/K-type CpG ODN, which is a poor IFN-I stimulator in pDCs (75). Unlike cDCs, pDCs do not support robust lytic infection with MHV68 (Fig 2-5B). However, latent infection is

likely, as it has previously been observed *in vivo* (104). I found that similar to uninfected and latently-infected cDCs, pDCs do not inhibit TLR-mediated signaling, when MHV68-exposed cells were exogenously stimulated with LPS, CpG, or R848 (Fig 2-7). Treatment of MHV68-exposed pDCs with phosphonoacetic acid, which inhibits herpesviral replication (120), did not affect IFN-I secretion (data not shown), further supporting the idea that MHV68 may not replicate in pDCs or actively interfere with its recognition.

IFN-I is a crucial cytokine in the defense against many viral infections including MHV68. Although the level of IFN-I in the serum of MHV68-infected mice is below detection level (Fig 2-1B), IFN-I clearly plays a role as evidenced by the fact that mice deficient for the IFN-I receptor succumb rapidly to MHV68 infection (106, 107). The cell type mediating this IFN-I response *in vivo* is still unknown. My observations show that both cDCs and pDCs are capable of producing IFN-I in response to MHV68 infection *in vitro*, albeit at very low levels.

My *in vitro* data indicate that MHV68 employs active mechanisms to inhibit TLR signaling in lytically-infected cells. However, these mechanisms appeared to be absent in cells, raising the question of why DC activation and cytokine secretion cannot be observed in latently-infected cells. I suspect that in addition to immune evasion mechanisms, MHV68 may not be well recognized.

CHAPTER 3

Suppression of TLR9-Immunostimulatory Motifs in MHV68

Chapter 3:

Suppression of TLR9-Immunostimulatory Motifs in MHV68

Introduction

TLR9 has been implicated in the recognition of different families of DNA viruses (65), including herpesviruses (42-49), poxviruses (40), adenoviruses (41), and most recently Torquetenoviruses (79). However, how this receptor discriminates between self and viral DNA is not yet fully understood. The localization of TLR9 in endolysosomes, vesicles normally devoid of self-nucleic acid but where viruses are degraded upon phagocytosis, is believed to account in part for this discrimination (74). TLR9 present in endolysosomes has undergone proteolytic cleavage of its ectodomain, and only the cleaved receptor is able to recruit its signaling adapter, MyD88 (68, 70). Additionally, TLR9 is thought to recognize unmethylated CpG dinucleotide motifs in DNA, a feature that is enriched in viruses but suppressed in host genomes (7, 65). The nature of the residues flanking the CpG motifs, as well as the methylation status of the cytosine, can also influence recognition by TLR9 (121).

An essential role for TLR9 has been demonstrated in the response to alphaherpesviruses (HSV-1 and HSV-2) (42, 44, 47, 98) and betaherpesviruses (MCMV) (43, 45, 46, 48). Cells from TLR9-deficient mice are impaired in their ability to recognize these viruses, and TLR9-deficient mice are highly susceptible to MCMV infection (43, 45, 46). The importance of TLR9 in controlling gammaherpesvirus infection is less evident. In two recent studies with murine gammaherpesvirus 68 (MHV68), a mouse model for gammaherpesvirus infection, no acute replication defect was observed in MyD88$^{-/-}$ or TLR9$^{-/-}$ mice following intranasal infection (99, 100). However, viral titers in TLR9$^{-/-}$ mice were significantly increased after intraperitoneal infection with MHV68. In TLR9$^{-/-}$ but not MyD88$^{-/-}$ mice, latent viral load was also only increased upon intraperitoneal but unaffected following intranasal infection (99, 100). Surprisingly, latency establishment was reduced in MyD88$^{-/-}$ mice following intranasal infection, suggesting that TLR signaling is important rather than detrimental for these events (100).

Here I show that MHV68 DNA is poorly recognized by TLR9. TLR9 immunostimulatory motifs are underrepresented in the MHV68 genome compared to MCMV. Interestingly, my analysis shows that immunostimulatory motifs have a lower frequency compared with non-stimulatory motifs in both the MCMV and MHV68 genome. Furthermore, loss of stimulatory motifs in the MHV68 but not the MCMV genome can be attributed to deamination. These observations may provide one explanation for the low level of DC activation in general and recognition by TLR9 in particular upon infection with MHV68.

Materials and Methods

TLR9 Reporter Assay

HEK293 cells stably expressing TLR9N4C and an NF-κB responsive luciferase reporter construct were plated into 96-well plates at 4×10^4 cells per well. Cells were incubated with unmethylated or methylated viral genomic DNA or phosphodiester CpG ODN (5' TCCNNRRCGYYNNTGATGCT 3', N any nucleotide, R purine, Y pyrimidine) at the indicated concentrations for 12 hours. Viral genomic DNA was denatured for 15 minutes at 100ºC and then immediately stored on ice prior to addition to TLR9N4C-HEK293 cells. Cells were lysed in 1x Passive Lysis Buffer (Promega) and luciferase activity measured using an LMAX II^{384} luminometer (Molecular Devices).

Isolation and Methylation of viral genomic DNA

To obtain genomic DNA from viral particles, virus was concentrated and purified over a sucrose cushion as described above. The viral pellet was resuspended in PBS. An equal volume of 2x Proteinase K buffer (20 mM Tris·Cl pH 8, 10 mM EDTA, 1% SDS, 100 μg/ml Proteinase K) was added and the mixture was incubated overnight at 50-60ºC. Viral genomic DNA was extracted twice with phenol-chloroform and once with chloroform only. The DNA was precipitated with an equal volume of isopropanol, washed once with 70% ethanol and resuspended in 10 mM Tris·Cl pH 8. The DNA was treated with RNase A at 25ºC for 30 min and then again extracted with phenol-chloroform, precipitated with isopropanol, washed with ethanol and resuspended in 10 mM Tris·Cl pH 8. Viral DNA such purified was used for stimulation of TLR9N4C-HEK293 cells. Viral DNA was methylated using the bacterial methyltransferase M.SssI (NEB) according to manufacturer's instructions. Methylated DNA was purified by phenol-chloroform extraction and isopropanol precipitation. Viral DNA from latent virus was co-purified with genomic DNA from S11e cells, which are latently infected with MHV68 (122). S11e cells were lysed in Proteinase K buffer and genomic DNA extracted as described for DNA from viral particles above.

Methylation Analysis

Viral DNA isolated from viral particles or latently-infected cells was subjected to bisulfite treatment using the EZ DNA Methylation™ Kit (Zymo Research) according to manufacturer's instructions. The following oligos were used to amplify a 307 bp region of the MHV68 genome (40242-40548): forward 5' GAATATTGTTATTTTGGTTTAATGGA 3' and reverse 5' AAACCTTAAATTAAATTTTTCCCTCTAC 3'. The resulting PCR product was cloned using the PCR cloning Kit (QIAGEN). Clones were analyzed by sequencing.

Statistical Analysis

An unpaired, two-tailed student's t test was used to determine statistically significant differences.

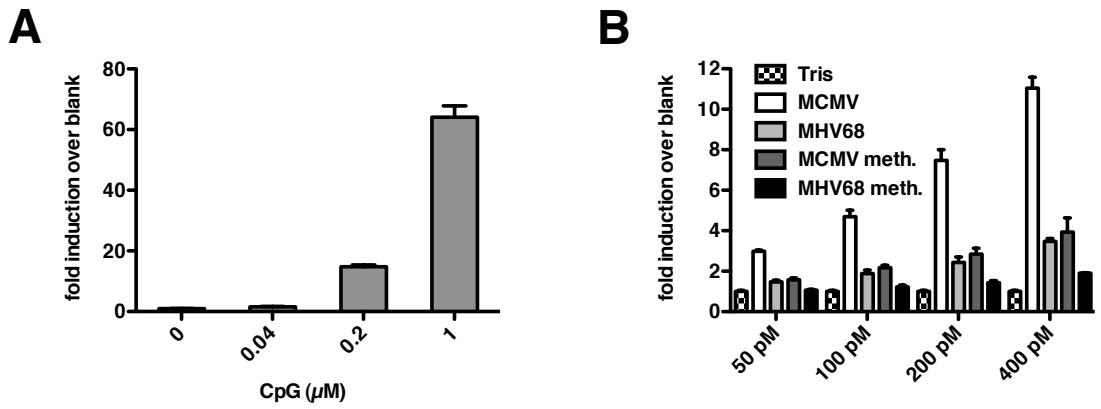
Results

The MHV68 genome poorly activates TLR9

Neither MCMV nor MHV68 replicate in pDCs, yet exposure of pDCs to MCMV leads to far greater IFN-I production compared with exposure to MHV68. This observation suggested, that TLR ligands presented by either virus are not equally well recognized. Both MHV68 and MCMV are dsDNA viruses. TLR9 is the only TLR implicated in the recognition of virally derived DNA. I therefore sought to test the possibility that direct recognition of the MHV68 genome by TLR9 is impaired. I purified genomic DNA from MHV68 and MCMV viral particles and tested their ability to activate TLR9 using a TLR9N4C-HEK293 reporter cell line (74). These cells express a chimeric version of TLR9 (the extracellular domain of TLR9 fused to the transmembrane and intracellular domain of TLR4), which is localized to the cell surface, and encode a NF-κB-responsive luciferase reporter. Without this chimeric receptor, responses to extracellular genomic DNA are very difficult to detect. TLR9N4C-HEK293 cells were incubated with various concentrations of MHV68 or MCMV DNA and TLR activation was measured using a luciferase reporter assay. As shown in Figure 3-1, MHV68 genomic DNA stimulated the reporter cells poorly compared to MCMV DNA. As expected, methylation of MHV68 and MCMV genomes on CpG motifs, prior to exposure to TLR9N4C-HEK293 cells, drastically reduced activation.

Gammaherpesviruses such as KSHV and EBV were shown to be methylated during their viral cycle, especially during latency (123, 124). It is therefore possible that the MHV68 genome is partially methylated, thus explaining the lack of efficient TLR9 activation. To test this hypothesis, I evaluated the methylation status of MHV68 genomic DNA isolated from viral particles. MHV68 DNA was treated with bisulfite, a reagent that converts unmethylated cytosines to uracil. Conversion of cytosine to uracil can then be detected by PCR and sequencing (cytosine to thymine). All cytosines present in the DNA sequence analyzed were converted to uracil, indicating that none of the original cytosines had been methylated (Table 2). A similar experiment using MHV68 genomic DNA isolated from a cell line latently infected with MHV68 (122) showed that cytosines within CpG motifs were not converted upon bisulfite treatment, and had thus been methylated (Table 1). By contrast, cytosines outside CpG motifs were never methylated (data not shown). Altogether, these results indicate that, in contrast to MHV68 DNA extracted from latently-infected cells, MHV68 DNA in viral particles is not methylated. Thus, the lack of TLR9 activation by MHV68 genomic DNA cannot be explained by the presence of methylation. This suggests that the primary sequence of the MHV68 genome itself is a poor TLR9 activator.

Figure 3-1: MHV68 genomic DNA stimulates TLR9N4C poorly



TLR9N4C-HEK293 cells were incubated with increasing amounts of CpG ODN (A) or unmethylated or methylated viral genomic DNA from either MCMV or MHV68 (B) and luciferase activity was measured 12 hours later. Viral DNA was denatured prior to addition to the cells.

Table 2: The MHV68 genome is methylated only during latency.

	Frequency of methylation	
CpG motif (40242-40548)	**DNA from lytic virus**	**DNA from latently infected cells**
GA**CG**CA	0%	75%
CC**CG**TG	0%	100%
GG**CG**TT	0%	75%
GG**CG**CT	0%	100%
AA**CG**CT	0%	100%
AT**CG**CC	0%	25%

A short sequence of the MHV68 genome corresponding to position 40242 to 40548 was subjected to bisulfite-based methylation analysis. Percentages indicate how often a particular cytosine in a CpG dinucleotide was found to have been methylated in viral DNA isolated from either viral particles or latently infected S11e cells. Cytosines outside CpG dinucleotides were never methylated.

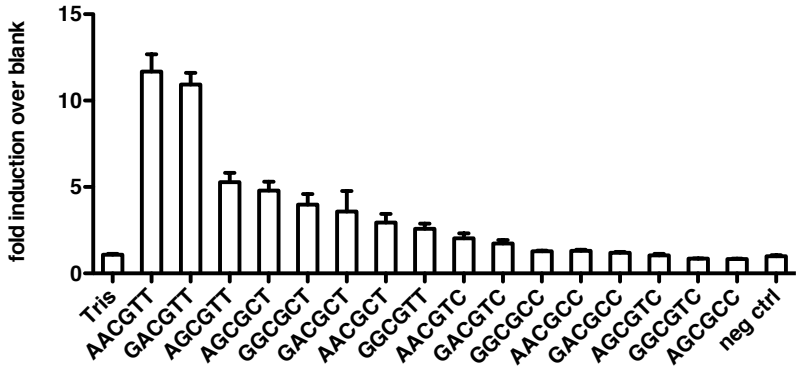
The MHV68 genome has few TLR9 stimulatory motifs

TLR9 is believed to recognize CpG dinucleotide motifs in single stranded DNA. The nature of the residues flanking CpG motifs has been shown to influence recognition by TLR9 (121, 125). However, mapping these residues has proven to be difficult mainly because natural ODN are highly sensitive to DNases (which cleave phosphodiester bonds between adjacent nucleotides). Chemically modified phosphorothioate-linked ODN alleviate most of these problems. An optimal motif recognized by murine TLR9 (A/G-A/G-CpG-C/T-C/T) has been defined using these modified ODN (125). It is not clear, however, if this consensus sequence also applies to natural PD DNA. Our current understanding of DNA recognition by TLR9 has recently been called into question. Haas *et al*. showed that TLR9 has a low intrinsic affinity for the DNA sugar backbone but that this affinity is drastically increased in the presence of DNA bases (22). Importantly, only activation of TLR9 by PS ODN showed a strict CpG dependency while CpG-containing PD ODN activated TLR9 only slightly better than some non-CpG PD ODN (22). Consequently, the consensus sequence, defined as the best activator of TLR9 using chemically modified ODN, might not be the same for natural DNA. The precise sequence motifs or structural elements that are recognized by TLR9 in natural DNA remain poorly defined. I thus decided to establish a hierarchy of motifs based on their ability to stimulate the TLR9N4C-HEK293 reporter cells described above. Phosphodiester-linked ODN comprising all 16 possible variations of the A/G-A/G-CpG-C/T-C/T murine TLR9 stimulatory motifs were synthesized and their ability to activate TLR9 was measured using the TLR9N4C-HEK293 reporter cells as before. As shown in Figure 3-2, these ODN exhibited a broad range of stimulatory capacity. The CpG ODN encoding the GACGTT context, which was previously described to be the optimal motif for murine TLR9 (126), is one of the most stimulatory motifs in our screen as well. Similar results were obtained with TLR9-HEK293 reporter cells (data not shown). However, a much higher ODN concentration was required, presumably due to inefficient uptake of the DNA.

Next, I determined the number and frequency of each of the 16 motifs in the MHV68 and MCMV genomes. All graphs in Fig 3-3 display 16 PD ODN ordered from most stimulatory on the left to least stimulatory on the right (Fig 3-3B and C, white bars on the primary y-axis) and contrasts this with the either the number (Fig 3-3A) or frequency (Fig 3-3B and C) of each motif within either the MHV68 or MCMV genome. The genome sizes of MHV68 and MCMV are 120 kb and 230 kb respectively. Strikingly, the total number of all 16 tested motifs as well as the 2 most stimulatory motifs (AACGTT and GACGTT) is 8 times lower (372 and 23) in the MHV68 genome compared to that of MCMV (2898 and 188) (Fig 3-3A), thus correlating with the differences in the ability of these two viral genomes to stimulate TLR9. Importantly, in both viral genomes, the frequency of stimulatory motifs was reduced compared to the non-stimulatory motifs (Fig 3-3B

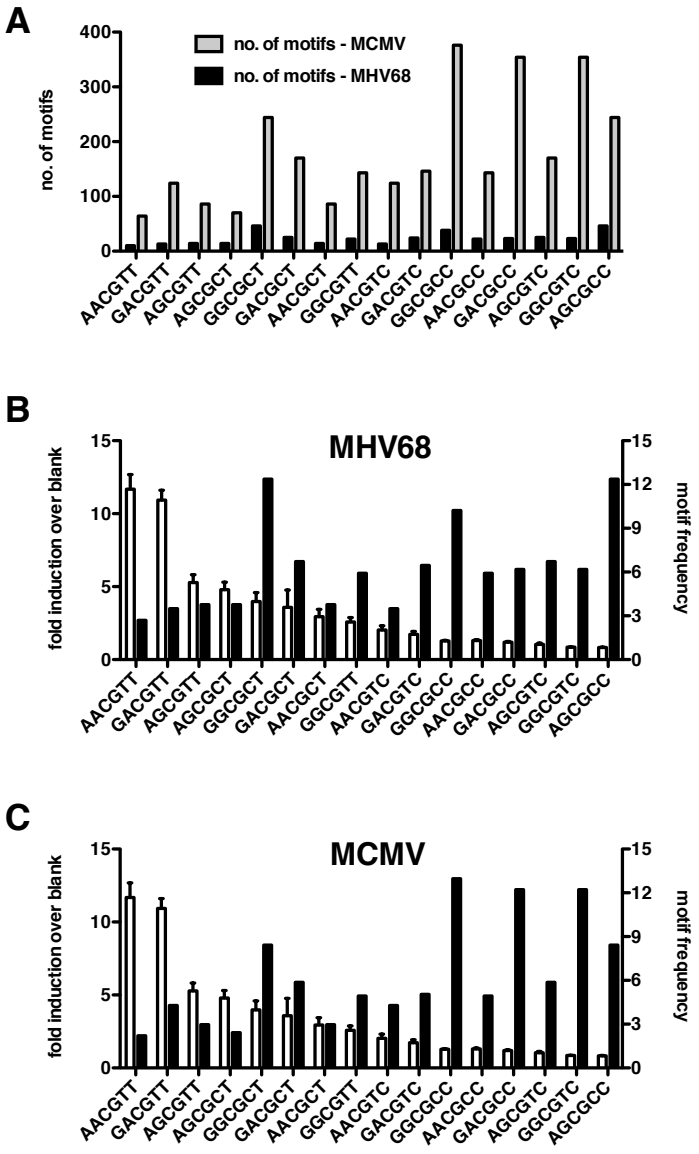
and C), suggesting that both viruses have suppressed the frequency of stimulatory motifs and possibly restricted their ability to stimulate TLR9.

Figure 3-2: Stimulation of TLR9N4C by DNA ODN containing the Pur-Pur-C-G-Pyr-Pyr consensus motif



TLR9N4C-HEK293 cells were incubated with 16 distinct CpG ODNs (1 μM) and luciferase activity measured 12 hours later.

Figure 3-3: Suppression of stimulatory CpG motifs in the MHV68 and MCMV genomes

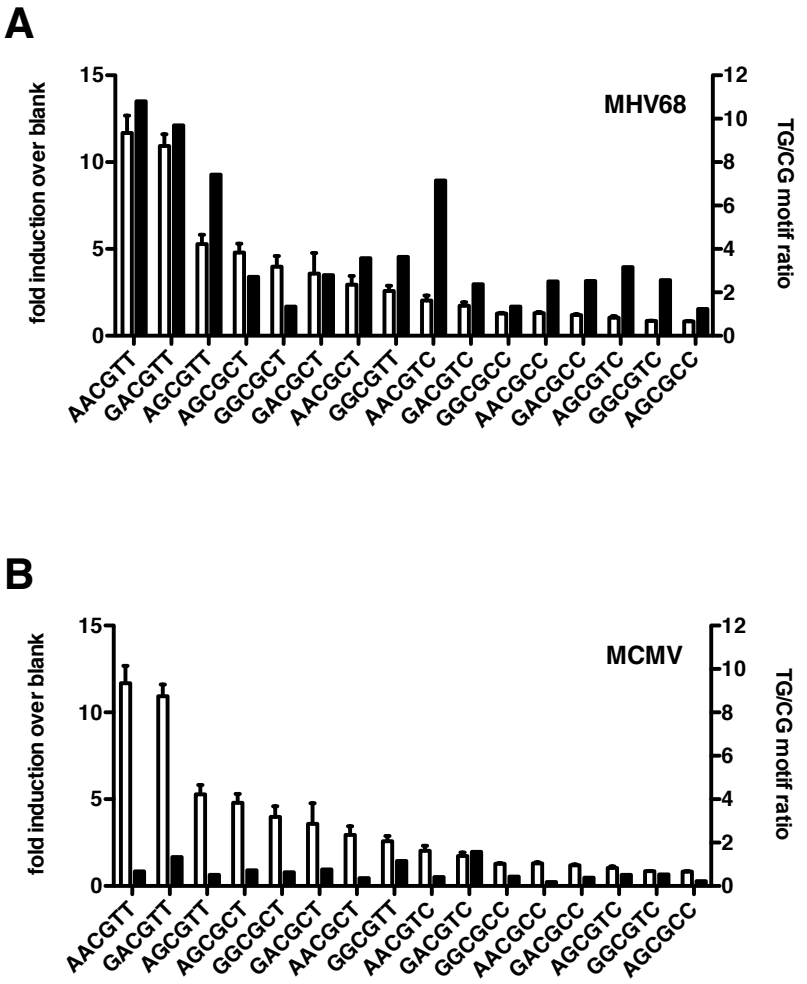


(A) Number of specific CpG motifs in either the MHV68 (black) or MCMV (grey) genome. Motifs are ordered as in Fig 3-2 with most stimulatory motif on the left and least stimulatory motif on the right.
(B, C) Data as in Fig 3-2 shown on primary y-axis (white bars) and frequency of specific CpG motifs in either the MHV68 (B) or MCMV (C) genome shown on secondary y-axis (black bars).

Selective loss of stimulatory sequences in the MHV68 genome by cytosine to thymine conversion

The low overall CpG content within the genomes of gammaherpesviruses is well documented and is believed to be largely the result of deamination, the conversion of a 5-methyl cytosine to thymine (127). As a result, the dinucleotide TpG is overrepresented in comparison to the CpG dinucleotide in these genomes (127). Spontaneous deamination of methylated cytosines would occur at random throughout the genome and be subject to DNA repair. However, if 5-methyl cytosine to thymine conversions are not repaired, they have the potential to be manifested within the genome if the mutant virus was positively selected for. Deamination of methylated cytosines within TLR9 stimulatory sequences might present such a selective advantage. We calculated the TG/CG motif ratio for each of the 16 CpG motifs within MHV68 and MCMV genomes. In the MCMV genome, TG/CG ratios were essentially the same among all the 16 motifs, with a value close to one (Fig 3-4B). However, comparing TG/CG ratios between stimulatory and non-stimulatory sequences in the MHV68 genome, we found that cytosine to thymine conversions were strikingly overrepresented among the stimulatory motifs (Fig 3-4A), suggesting that positive selection of mutated TLR9-immunostimulatory motifs may have occurred in MHV68.

Figure 3-4: Deamination of stimulatory CpG motifs in MHV68 but not MCMV



Data from Fig 3-2 (white bars) shown on the primary y-axis. Data on the secondary y-axis (black bars) shows the ratio of TpG motif frequency (CpG motif in which CG is replaced by TG) over corresponding CpG motif frequency (black bars). (A) MHV68. (B) MCMV.

Discussion

Of all currently identified receptors, the PRR that is most likely playing a role in the recognition of MHV68 is TLR9. Does TLR9 participate at all in the control of MHV68 infection *in vivo*? I clearly showed that MHV68 genomic DNA is a weak activator of TLR9 (Figure 3-1). Nevertheless, pDCs produce low levels of IFN-I in response to MHV68, and this production is dependent on MyD88, suggesting that TLR9 is capable of detecting MHV68 genomic DNA in these cells. Mice deficient for TLR9 or MyD88 do not show increased viral replication during acute replication following intranasal infection (99, 100), suggesting that TLR9 is not important under these conditions. However, viral loads were increased 10 fold in TLR9-deficient mice compared to wildtype mice when MHV68 was injected intraperitoneally (99). Strikingly, in similar experiments performed with MCMV viral titers increased three orders of magnitude (45). This is consistent with my observation that MCMV genomic DNA was three times as stimulatory as MHV68 genomic DNA when incubated with TLR9N4C-HEK293 cells. The question remains why differences between intranasal and intraperitoneal infection with MHV68 in wildtype and $TLR9^{-/-}$ mice were observed. Intranasal infection is characteristic for herpesviral transmission (128), and is believed to be the natural route of infection. In addition, previous studies have shown that lung DCs express much lower levels of TLR9 compared to splenic DCs (129), the latter of which likely interact with MHV68 during intraperitoneal infection. Thus, suppression of TLR9 immunostimulatory motifs in MHV68 masks infection and makes this virus uniquely adapted to the intranasal route of infection. Additionally, splenic DCs respond well to TLR9 stimulation and because MHV68 is not as well adapted to the intraperitoneal route of infection, the degree of suppression in TLR9 immunostimulatory motifs may simply not be sufficient to evade recognition by the innate immune system. The discrepancies between intraperitoneal infection in $TLR9^{-/-}$ and $MyD88^{-/-}$ mice, the latter of which show no increase in latently-infected cells and a dramatic reduction in reactivation from latency, remain unexplained and require further analysis.

My studies did not address the involvement of other TLRs that have been implicated in the recognition of large double-stranded DNA viruses. TLR 3 and 7, which sense double-stranded and single-stranded RNA respectively, contribute to the innate response to MCMV infection in addition to TLR9 (45, 48). However, TLR3 is dispensable during MHV68 infection (100). TLR2, which was initially found to recognize microbial lipopeptides, has since been shown to play a role in various viral infections including those with Herpes simplex viruses types 1 and 2 (51, 52), Varicella-zoster virus (53, 54), Human Cytomegalovirus (55, 56), MCMV (57), vaccinia virus (58, 59), measles virus (60), hepatitis C virus (61) and lymphocytic choriomeningitis virus (62). It is thus likely that TLRs other than TLR3 or TLR9 may contribute to immune responses against MHV68. Future studies to evaluate such contributions would require using multiple routes of infection.

Surprisingly, I observed that both MCMV and MHV68 have lower frequencies of highly stimulatory CpG motifs in their genomes, though only MHV68 DNA is able to evade TLR9 recognition efficiently. Although suppression of TLR9 stimulatory motifs might have been driven by TLR9 evasion in both viruses, it may have been sufficient for MCMV to eliminate only a few TLR9 stimulatory motifs in order to maintain a successful infection. Alternatively, other evolutionary forces may have contributed to the suppression of these stimulatory CpG motifs. Herpesviral genomes were shown to be methylated during some stages of the viral lifecycle, in part to control viral gene expression (123, 124, 130). It is thus conceivable that viruses may have evolved to mutate certain CpG motifs within their genomes during evolution to allow for more targeted gene expression. Though presently unknown, cellular methyltransferases may be more specific for particular CpG contexts in order for the host to preferentially methylate TLR9 stimulatory CpG motifs in its own genome to avoid self-recognition by TLR9. Consequently, elimination of methylated sites in viral genomes through deamination would thus specifically remove TLR9 stimulatory motifs. Regardless of the means by which suppression of TLR9 stimulatory motifs was achieved, only gammaherpesviruses but not alpha- or betaherpesviruses are generally CpG-suppressed (127). As a result, the additional reduction of TLR9 stimulatory motifs renders MHV68 almost invisible to TLR9 recognition. One prediction from my observation is that TLR9 recognition of MHV68 may be improved by increasing the stimulatory CpG content in the viral genome. To this end, I introduced a 1.4-kb sequence containing 54 stimulatory CpG motifs into the MHV68 genome by BAC recombination, increasing the overall stimulatory CpG content of the virus 2-fold. However, it has so far been insufficient to increase innate immune recognition by this mutant virus (Chapter 4).

Differences in viral lifecycles could play an important role in avoiding TLR9 recognition. Interestingly, virtually all small eukaryotic viruses are CpG suppressed (127). Among those with the lowest CpG content are polyomaviruses and papillomaviruses whose lifecycles are characterized by persistent infections (127). Viral persistence is also a hallmark of herpesviruses. How might persistence or latency select for viruses that can more effectively evade innate recognition? It is unlikely that selection occurs during acute viral infection simply due to the vast amount of virus produced. Interestingly, it has previously been shown that establishment and maintenance of latency are independent of infectious dose and route of infection for MHV68 (131). Furthermore, several deletions in MHV68 genes important for acute replication did not affect establishment of latency (132-134). However, reactivation events during persistent infection are rare, rendering reactivating cells an easier target for the immune system. For successful dissemination, reactivation of persistent viruses needs to go unnoticed. Viruses that have evolved to reduce stimulation of innate pattern recognition receptors like TLR9 may be able to spread more successfully and could thus be positively selected. Further studies are necessary to

definitively link viral persistence with TLR9 evasion. Interestingly, evasion of adaptive immune responses during reactivation has previously been suggested to be important for virus spreading (135, 136).

There are several known examples of pathogens avoiding TLR recognition by modifying TLR ligands. Several human pathogens, such as *Salmonella typhimurium* and *Yersinia pestis* produce modified lipid A moieties (the major signaling component of LPS) that are poorly recognized by TLR4 (137). To my knowledge, this strategy has not yet been described for viruses. Interestingly, modification of the herpesvirus genome as a mechanism of immune evasion has recently been documented. During latency, Epstein Barr virus expresses the EBNA-1 protein. Tellam *et al.* showed that the coding sequence of EBNA-1 is enriched in purine residues in the third base wobble position. As a consequence, EBNA-1 is translated with a low efficiency, thus reducing the number of EBNA-1 derived peptides that can be displayed at the surface of an infected cell for recognition by CTL (138). Together with the work of Tellam *et al.*, my study highlights the fact that during evolution, herpesviruses have modified their genomes to minimize immune recognition.

CHAPTER 4

Generation and Characterization of a CpG-Enriched MHV68 Mutant

Chapter 4:

Generation and Characterization of a CpG-Enriched MHV68 Mutant

Introduction

Toll-like receptors are a crucial component of the innate immune system in the detection of non-self. They recognize PAMPs, that are found in microbes but absent in the host. Bacteria provide PAMPs such as LPS, flagellin or components of the bacterial cell wall, which are recognized by TLRs located on the cell surface (5). Viruses, as they replicate within host cells, often lack these unique biochemical products. Instead the innate immune system uses the recognition of viral nucleic acids as an indicator of viral infection (6, 7). Viruses that replicate within the cytosol can be recognized by cytosolic nucleic acid-sensing receptors such as RIG-I, MDA5, or AIM2 (1). Nucleic acid-sensing TLRs comprised of TLR3, 7, 8, and 9 are located within endosomes and lysosomes. TLR3 recognizes dsRNA and mice deficient in this receptor are susceptible to infection with West Nile virus (35) and influenza virus (36). It also differs from the other nucleic acid sensing TLRs in that it signals through the adapter TRIF (37, 38), while MyD88 is the adapter interacting with the TIR domains of TLR7, 8 and 9 (8). TLR7 detects single-stranded RNA molecules, and has been shown to be important for orthomyxovirus infection. TLR8 has also been implicated in the recognition of viral RNA; however, its precise function is still unclear. TLR9 is the only TLR to recognize DNA. In particular, unmethylated single stranded DNA containing a CpG motif mediates TLR9 activation (39). The receptor has been implicated in the recognition of a wide range of DNA viruses, including poxviruses (40), adenoviruses (41) and herpesviruses (42-49). TLR7 and 9 are particularly important in the innate immune response against viruses, as they are the only PRRs expressed in plasmacytoid DCs, which produce large amounts of IFN-I in response to nucleic acid recognition (50).

TLR9 has recently been implicated in the recognition of both human gammaherpesviruses, EBV and KSHV (49, 139). As host-pathogen interaction studies are difficult to pursue with the human viruses, I utilized MHV68, a murine gammaherpesvirus most closely related to KSHV with a dsDNA genome of 120 kb (140). Previous research into the role of TLR9 in infection with MHV68 has revealed only a role when mice were infected intraperitoneally but not intranasally (99), the latter of which is believed to mimic the natural route of infection (128). I have shown in Chapter 3 that TLR9 immunostimulatory motifs are suppressed in the MHV68 genome and that MHV68 genomic DNA poorly stimulates TLR9.

Here I have generated a 1.4 kb sequence containing 54 highly stimulatory CpG motifs and integrated this sequence into MHV68 in order to increase TLR9

recognition of the virus. I show that TLR9 can be activated when exposed to these stimulatory CpG repeats. However, presentation of the same sequence in the context of the MHV68 genome did not enhance TLR9 activation compared to wildtype or GpC control virus.

Materials and Methods

Viruses and Mutagenesis

MHV68 BAC was obtained from Brigitte Rupp. Mutagenesis was performed as outlined in detail in Supplementary Protocol at the end of this chapter. Briefly, a truncated version of the *E. coli* thymidylate synthase A (*thyA)* gene (thyAΔ3') was PCR amplified with the following primers: Forward 5' caccgcaccaaggggtatttttgtgtgtgaataatcaataataaacacGCTGCTGCTGGAAGGTG TGGT 3' and Reverse 5' tgctgtaagcatgtaattaataaaagacaaaacagatatgcagttcaattGGGTAAAAAAACCGACG CACAC 3' (sequences in upper case letters corresponds to the *thyA* gene, sequences in lower case letters corresponds to MHV68 region 77128-77177 and 77178-77227, respectively). QW1 bacteria (141) carrying the MHV68 BAC were electroporated with the above PCR product and bacteria having undergone recombination were selected in the absence of thymine. MHV68 region 77106-77565 encoding the 3' ends or ORF57 and ORF58 was cloned into BamHI and EcoRV digested pcDNA3.1(+). An XhoI restriction site was inserted into the MfeI site between ORF57 and ORF58 and the CpG or GpC repeats were cloned into this XhoI restriction site. The CpG or GpC repeats with the MHV68 flanking region were excised with BamHI and EcoRV and gel-purified. The restriction digest product was electroporated into QW1 bacteria carrying the MHV68 BAC with the *thyA* gene integrated into the MfeI site between ORF57 and ORF58. Bacteria having undergone recombination to replace the *thyA* gene with either the CpG or GpC repeat were selected for in the presence of thymine and trimethoprim. After each recombination step BACs from resulting colonies were screened for the desired recombination event by EcoRI restriction digest of the BAC, PCR (76982-77001 Forward 5' CTCTGCTGACACAGTGTAAG 3'; 77912-77931 Reverse 5' TTGCTTTCCACATGGGTTCC 3') and BamHI and PstI restriction digest of the PCR product.

Virus from BACs was obtained by transfecting BAC DNA into Vero-Cre cells (generously provided by Sam Speck), which also mediate excision of BAC backbone sequences. Resulting virus was further amplified in NIH3T12 cells (ATCC CCL-164). Virus-containing supernatants were cleared of cellular debris by low speed centrifugation for 20 min. Virus was subsequently concentrated by centrifugation at 24,000 × g for 2 hrs and purified over a 30% sucrose cushion by centrifugation at 85,000 × g. Pelleted virus was resuspended in PBS and stored at -80 ºC. Viruses were titered on Balb/c 3T3 cells (ATCC CCL-163). Viral titers reflect the titer of the stock at the time of the infection (i.e. after freeze-thawing). All cell lines were grown in DMEM supplemented with 10% FBS and 100 Units/ml penicillin and 100 μg/ml streptomycin. Mice were injected intraperitoneally with MHV68 or MCMV (2×10^6 pfu per mouse) in 200 μl volumes and sera collected at the indicated time points.

Isolation of Bone Marrow and Culture of DC

Bone marrow cells were isolated from the femurs and tibiae of C57BL/6 or MyD88$^{-/-}$ mice and red blood cells were removed by ammonium chloride lysis. To derive cDCs, bone marrow cells were plated into 24-well plates at 7×10^5 cells per well in RPMI 1640 medium supplemented with 10% FBS, 100 Units/ml Penicillin, 100 μg/ml Streptomycin, 100 μM MEM non-essential amino acids, 1 mM sodium pyruvate, 2 mM L-glutamine, 50 μM 2-mercaptoethanol, and GM-CSF for 7 days. Cells were fed every other day by adding 50% fresh medium containing GM-CSF. By day 7, cultures contained 70-80% CD11c$^+$ CD11b$^+$ conventional DCs (data not shown). GM-CSF-DCs or bone marrow cells were plated into 6-well plates at 2×10^6 cells/ml per well and infected with MHV68 at the indicated MOIs or treated with phosphorothioate-linked CpG ODN (5'-TCCATGACGTTCCTGACGTT-3') at 1 μM or R848 at 2 μg/ml.

Flow Cytometry

Intracellular cytokine staining was performed using the BD Cytofix/Cytoperm™ Fixation/Permeabilization Solution Kit with BD GolgiPlug™ according to manufacturer's instructions. Antibodies were obtained from BD Biosciences (CD11c clone HL3, CD11b clone M1/70, IL-12(p40/p70) clone C15.6) and eBioscience (TNFα clone Mab11, B220 clone RA3-6B2). Data were collected on a LSR II flow cytometer (BD Biosciences) and analyzed using FloJo software (TreeStar).

TLR9 Reporter Assay

HEK293 cells stably expressing TLR9N4C and an NF-κB responsive luciferase reporter construct were plated into 96-well plates at 4×10^4 cells per well. Cells were incubated with viral genomic DNA, 1.4 kb CpG or GpC repeats, or phosphodiester CpG ODN (5' TCCNNRRCGYYNNTGATGCT 3', N any nucleotide, R purine, Y pyrimidine) at the indicated concentrations for 12 hours. Double stranded DNA was denatured for 15 minutes at 100ºC and then immediately stored on ice prior to addition to TLR9N4C-HEK293 cells. Cells were lysed in 1x Passive Lysis Buffer (Promega) and luciferase activity measured using an LMAX II^{384} luminometer (Molecular Devices).

To obtain genomic DNA from viral particles, virus was concentrated and purified over a sucrose cushion as described above. The viral pellet was resuspended in PBS. An equal volume of 2x Proteinase K buffer (20 mM Tris·Cl pH 8, 10 mM EDTA, 1% SDS, 100 μg/ml Proteinase K) was added and the mixture was incubated overnight at 50-60ºC. Viral genomic DNA was extracted twice with phenol-chloroform and once with chloroform only. The DNA was precipitated with an equal volume of isopropanol, washed once with 70% ethanol and resuspended in 10 mM Tris·Cl pH 8. The DNA was treated with RNase A at 25ºC for 30 min and then again extracted with phenol-chloroform, precipitated with isopropanol, washed with ethanol and resuspended in 10 mM Tris·Cl pH 8. Viral DNA such purified was used for stimulation of TLR9N4C-HEK293 cells.

Generation of CpG and GpC repeats

The three 10-mer motifs (GCAACGTTTT, CTGACGTTGG, ATAGCGTTTG) within the following 20 nt context (5' TCCNNRRCGYYNNTGATGCT 3', N any nucleotide, R purine, Y pyrimidine) were randomly assembled into two 60 nt ODN (60-1 5' TCCGCAACGTTTTTGATGCTTCCCTGACGTTGGTGATGCTTCCATAGCGTTT GTGATGCT 3'; 60-2 5' TCCCTGACGTTGGTGATGCTTCCGCAACGTTTTTGATGCTTCCATAGCGTTT GTGATGCT 3'). Each of the 60 nt ODN was preceded by a XhoI and followed by a SalI restriction site (digestion with both enzymes results in sticky ends that are compatible with one another). The two 60 nt ODN were assembled and cloned in a random fashion into a 1.4 kb sequence with 18 repetitions of the 60 nt ODN (1-2-1-2-2-2-2-1-1-2-2-1-2-1-2-2-1-1) into pDrive (Invitrogen). The GpC repeat was created in the same manner with the difference that the CpG dinucleotides were inverted to GpC dinucleotides.

Results

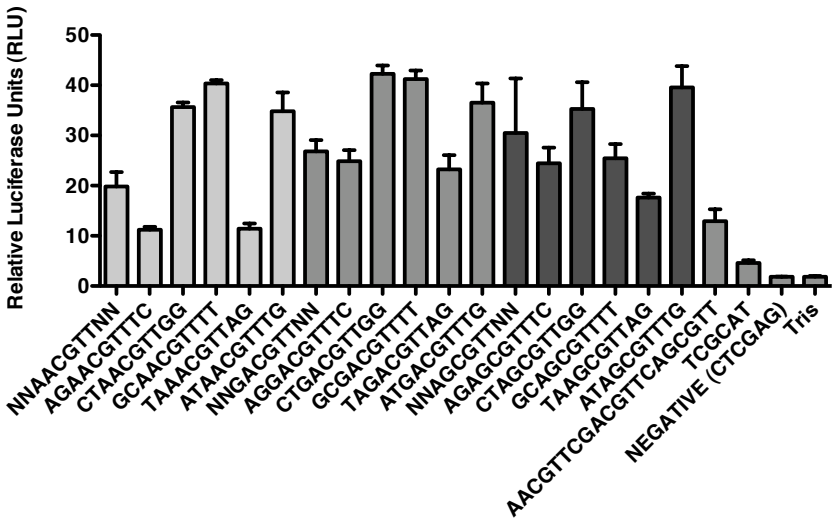
Generation of a Stimulatory CpG and a Non-stimulatory GpC Repeat

To generate a CpG-enriched mutant virus I first determined whether the sequences surrounding the 6-mer stimulatory CpG motifs (Fig 3-2) influenced TLR9 stimulation. This was necessary because each 6-mer motif was tested in this context, 5' TCCNNRRCGYYNNTGATGCT 3' (N – any base, R – A or G, Y – C or T), where the 2 bases preceding and following the 6-mer motifs were chosen randomly. Using the three most stimulatory 6-mer CpG motifs (AACGTT, GACGTT, AGCGTT) I randomly changed the 2 bases preceding and following this motif and identified the 3 most stimulatory 10-mer motifs to use in the generation of a CpG repeat. Figure 4-1 below shows the 10-mer motifs tested in our TLR9 reporter assay. Importantly, inversion of the CpG to a GpC resulted in a loss of TLR9 stimulation (data not shown).

The three 10-mer motifs (gcAACGTTtt, ctGACGTTgg, atAGCGTTtg) within the above 20 nt context were randomly assembled into two 60 nt ODN. The two different 60 nt ODN were then combined into a 1.4 kb sequence containing 54 highly stimulatory CpG repeats. As a negative control, I used the same sequences with the CpG dinucleotide inverted to a non-stimulatory GpC dinucleotide. At each step I tested stimulation of TLR9 using our TLR9 luciferase reporter assay. Figure 4-2A shows dose-dependent stimulation of TLR9 reporter cells by the three most stimulatory 20 nt ODN identified in Fig 4-1 above. In addition, I also tested the two 60 nt ODN. Especially at the lower concentrations the 60 nt ODN were more stimulatory compared to the 20 nt ODN. Again, ODN in which the CG dinucleotide was inverted to a GC dinucleotide were not stimulatory at all (Fig 4-2B).

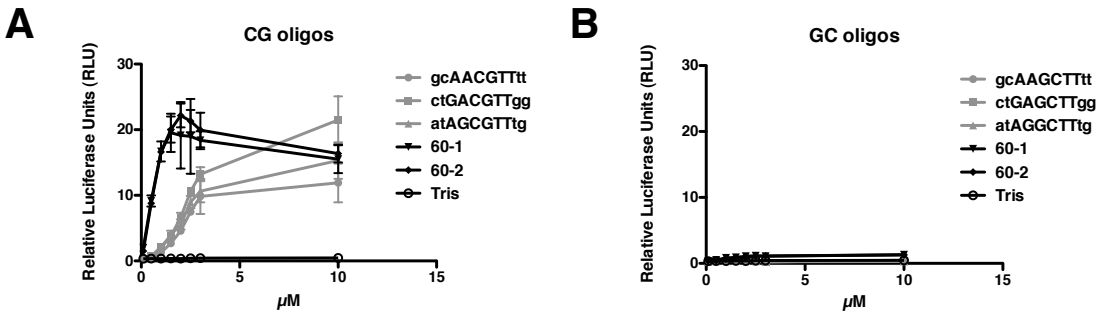
Next, I assembled the two 60 nt ODN in a random fashion to form a 1.4 kb sequence containing a total of 54 stimulatory CpG or 54 non-stimulatory GpC repeats. Figure 4-3 shows that this 54 CpG-repeat containing DNA was able to stimulate the TLR9 reporter cells, while the GpC-repeat containing DNA did not.

Figure 4-1: Defining the context around the stimulatory 6-mer CpG motifs



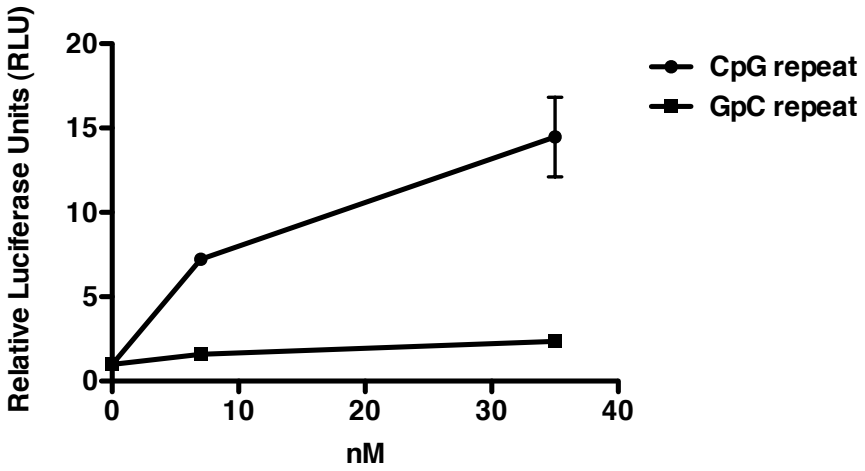
TLR9N4C-HEK293 cells were incubated with 20 nt ODNs with the indicated sequences at 1 μM and luciferase activity measured 12 hours later. (ODN sequence 5' TCC NNRRCGYYNN TGATCGT 3', N – any nucleotide, R – Purine, Y – Pyrimidine)

Figure 4-2: Dose-dependent stimulation of TLR9N4C by 20-mer and 60-mer ODN containing stimulatory CpG or non-stimulatory GpC motifs



TLR9N4C-HEK293 cells were incubated with 20 nt or 60 nt ODNs containing either stimulatory CpG (A) or non-stimulatory GpC (B) sequences and luciferase activity measured 12 hours later.

Figure 4-3: Stimulation of TLR9N4C with 1.4 kb containing 54 stimulatory CpG or non-stimulatory GpC motifs



TLR9N4C-HEK293 cells were incubated with the 1.4 kb sequence containing 54 stimulatory CpG or 54 non-stimulatory GpC repeats and luciferase activity was measured 12 hours later. DNA was denatured prior to addition to cells.

A CpG enriched MHV68 mutant does not increase innate immune recognition

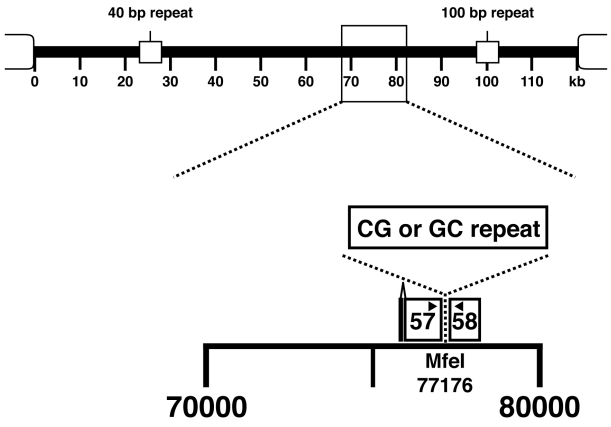
The 1.4 kb sequence containing either 54 highly stimulatory CpG repeats or non-stimulatory GpC repeats was introduced into the MHV68 genome by bacterial artificial chromosome (BAC) mutagenesis (Supplementary Protocol and Figure 4-4). I chose to insert the CpG repeats between the polyadenylation signals of ORFs 57 and 58 as integration into this site had previously been shown not to affect expression of neighboring genes (142).

I then generated virus from wildtype, CpG-enriched or GpC-enriched MHV68 BACs, isolated viral genomic DNA from viral particles, and tested stimulation of TLR9 using a TLR9 luciferase reporter assay. While the 1.4 kb sequence containing 54 highly stimulatory CpG motifs by itself was stimulatory (Fig 4-3), I did not observe any increased stimulation when this 1.4 kb stimulatory sequence was presented in the context of MHV68 DNA (120 kb) compared to DNA derived from wildtype virus (Fig 4-5). By inserting 54 stimulatory CpG repeats I only increased the CpG content 2-fold. This is still significantly lower than the stimulatory CpG motif content in the MCMV genome, thus explaining in part the absence of TLR9 stimulation.

Despite the absence of increased TLR9 stimulation when CpG-repeats were presented in the context of the MHV68 genome in our TLR9 reporter assay, I decided to test whether this virus would elicit a stronger cytokine response during infection of dendritic cells *in vitro*. Wildtype, CpG-enriched, and GpC-enriched MHV68 grew to similar titers *in vitro* (Fig 4-6). Next, I GM-CSF-derived DCs were infected with either wildtype MHV68, CpG-MHV68, or GpC-MHV68 and cytokine responses assessed by intracellular cytokine staining for TNFα, a cytokine produced in response to TLR signaling in cDCs. No increased cytokine production in response to CpG-enriched MHV68 was observed compared to infection with wildtype or GpC-enriched MHV68 (Fig 4-7). These results suggest that either TLR recognition was not enhanced or that active immune evasion mechanisms employed by MHV68 are sufficient to overcome any increase in TLR9-mediated activation.

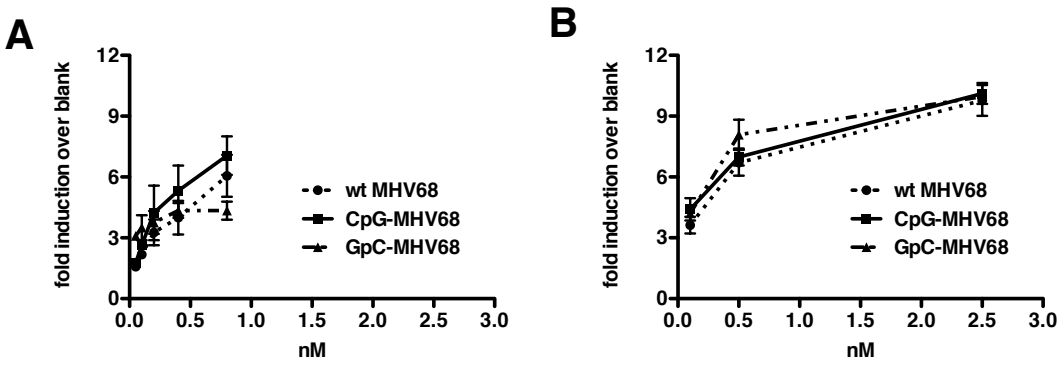
MCMV infection in pDCs, a cell type in which the virus does not replicate (115), leads to robust induction of cytokines (Fig 2-6). This suggests that replication is not required for efficient recognition by TLR 7 or 9, the two PRRs expressed in pDCs. Plasmacytoid DCs also do not support replication of MHV68 (Fig 2-5); however, infection with MHV68 does not cause robust cytokine secretion. These observations suggested that MHV68 is not well recognized in pDCs. Next, I tested if TLR9 recognition in pDCs could be increased by infection with CpG-enriched MHV68. Similarly to infection of cDCs, infection of pDCs with CpG-MHV68 did not lead to increased cytokine production compared to wildtype or GpC-MH68 (Fig 4-8). Several reasons for these negative results are discussed below.

Figure 4-4: Construction of CpG or GpC enriched MHV68



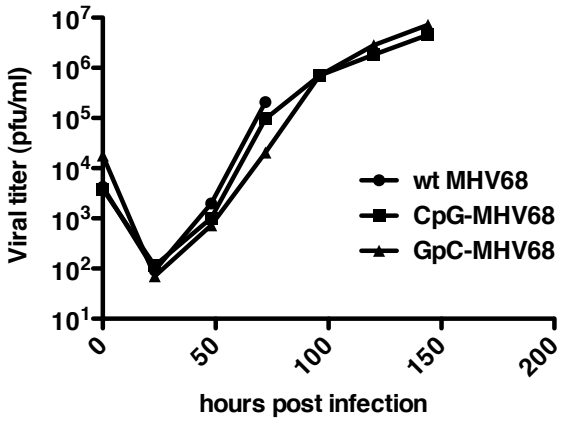
A 1.4 kb sequence containing 54 CpG or CpG repeats was integrated into the MfeI site between the polyadenylation signals of ORF57 and ORF58. Generation of these 2 viruses is outlined in greater detail in the supplementary protocol at the end of this chapter.

Figure 4-5: Stimulation of TLR9N4C with genomic DNA from wildtype, CpG, or GpC MHV68



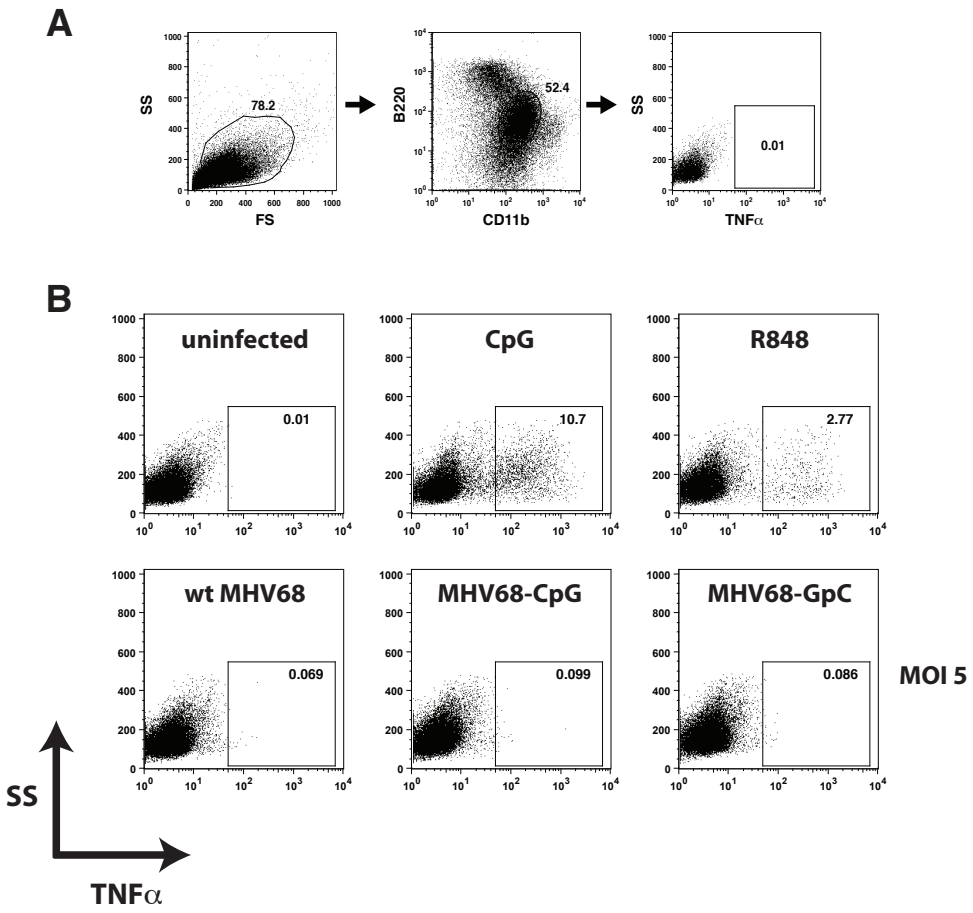
TLR9N4C-HEK293 cells were incubated with increasing amounts of viral genomic DNA from either wildtype MHV68, CpG-MHV68, or GpC-MHV68 and luciferase activity measured 12 hours later. Viral DNA was denatured prior to addition to cells. (A) Concentration of viral DNA: 0.1 nM, 0.2 nM, 0.4 nM, and 0.8 nM. (B) Concentration of viral DNA: 0.1 nM, 0.5 nM, 2.5 nM.

Figure 4-6: Growth curve of wildtype, CpG and GpC MHV68 viruses



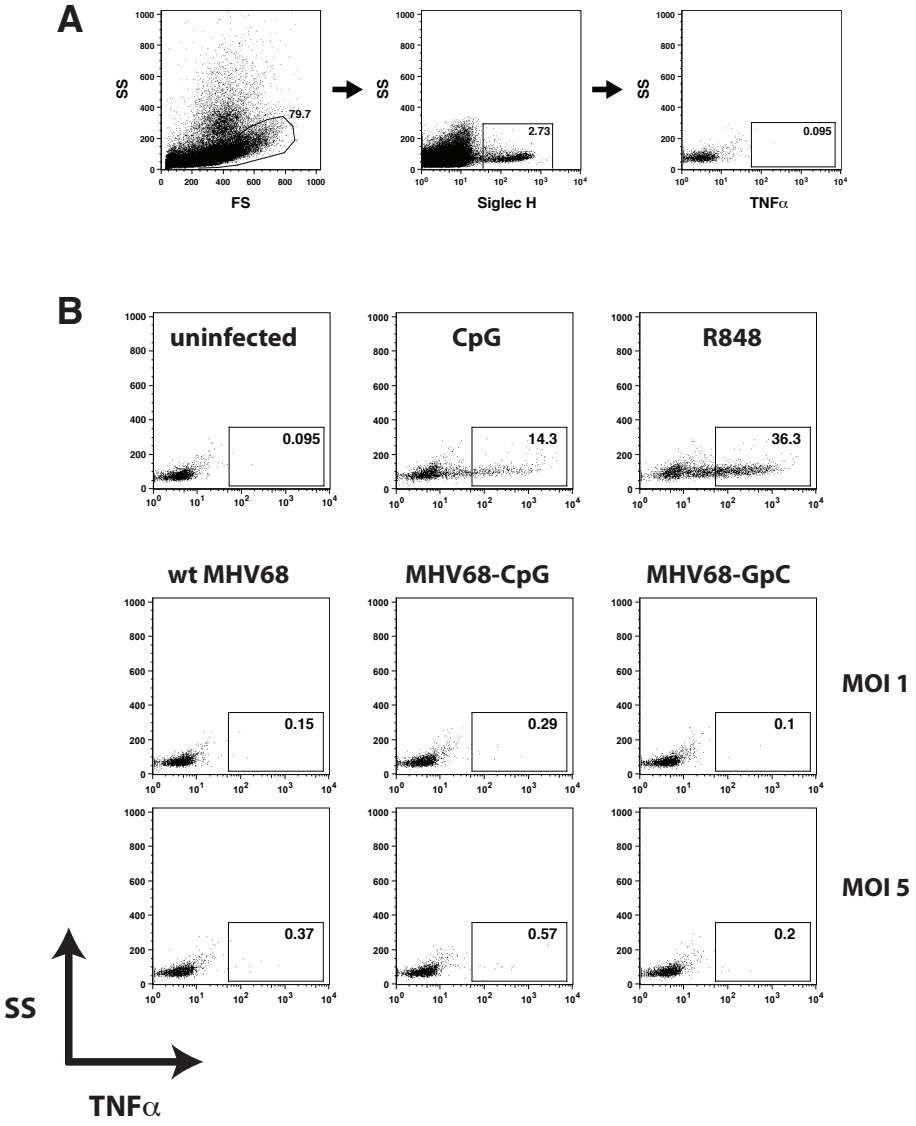
3T12 cells were infected at an MOI of 0.05. Supernatants were recovered at various time points post infection and viral titers determined by Plaque Assay. (Not all time points for wt MHV68 were collected in this assay. However, wt MHV68 generally grows to the same titers as CpG-MHV68 and GpC-MHV68.

Figure 4-7: TNFα production by conventional DCs infected with either wildtype, CpG or GpC MHV68



(A, B) GMCSF-derived DCs were isolated and untreated, treated with CpG or R848, or infected with wildtype MHV68, CpG-MHV68, or GpC-MHV68 at the indicated MOIs. TNFα production in $CD11b^{+}$, $B220^{-}$ conventional dendritic cells (A) was assessed by intracellular cytokine staining (B).

Figure 4-8: TNFα production by plasmacytoid DCs infected with either wildtype, CpG or GpC MHV68



(A, B) Bone marrow cells were isolated and untreated, treated with CpG or R848, or infected with wildtype MHV68, CpG-MHV68, or GpC-MHV68 at the indicated MOIs. TNFα production in Siglec H^+ plasmacytoid dendritic cells (A) was assessed by intracellular cytokine staining (B).

Discussion

TLR9 is activated upon stimulation with CpG ODN as well as viral and bacterial DNA (65). Here, I attempted to enhance TLR9-mediated recognition of and responses against the gamma-herpesvirus MHV68 by introducing highly stimulatory CpG motifs into the viral genome.

My previous work shows that TLR9 immunostimulatory motifs are underrepresented in the MHV68 genome compared to non-stimulatory motifs, in part explaining the lack of TLR9 stimulation observed with this virus. Deamination contributed strongly to the loss of TLR9 stimulatory motifs. As a result, the MHV68 genome contains a far greater number of motifs with a stimulatory context in which the central CpG dinucleotide was converted to a TpG dinucleotide. To rescue TLR9-mediated recognition I decided to increase the stimulatory CpG context within the MHV68 genome. As the MHV68 genome is 120 kb in size and previous stimulatory motifs now containing the TpG dinucleotide are scattered throughout the MHV68 genome, it was not feasible to convert individual motifs. Instead I decided to use a strategy previously employed by Krieg *et al*. in the generation of a DNA vaccine. The authors introduced as many as 50 stimulatory CpG motifs into an existing DNA vaccine vector markedly increasing its Th1-like function *in vivo* (143). I constructed a CpG repeat containing 54 highly stimulatory CpG motifs based on our characterization of TLR9 stimulation by ODN containing the A/G-A/G-C-G-C/T-C/T consensus motif (Fig 3-2). My analysis showed that increasing the number of CpG motifs did increase TLR9-mediated activation of a NF-κB responsive luciferase reporter, and that this stimulation was CpG-dependent, as ODN containing a GpC dinucleotide within the same DNA context were unable to stimulate TLR9.

Surprisingly, while the 1.4 kb sequence containing 54 stimulatory CpG motifs was able to stimulate TLR9, no increased stimulation was observed when this repeat was presented within the context of the MHV68 genome compared to its wildtype or GpC motif-containing counterparts. Several reasons may account for these observations. First, given the size of the MHV68 genome (120 kb), introduction of 54 stimulatory CpG motifs only doubled the stimulatory CpG content of virus. In a TLR9 reporter assay, only a 3-fold difference in stimulation between MCMV and MHV68 was observed, even though the former contains 8 times as many stimulatory motifs. Thus, increasing the stimulatory CpG content in MHV68 should yield a less than 2-fold increase in stimulation at best, suggesting that stimulation in the TLR9 reporter assay may not be sensitive enough to observe an enhancement in TLR9 stimulation. Additionally, it is possible that other as of yet uncharacterized stimulatory CpG motifs are present in both the MCMV and MHV68 genome, in which case a less than two-fold increase in stimulatory CpG motifs would have been achieved. Thus, the level of CpG enrichment in our mutant CpG-MHV68 virus may simply not be sufficient to increase recognition by TLR9. Furthermore, the stimulatory CpG motifs were introduced in one continuous sequence. Due to the limited understanding of

TLR9 – DNA interaction, it is unknown whether this is would lead to TLR9 stimulation in the context of a large viral genome or in the context of a viral infection. It may be preferable to distribute stimulatory CpG motifs throughout the MHV68 genome. However, the genome size and the limitations of BAC mutagenesis make this approach not feasible at this time.

To increase the sensitivity of TLR9 stimulation, I decided to test stimulation in the context of DC infection. Cytokine production was neither increased in cDCs nor pDCs infected with CpG-MHV68 compared to wildtype or GpC-MHV68 (Fig 4-7 and 4-8). As MHV68 replicates in conventional DCs and IFN-I production diminished with increasing MOI of virus, my previous observation suggested that the virus might utilize active immune evasion mechanisms to evade recognition by the immune system and subsequent cytokine production. These reasons cannot, however, account for the lack of cytokine production observed in pDCs. MHV68 does not replicate in pDCs within the first 24 hours of infection, suggesting that virus either enters latency as previously observed (104) or does not infect this cell type at all. Infection of or replication within pDCs is not prerequisite to recognition by TLRs expressed in this cell type. MCMV does not replicate in pDCs either, yet it induces robust cytokine secretion in a TLR7 and 9-dependent manner (115). What then accounts for the lack of TLR9 stimulation observed? As discussed above, it is possible that presenting stimulatory CpG motifs in one continuous sequence rather than distributed around the genome may not be sufficient to stimulate TLR9. Furthermore, if the MHV68 contains additional as yet unidentified TLR9 stimulatory motifs, introducing 54 additional motifs may simply not be enough to enhance TLR9 stimulation significantly. In addition, the MHV68 genome contains a GC-rich 100 bp repeat containing motifs that have previously been characterized is inhibitory. Their number is roughly equal to the number of stimulatory motifs I previously identified. The additional motifs introduced in CpG-MHV68 might not be enough to overcome a potential inhibitory effect.

Taken together, my data suggest, that MHV68 presents a complex system, which is not yet fully understood with regard to TLR9 activation. Rather than further modifying the MHV68 genome, introducing CpG repeats into a smaller DNA virus, that is easier to manipulate genetically, may be more feasible.

Supplementary Protocol

Overview of Thymidylate synthase A (thyA)-mediated BAC mutagenesis

With a genome size of 120 kb, MHV68 cannot be easily manipulated genetically. Cloning of the MHV68 genome as a bacterial artificial chromosome (BAC) has facilitated this process (144). BAC vector sequences are flanked by loxP sites, allowing for excision of these sequences by Cre recombinase. Modification of the MHV68 genome through BAC mutagenesis usually involves a two-step process. In the first step, a selection marker such as an antibiotic resistance replaces or is inserted into the gene or region of interest. In the second step, the selection marker is replaced by the gene or region of interest containing the desired modification. Infectious virus can be reconstituted by transfecting the MHV68 BAC into a permissive cell line. If desired, the BAC vector sequences can be removed by passaging the virus in Cre-expressing permissive cells.

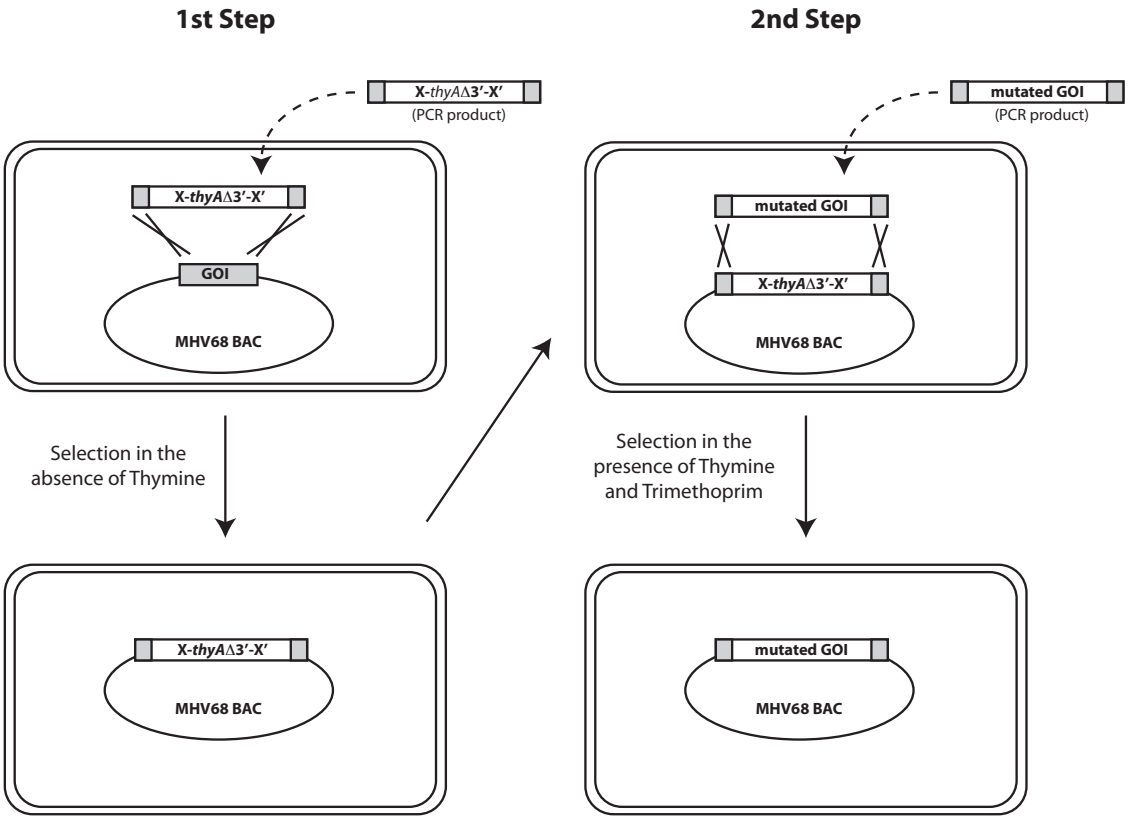
The nature of the selection process in the first and second step greatly influences the efficiency of BAC mutagenesis. Recently, a DNA recombineering strategy using a single selectable marker, the *thyA*, has been developed (141). In general, this method is based on the bacteriophage λ-Red recombination system (145, 146). The Red system encodes for three proteins, Exo, Beta, and Gam, which mediate recombination between linear double-stranded DNA and its homologous target sequence. The selection approach recently developed by Wong *et al*. utilizes the bacterial *thyA* gene, which is involved in the synthesis of dTTP from dUMP. In the absence of the *thyA* gene product, bacteria cannot synthesize DNA and are thus unable to grow in the absence of thymine. ThyA function requires an additional cofactor, tetrahydrofolate (THF), which is important in many other essential cellular pathways as well. During these biochemical processes THF is converted to dihydrofolate (DHF). The enzyme dihydrofolate reductase, which is sensitive to the chemical agent trimethoprim, replenishes the cell's THF supply from DHF.

The BAC mutagenesis strategy developed by Wong *et al*. uses these biochemical dependencies in the following way. *E. coli* deficient in *thyA* and carrying the Red genes, whose expression is controlled by a temperature-sensitive repressor, and the BAC of interest to be mutated are transformed with a PCR product encoding the *thyA* gene flanked by ~50 bp homologous to the region of interest. Bacteria that have successfully undergone recombination and integrated the *thyA* gene will be able to grow in the absence of thymine (Fig 4-9, 1st step). Next, bacteria carrying the *thyA*-proficient BAC are transformed with a PCR product encoding the mutated gene of interest flanked by ~50 bp homologous to the region of interest. Bacteria that have successfully undergone this 2nd recombination event are selected for in the presence of thymine and trimethoprim (Figure 4-9, 2nd step). Successful recombination would result in bacteria being *thyA*-deficient and therefore they require thymine. However,

bacteria that have not undergone recombination and are still *thyA*-proficient will grow in the presence of thymine as well. To selectively inhibit growth of the latter, the growth medium is also supplemented with trimethoprim, which prevents replenishment of the essential cofactor THF. The former *thyA*-deficient bacteria will be largely unaffected by trimethoprim, as THF cannot be exhausted in a thyA-dependent biochemical process and is thus still available for the remaining essential cellular reactions. On the other hand, bacteria carrying a *thyA*-proficient BAC that failed to undergo recombination will exhaust the cofactor THF in a ThyA-dependent manner. As trimethoprim prevents THF from being replenished, these bacteria will not have sufficient levels of THF to support other essential pathways and thus are unable to grow.

I used *thyA*-mediated BAC mutagenesis to create three different mutant MHV68 BACs, mCherry-ORF45 MHV68, CpG MHV68 and GpC MHV68. Their construction is described in greater detail below.

Figure 4-9: BAC mutagenesis strategy

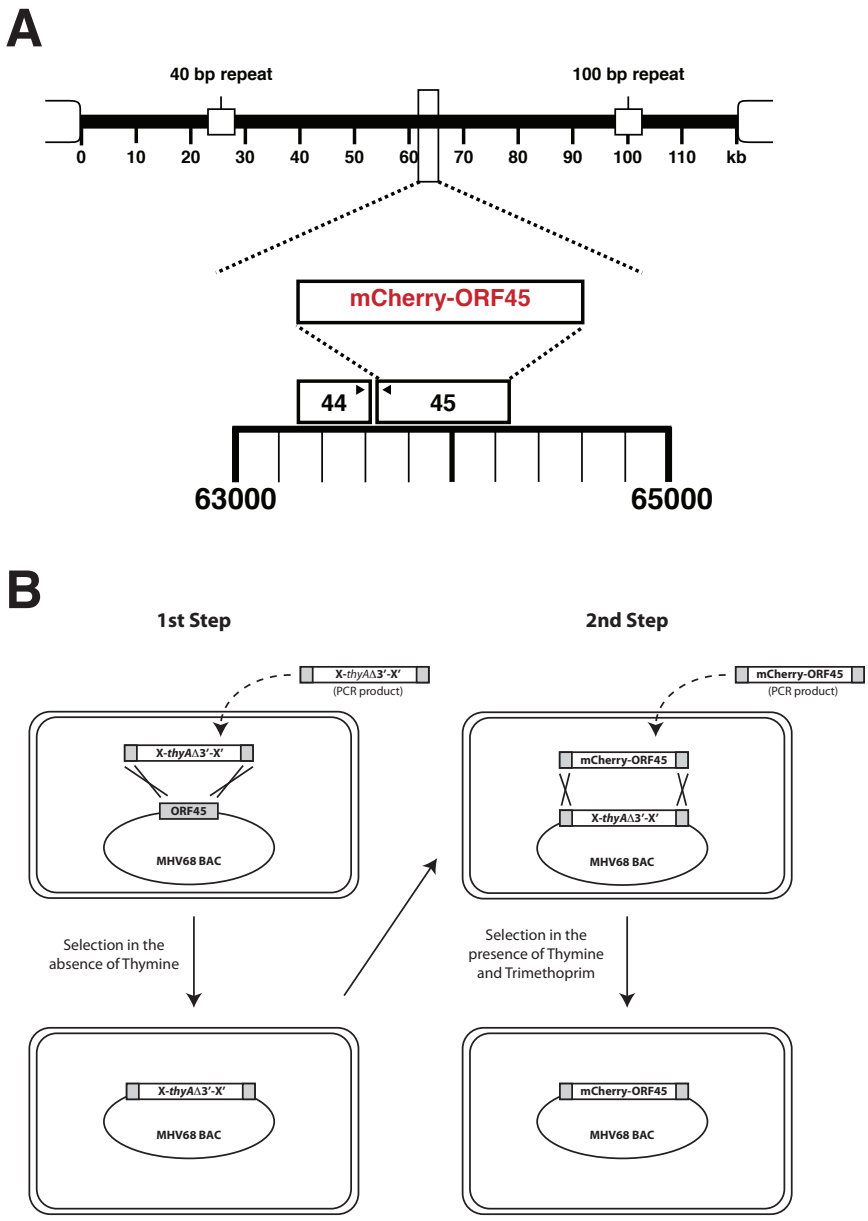


1st Step: Thymidylate synthase A-deficient bacteria carrying the MHV68 BAC are transformed with a PCR product encoding the *thyA* gene flanked by ~50 bp of sequences homologous to the gene of interest (GOI) to be changed. Bacteria that have undergone recombination and integrated the *thyA* gene in the region of interest are selected for by the absence of thymine.
2nd step: ThyA-proficient bacteria carrying the MHV68 BAC with *thyA* integrated into the region of interest are transformed with a PCR product encoding the mutated gene of interest flanked by ~50 bp of sequences homologous to the locus of interest to be changed. The 2nd step selection occurs in the presence of thymine and trimethoprim.

Generation of mCherry-ORF45 MHV68

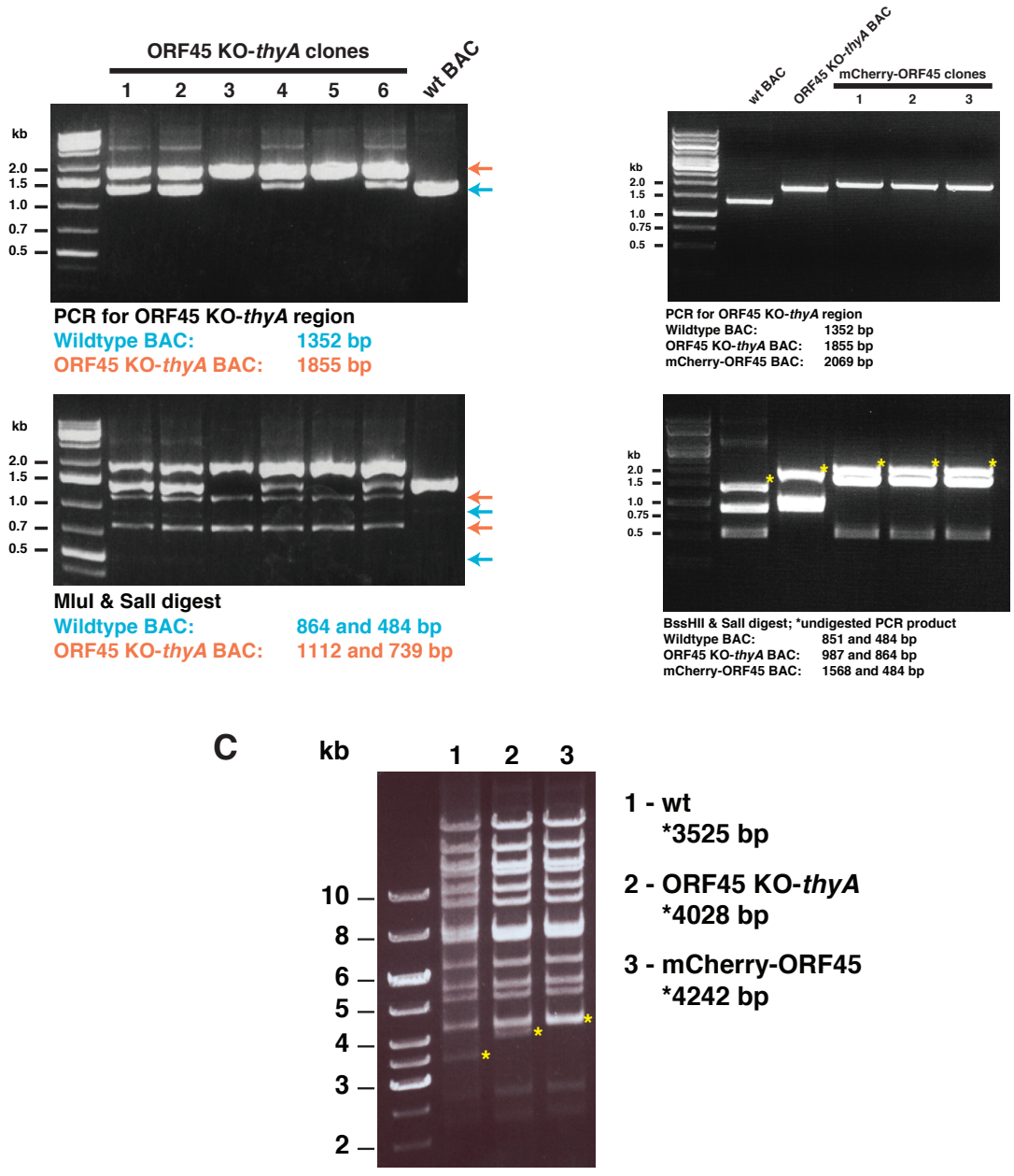
The mCherry-ORF45 BAC is different from wildtype MHV68 in that the ORF45 gene is fused to the C terminus of mCherry to create a fluorescently-tagged gene product (Fig 4-10A). For the first step of the mutagenesis process (Fig 4-10B), a truncated version of the *E. coli thyA* gene (thyAΔ3') was PCR amplified with the following primers: Forward 5' tacacaacccaaaaacattacttgtatattaatttttattgaataaagttGCTGCTGCTGGAAGGTGTG GT 3' and Reverse 5' aacacatatttaacgcagcacaacaaaccctcaatttcttggaacttataGGGTAAAAAAACCGACG CACAC 3'. Sequences in upper case letters corresponds to the 5' and 3' end of the truncated *thyA* gene, whereas sequences in lower case letters corresponds to MHV68 regions flanking the ORF45 gene (63602-63651 and 64273-64322, respectively). QW1 bacteria (141) carrying the MHV68 BAC were electroporated with the above PCR product and bacteria having undergone recombination were selected for in the absence of thymine. MHV68 BACs in which the ORF45 gene was replaced with *thyA* (ORF45 KO-*thyA*) were screened by PCR and restriction digest with MluI and SalI. The MHV68 region of interest was amplified with the following primers: Forward 5' TGGGCTGCACAGGAGATTATGGAA 3' (63359-63382 bp in the MHV68 genome) and Reverse 5' AGTCCCACCGAGCTTACACAACAT 3' (64687-64710 bp in the MHV68 genome). Figure 4-11A, top panel shows that clones 3 and 5 produced the expected 1855 bp band, suggesting that the ORF45 gene has been replaced with *thyA*. Similarly, both clones produced the expected banding pattern, when the PCR product was digested with MluI and SalI (Fig 4-11A, bottom panel). Clone 3 was used for the second step of BAC mutagenesis. ORF45 was fused to mCherry and amplified with the following primers: Forward 5' AACACATATTTAACGCAGCACAACAAACCCTCAATTTCTTGGAACTTATAatggt gagcaagggcgagg 3' and Reverse 5' TACACAACCCAAAAACATTACTTGTATATTAATTTTTATTGAATAAAGTTtcaatc caaccatggccagttatattttcca 3'. Sequences in upper case letters corresponds to MHV68 regions flanking the ORF45 gene (63602-63651 and 64273-64322, respectively), whereas sequences in lower case letters corresponds to the 5' and 3' end of the mCherry-ORF45 fusion construct. Clone 3 carrying the ORF45 KO-*thyA* MHV68 BAC was electroporated with the above PCR product and bacteria having undergone recombination were selected for in the presence of thymine and trimethoprim. MHV68 BACs in which the *thyA* gene was replaced with mCherry-ORF45 were screened by PCR (using above primers) and restriction digest with BssHII and SalI. PCR and restriction digest analysis of clones 1-3 show that all have undergone the desired recombination in which the *thyA* gene was replaced with mCherry-ORF45 (Fig 4-11B). EcoRI digestion of the wildtype, ORF45 KO-*thyA* and mCherry-ORF45 KO MHV68 BACs also show the expected banding pattern. The band expected to shift in size is marked with an asterisk (Fig 4-11C).

Figure 4-10: Mutagenesis strategy for mCherry-ORF45 MHV68



(A) ORF45 in the MHV68 BAC is replaced with ORF45 fused to the C terminus of mCherry. (B) 1st and 2nd step of thyA-mediated BAC mutagenesis for the generation of mCherry-ORF45.

Figure 4-11: Generation of mCherry-ORF45 MHV68

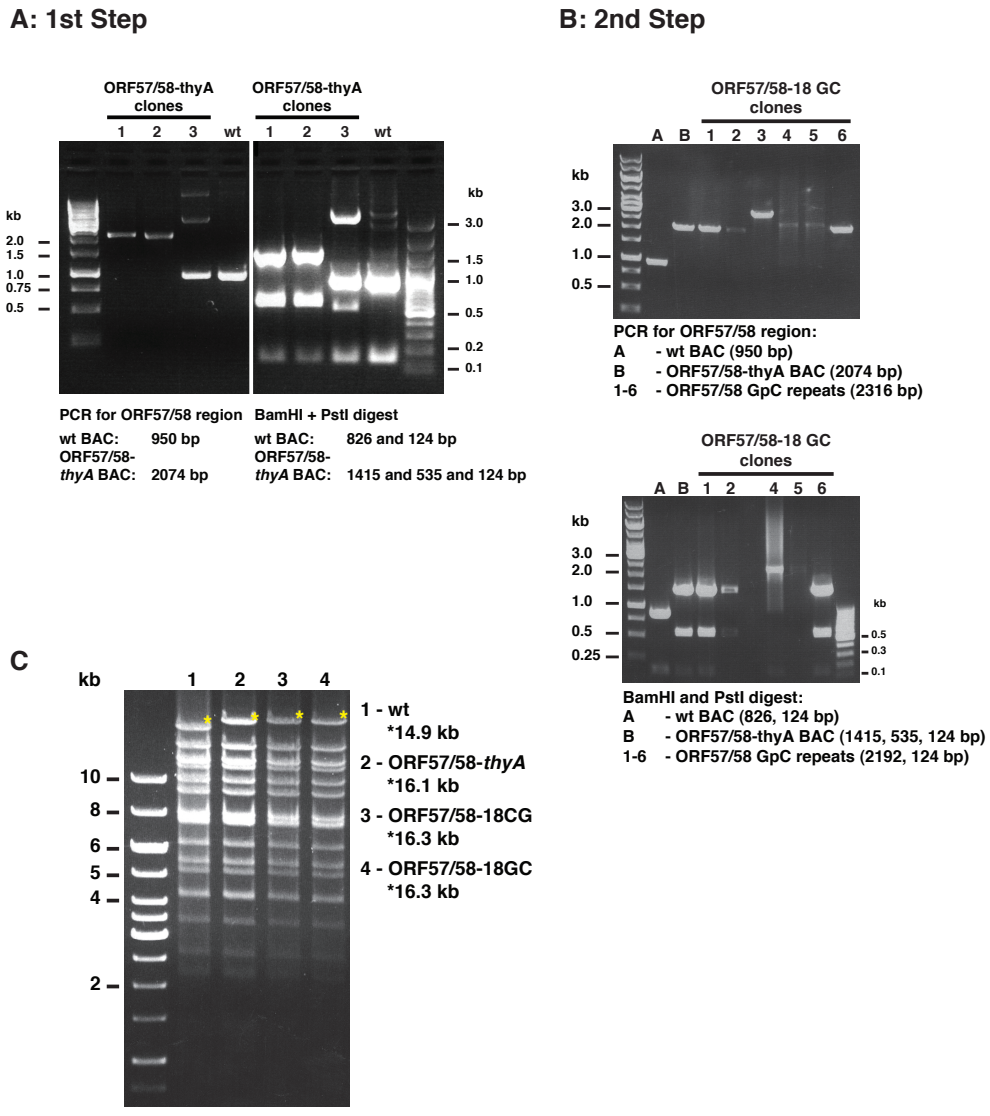


(A) ORF45 KO-*thyA* clones were screened by PCR and restriction digestion with MluI and SalI. (B) mCherry-ORF45 clones were screened by PCR and restriction digestion with BssHII and SalI. (C) EcoRI restriction digestion of wildtype, ORF45 KO-*thyA* and mCherry-ORF45 MHV68 BAC. Asterisks indicate bands that shift as a result of mCherry-ORF45 integration.

Generation of CpG MHV68 and GpC MHV68

To generate a CpG and GpC-enriched virus, a 1.4 kb sequence containing 54 highly stimulatory CpG or non-stimulatory GpC repeats was constructed and integrated in to the MfeI site between the polyadenylation signals of ORF57 and ORF58 (Fig 4-4). Generation of MHV68 GpC is documented in Figure 4-12, panels A and B below. For the first step of the mutagenesis process, a truncated version of the *E. coli thyA* gene (thyAΔ3') was PCR amplified with the following primers: Forward 5' caccgcaccaaggggtatttttgtgtgtgaataatcaataataaacacGCTGCTGCTGGAAGGTG TGGT 3' and Reverse 5' tgctgtaagcatgtaattaataaaagacaaaacagatatgcagttcaattGGGTAAAAAAACCGACG CACAC 3'. Sequences in upper case letters corresponds to the 5' and 3' end of the truncated *thyA* gene, whereas sequences in lower case letters corresponds to positions 77128-77177 and 77178-77227 in the MHV68 genome, respectively. QW1 bacteria (141) carrying the MHV68 BAC were electroporated with the above PCR product and bacteria having undergone recombination were selected for in the absence of thymine. MHV68 BACs in which the *thyA* gene was integrated between ORF57 and 58 (ORF57/58-*thyA*) were screened by PCR and restriction digest with BamHI and PstI. The MHV68 region of interest was amplified with the following primers: Forward 5' CTCTGCTGACACAGTGTAAG 3' (position 76982-77001 in the MHV68 genome) and Reverse 5' TTGCTTTCCACATGGGTTCC 3' (position 77912-77931 in the MHV68 genome). Figure 4-12A (left panel) shows that clones 1 and 2 produced the expected 2074 bp band, suggesting that the *thyA* was successfully integrated between ORF57 and 58. Similarly, both clones produced the expected banding pattern, when the PCR product was digested with BamHI and PstI (Fig 4-12A, right panel). For the 2nd step of the mutagenesis process, MHV68 region 77106-77565 encoding the 3' ends or ORF57 and ORF58 was cloned into pcDNA3.1(+) digested with BamHI and EcoRV. An XhoI restriction site was inserted into the MfeI site between ORF57 and ORF58 and the CpG or GpC repeats were cloned into this XhoI restriction site. The CpG or GpC repeats with the MHV68 flanking region were excised with BamHI and EcoRV and gel-purified. The restriction digest product was electroporated into QW1 bacteria carrying the ORF57/58-*thyA* MHV68 BAC (clone 1). Bacteria having undergone recombination to replace the *thyA* gene with either the CpG or GpC repeat were selected for in the presence of thymine and trimethoprim. Again, BACs from resulting colonies were screened for insertion of either repeat by PCR (using above primers) and BamHI and PstI restriction digest of the PCR product. For ORF57/58-GpC MHV68, 2 clones (4 and 5) with the correct insertion were obtained (Figure 4-12B). In addition, EcoRI digestion of the wildtype, ORF57/58-*thyA*, ORF57/58-CpG and ORF57/58-GpC MHV68 BACs also show the expected banding pattern. The band expected to shift in size is marked with an asterisk (Fig 4-12C).

Figure 4-12: Generation of CpG or GpC enriched MHV68



Generation of CpG and GpC enriched virus is shown with data from GpC-MHV68. (A) ORF57/58-*thyA* clones were screened by PCR and restriction digestion with BamHI and PstI. (B) ORF57/58-GpC clones were screened by PCR and restriction digestion with BamHI and PstI. (C) EcoRI restriction digestion of wildtype, ORF57/58-*thyA*, ORF57/58-CpG and ORF57/58-GpC MHV68 BAC. Asterisks indicate bands that shift as a result of CpG or GpC integration.

Wong et al. thyA-mediated BAC mutagenesis protocol

Outline:

1. Prepare QW1 for electroporation and prepare BAC fresh.
2. Transform BAC into QW1. Select by Chloramphenicol (resistance provided by BAC) in either LB plate (need 1 day to grow up) or better still in M9 minimal plate supp. with thymine and trimethoprim (need 2 days to grow up).
3. Perform PCR and enzyme digestion to check that BAC is okay and ensure no rearrangements occurred.
4. Prepare QW1-BAC for RED induction. Prepare ThyA fusion fragment for transforming into it (DpnI digested).
5. Transform ThyA fusion fragment into RED induced QW1-BAC. Select for correct recombination by M9-chloramphenical plate without thymine or trimethoprim. Bugs without ThyA fusion fragment would die in medium without thymine (need 2 days to grow up). Check efficiency with and without RED induction.
6. Check by PCR and RE digestion to ensure that the selected clone only contains BAC with ThyA fragment, in case the clone actually contains the pThyAFL plasmid, or more than one copy of BAC. If contamination of unwanted plasmid or BAC occurs, retransform into QW1. Could double check by growing bacteria on Amp plate. Correct recombinants would not grow up on Amp plate.
7. Grow up QW1-ThyA BAC for 2nd round of RED recombination. Prepare fragment harboring desired mutation for recombination.
8. Electroporate aforesaid fragment into RED induced QW1-ThyA BAC. Select using M9/CM/thymine/trimethoprim noble agar plate at a few different dilutions e.g. 1/10, 1/100, 1/1000. Sometimes when dilution is not high enough unrecombined clones could also grow causing background. Correct recombinants should now contain no functional ThyA fragment and thus can survive trimethoprim selection. Usually takes 2 days to grow up but may take up to 4 days for growth.
9. Pick colonies and grow in a small volume (~1ml) of M9/CM/TMP/T medium. Takes 2 – 4 days to grow up. If it does not show growth after 4 days, discard.
10. Check that recombination is okay by sequencing through the junctions. Perform RE digest to ensure no rearrangements are present.

Materials Needed:

Prepare the following stock solutions separately and sterilize accordingly:

Autoclave:
5x M9 solution:
240mM Na_2HPO_4
110mM KH_2PO_4
43mM NaCl
93.5mM NH_4Cl

0.1M $MgSO_4$
0.5M $CaCl_2$
LB Broth
500X MM1 (optional, is not absolutely necessary but grows better with it)
0.5mM each of $ZnSO_4$, $CuSO_4$, Na_2MoO_4, $CoCl_2$, $MnSo_4$, $CrCl_3$, $NiCl_2$

Filter sterilize:
60mM leucine (dissolve by addition of HCl)
60mM isoleucine (dissolve by addition of HCl)
60mM valine
20% Glucose
15μM Vitamin B1 (thiamine hydrochloride)
50mg/ml thymine (T) (dissolve in 0.5M NaOH solution, heat if necessary)
50mg/ml trimethoprim (TMP) (I made stock solution in DMF instead of water or DMSO) (is not too stable, keep stock at 4^{o}C for 1 month. May precipitate out at -20^{o}c)

To make 100ml modified M9 medium, mix together:

Autoclaved ddH_2O	73ml
0.5M $CaCl_2$	0.1ml
5x M9 salts	20ml
LB broth	1ml
0.1M $MgSO_4$	1ml
500x MM1	200μl
-- cool down --	
60mM leucine	1ml
60mM isoleucine	1ml
60mM valine	1ml
20% Glucose	2ml
15μM Vitamin B1	200μl

add selective agents if needed:

50mg/ml thymine	200μl
50mg/ml trimethoprim	20μl
34mg/ml chloramphenicol	36.76μl

Filter sterilize medium again if required

To make M9 plates, autoclave 2.5 – 3% noble agar with required amount of ddH_2O, then add the stock solutions following the above order. Note that noble agar is very, very soft and therefore is slightly easier to manipulate at 3%. Using a new spreader each time you spread the plates also helps to prevent damaging the delicate surface of the agar. If that happens, it would be rather difficult to spot the colonies. When spreading plates, first wet the spreader with the recovered culture on the plate. Then, try to hold the spreader with a slight lifting force, i.e. try not to let the weight of the spreader press down onto to agar. Spread by rotating the plate and hold the spreader steady. Stop once the culture is absorbed into the agar. Drawing the spreader across the dry agar surface will damage the surface.

Transforming BAC into QW1

Just follow standard electroporation procedure. Grow QW1 up in LB-thymine until OD600=0.5. Harvest cell, wash three times in ice-cold ddH_2O, resuspend in ice-cold ddH_2O, or 10% glycerol for long-term storage in -80^{o}c. Prepare BAC from 5ml culture, and electroporate fresh into competent QW1. Time constant of electroporation should be around 5. Select on LB-CM-T plate at 32^{o}c

Preparing ThyA fusion fragment

Design primers with 50-70bp flanking arms on each side. Perform PCR using pThyAFL or DY380 as template. If using DY380, spin down a small amount ~10ul culture, remove medium, resuspend in 10ul water, and boil at 95min for 10min. Use ~ 2ul as template. Digest away the plasmid template in the PCR using DpnI. It is important to remove plasmid template, or else it may cause false positive in the subsequent recombination step. Purify your ThyA fusion fragment. Perform gel purification if required. Try to resuspend in water or in buffer with low salt content. Measure absorbance to determine concentration.

Preparing for ThyA kick-in recombination

Follow standard RED-induced recombination procedures. Grow O/N pilot QW1-BAC at 32°c in M9-CM-TMP-T. Subculture 1ml into 50ml LB-CM-T, grow at 32°c until OD600=0.5 (3-6hrs). Induce 15ml culture in >=125ml flask (culture should be smaller than 1/6 of the flask volume) at 42°c, with shaking, for 10-15min. Immediately chill on ice slurry by shaking quickly with hand. From then on, keep cells on ice. When culture is completely chilled (~8min), spin down cell, 4°c (remember to pre-chill rotors and ALL containers for QW1). Wash once with 50ml ice-cold ddH_2O. Transfer to 1.5ml eppendorf and wash three more times with 1ml ice-cold ddH2O. Resuspend in 80μl ice-cold ddH_2O. Mix with 0.5 - 1μg ThyA fusion fragment. Electroporate in a chilled 0.1cm cuvette at 1.8kV. Resuspend cells immediately in 1ml M9 and recover, with gentle shaking / rotation (I stick the eppendorf on a rotating wheel in the incubator), at 32°c for 1.5 hours. Spin down culture, wash twice with ddH_2O and resuspend in ddH_2O. Spread onto M9-CM plate (no thymine!) and incubate at 32°c. Wrap with parafilm if plate begins to dry out.

Normally there would not be a background; but for instances when there is, respread the culture on the first plate to a second M9-CM plate.

For harder recombinations, try increasing the ThyA fusion fragment amount and also try to denature fragment at 95°c for 10min prior to electroporation.

Colonies on M9 plate would be rather small, it would be easier to observe for colonies with a backlight.

After having screened out the ThyA-BAC, do a pilot test to ensure that your bug would not grow on the M9-CM-TMP-T plates even after 4 days. If it does, then you would need to perform a TMP dilution test to determine the best concentration that would inhibit the growth of your ThyA-BAC.

Preparing for Second Round Mutation

Procedures would be exactly the same as the first round mutation with the exception that the O/N pilot should be grown in M9-CM. After electroporation, recover the cells in M9-CM-TMP-T. Using LB to recover will sometimes increase the background. For small plasmids, spread onto M9-CM-TMP-T plates in a few different dilutions, eg. 1/10, 1/100, and 1/1000. For BACs, just spread all the cells

onto a single plate. Save the remaining culture and store at 4°c. Those could be screened at a later stage if required. Use water instead of medium to dilute the cells. Wrap the plates with parafilm to prevent them from drying out, and incubate at 32°c for up to 4 days. Normally very tiny colonies would start to appear at 72 hrs but it varies. You would just have to observe for appearance of colonies with a backlight each day.

Culture colonies at 32°c in 1-1.5ml M9-CM-TMP-T. If the culture volume is too large, sometimes the colony would refuse to grow up. It would take around 2 days for the culture to grow.

Retransform the final mutated BAC into eg. DH10B for propagation or maintaining.

CHAPTER 5

Characterizing DNA Motifs that Interact with TLR9

Chapter 5:

Characterizing DNA Motifs that Interact with TLR9

Introduction

The innate immune system encodes several families of PRRs that distinguish self from non-self through the recognition of unique microbial and viral features. One such family is comprised of TLRs. A subset of TLRs is located on the cell surface and predominantly involved the detection of bacterial ligands such as LPS, flagellin or bacterial cell wall components (5). The subset of TLRs that recognize viral ligands is localized in the endosomal compartment. As viruses often lack unique biochemical products, endosomally located TLRs recognize distinctive features in their genomic material, which are rare or absent in host-derived DNA or RNA (6, 7). Of the nucleic acid-sensing TLRs only TLR9 has been implicated in the detection of DNA (39).

The TLR9 protein consists of an N-terminal portion containing 26 LRRs, followed by a transmembrane and a cytoplasmic TIR domain (65). To encounter its cognate ligand and induce a downstream signal transduction cascade TLR9 needs to be transported from the endoplasmic reticulum to an endolysosomal compartment in a process that requires the multi-pass transmembrane protein UNC-93B (66-69). Ligand binding occurs within the LRRs, may require endosomal acidification (71, 72), and is believed to induce a membrane-proximal conformational change (70, 73). Further required for subsequent activation is a proteolytic cleavage event within or distal to LRR 14, removing approximately half of the extracellular domain (68, 70).

In the mouse TLR9 is expressed in various cell types including macrophages, B cells, cDCs and pDCs, whereas in humans TLR9 is only expressed in B cells and pDCs (86). Generally, activation of TLR9 in macrophages and cDCs leads to the expression of proinflammatory cytokines. In addition, activation of TLR9 also leads to the expression of IFN-I. In cDCs IFNβ expression is mediated by the transcription factor IRF1 (94). However, robust expression of IFNα and is only observed in pDCs. This is in part mediated by the transcription factor IRF7, which is highly expressed in pDCs but not other cells types (95).

The ligands for TLR9 are CpG ODN, bacterial and viral DNA (65). Two subtypes of CpG ODN exist, B/K-type and A/D-type. The former have a phosphorothioate-linked backbone and induce DC maturation and B cell proliferation. In contrast, A/D-type CpG ODN carry the CpG motif within a phosphodiester-linked sequence, but are flanked with phosphorothioate-modified poly G stretches on either end. Stimulation with these ODN induces IFN-I in pDCs (75). TLR9 has previously been shown to play a role in the response

against several bacteria including Mycobacterium tuberculosis, Brucella, and Streptococcus pneumonia (76-78). Viral DNA may also contain unmethylated CpG motif and thus present a ligand for TLR9. Some viruses that previously been shown to be recognized by TLR9 are MCMV (43), HSV-1 (44) and HSV-2 (42), and adenovirus (41). However, that the ligands recognized in viral DNA are indeed CpG motifs remains to be shown. In addition, TLR9 has been reported to be activated by ODN containing nucleotide derivatives, the phosphorothioate backbone along with a bicyclic heterobase structure, or the DNA sugar backbone alone (80-83). In the latter case, addition of bases increased TLR9-mediated stimulation. A phosphorothioate backbone by itself inhibited TLR9 activation, but was converted to an agonist with the addition of CpG motifs (80). In addition to DNA, TLR9 has also been shown to recognize the malarial heme-detoxification byproduct, hemozoin (84, 85). Despite the wealth of research into TLR9 – ligand interactions, the nature of the DNA sequence motifs that are recognized by and stimulate or inhibit TLR9 in the context of a natural infection are still poorly understood.

Recently, a high-throughput microfluidic platform has been developed that measures binding interactions at equilibrium on the basis of mechanical trapping of molecular interactions (MITOMI) (147, 148). This approach has been successfully employed in the *de novo* discovery and quantitative biophysical characterization of DNA – transcription factor binding sites (147). Here, I show that TLR9 interaction with known stimulatory, inhibitory, and neutral ODN can be observed using microfluidic-based MITOMI. My experiments demonstrate that this platform may be useful in the identification of all DNA motifs within a 6-mer or 8-mer context that interact with TLR9. DNA motifs identified using this method will then be screened to determine the functional outcome of this binding.

Materials and Methods

Generation of TLR9 fusion constructs

Mouse and human TLR9 cDNA fragment corresponding to their extracellular domains were amplified by PCR and inserted into the Xho I cloning site of a modified pcDNA3.1(+) expression vector that contained a mouse CD150 leader segment at the N terminus (MDPKGSLSWRILLFLSLAFELSYG) and the Fc segment of human IgG1 (aa 243-273) fused to eGFP at the C terminus.

TLR9 – CpG ODN in vitro binding assay

293T cells were transfected with HA-tagged TLR9, TLR9 or TLR7 fusion constructs using calcium phosphate. Cells were lysed 48 hours post transfection in either TNT (20 mM Tris pH 8.0, 200 mM NaCl, 1% Triton X-100), MES (50 mM MES, 150 mM NaCl, 1mM MgCl2, 1% Triton X-100), or MNT (50 mM MES pH 6.0, 200 mM NaCl, 1 mM EDTA pH 8.0, 1% Triton X-100) lysis buffer supplemented with Complete protease inhibitor cocktail (Roche Cat # 04693159001), cleared of insoluble debris, incubated with biotinylated phosphorothioate (0.4 μM) or phosphodiester-linked (0.4 or 4 μM) CpG ODN (5' TCCATGACGTTCCTGACGTT 3') and streptavidin agarose at 4ºC for 1 hour each. ODN – TLR9 complexes were boiled in SDS buffer, separated by SDS-PAGE, and probed by immunoblotting.

TLR9 Reporter Assay

HEK293 cells stably expressing TLR9N4C and an NF-κB responsive luciferase reporter construct were plated into 96-well plates at 4×10^4 cells per well. Cells were incubated with the indicated phosphodiester-linked CpG ODN (see Table 3 for a complete list) at the indicated concentrations for 12 hours. Cells were lysed in 1x Passive Lysis Buffer (Promega) and luciferase activity measured using an LMAX II^{384} luminometer (Molecular Devices).

Microfluidic device fabrication and experimental procedure

Devices were constructed as previously described (147, 148). Briefly, flow and control molds were fabricated on 4″ silicon wafers and devices were fabricated in polydimethylsiloxane (PDMS). MITOMI to identify nucleotide sequences that bind TLR9 was performed as follows. ODN are based on existing sequences (Table 3) preceded by a 5nt spacer (CTGAC), followed by a 3 nt spacer (CCC) and a 14 nt sequence (TCCGGCGGTATGAC) complimentary to a Cy5-labelled oligo (AGGCCGCCATACTG-Cy5). ODN and Cy5-labelled oligo are hybridized and the resulting Cy5-labelled ODN noncovalently spotted on a DNA microarray that is subsequently overlaid with PDMS creating a 3-dimensional space. Neck valves are closed to protect the DNA chamber and the protein chamber is derivatized with anti-GFP antibody below the button valve and passivated elsewhere. Introduction of lysates containing a mouse TLR9 fusion protein solubilized spotted ODN, allowing both to interact. TLR9 – ODN

complexes are captured on the surface beneath the button valve. Rapid closure of the button valve traps complexes, and slides are imaged following a final wash to remove unbound material.

Results

Optimizing TLR9 – CpG ODN binding in vitro

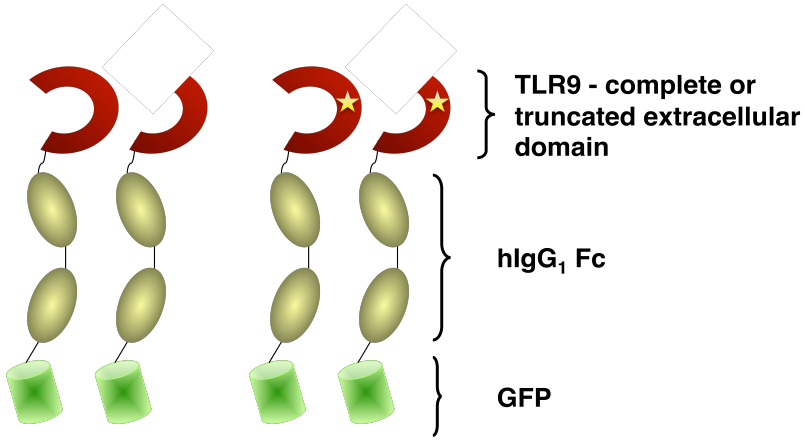
The extracellular LRR domain of TLR9 mediates substrate binding, while the intracellular TIR-containing domain is important for initiating the downstream signal transduction cascade (65). To demonstrate that TLR9 binds unmethylated CpG motifs in single stranded DNA, a previous study utilized a TLR9 fusion construct, in which the extracellular domain of TLR9 was fused to the Fc region of human IgG1 (149). I decided to construct similar TLR9 fusion proteins to be used in a microfluidic-based approach aiming to identify all 6-mer and 8-mer DNA motifs that bind to TLR9. Figure 5-1 shows a schematic of these fusion proteins. Similar to Rutz *et al.*, the extracellular domain of TLR9 was fused to the Fc region of human IgG1 (149). GFP was attached to the C terminus of this construct, as high affinity antibodies are available that would facilitate efficient trapping of the TLR9 fusion proteins to the anti-GFP-derivatized surface of the microfluidic device. Recent advances in our understanding of TLR9 biology have shown that only N-terminally cleaved TLR9 is present in the endolysosomal compartment where receptor – ligand interaction occurs and that only cleaved TLR9 interacts with its downstream adapter MyD88 (70). While ligand binding is thought to be confined to the portion of the extracellular domain of TLR9 that is unaffected by the cleavage event, it is still formally possible, that the N-terminal extension in the uncleaved construct affects binding characteristics. Therefore, TLR9 fusion constructs with a truncated extracellular domain that mimic this cleavage event were constructed also. Furthermore, Rutz *et al.* have shown, that amino acids D535 and Y537 are crucial for CpG-sequence-specific binding to TLR9 and that D535A Y537A double mutants cannot be activated in HEK293 cells (149). Fusion constructs encompassing the full-length or truncated TLR9 extracellular domain carrying these mutations will be used as negative controls in our microfluidic binding studies.

In order to determine optimal binding conditions for TLR9 – CpG ODN interaction *in vitro*, I incubated cell lysates from TLR9-expressing cells with biotinylated CpG ODN containing a phosphorothioate backbone and then precipitated CpG-ODN associated proteins using streptavidin beads. When TLR9 – CpG ODN complexes were precipitated under alkaline (pH 8.0) conditions, specific binding to TLR9 was relatively weak (Fig 5-2). As TLR9 encounters its cognate ligand in the slightly acidic environment of an endolysosomal compartment, I wanted to test whether *in vitro* binding could be improved at a lower pH. Low pH conditions have successfully been used previously to measure TLR9 – ODN interactions in Surface Plasmon Resonance-based experiments (149). TLR9-expressing cells were lysed in TNT, MES, or MNT buffer, which differ either in composition and/or pH. Strikingly, binding of TLR9 to phosphorothioate-modified CpG improved dramatically at pH 6.0 compared to pH 8.0 (Fig 5-3).

Having optimized the *in vitro* binding conditions, I next wanted to test binding of TLR9 to CpG ODN with a phosphodiester backbone. Despite the much-improved binding to a phosphorothioate-modified ligand, binding to CpG ODN with a phosphodiester backbone was still significantly lower (Fig 5-4). One reason for this difference in binding could be the DNase sensitivity of the phosphodiester backbone of natural DNA. In contrast, the phosphorothioate backbone is largely DNase resistant. Another possibility derives from the recent observation that TLR9 undergoes an N-terminal cleavage event in the endolysosomal compartment (68, 70). When comparing CpG ODN binding of both full-length and cleaved TLR9, more ligand was found binding to the latter (70). In addition, the downstream adapter MyD88 is only recruited to the processed form of TLR9 (70). To address whether cleavage may improve binding to CpG ODN with a phosphodiester backbone, I used a RAW264 macrophage cell line stably expressing HA-tagged TLR9. Unlike 293T cells, RAW264 cells express the ER transmembrane protein UNC-93B, which is required for trafficking and cleavage of TLR9 (69). I found that TLR9 was still more efficiently precipitated with biotinylated CpG ODN containing a phosphorothioate compared to a phosphodiester backbone (Fig 5-5). Similarly, mouse and TLR9 fusion proteins containing the full-length extracellular domain were also precipitated more efficiently with phosphorothioate-modified CpG ODN (Fig 5-6).

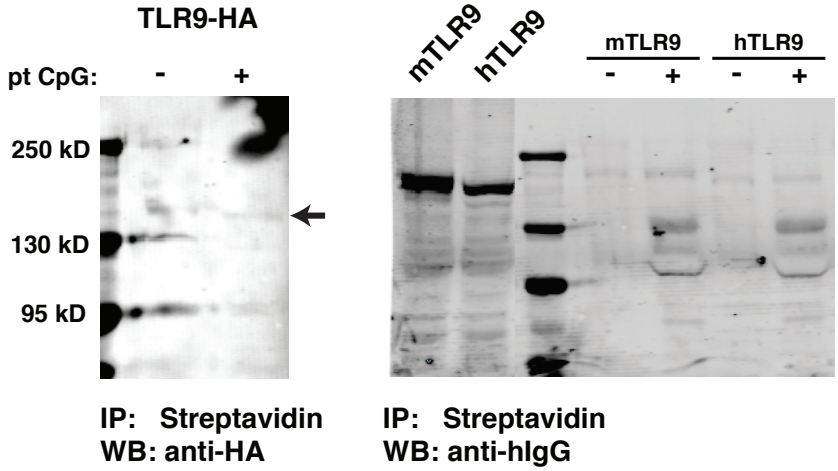
Altogether, these experiments showed that binding of TLR9 – ligand binding *in vitro* is dramatically improved at pH 6.0. However, binding of TLR9 to CpG ODN containing a phosphodiester backbone was always weaker compared to phosphorothioate-backboned CpG ODN. These differences may be due to the DNase sensitivity of natural phosphodiester DNA.

Figure 5-1: TLR9 fusion constructs



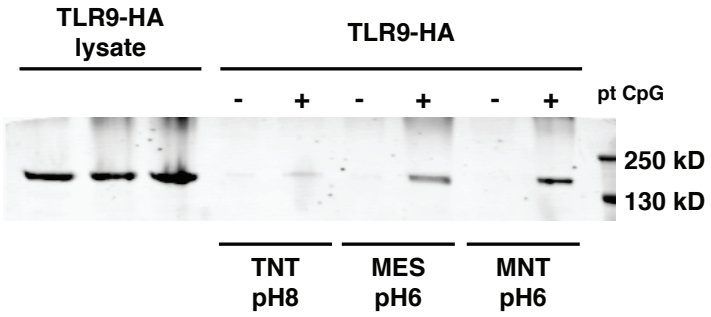
The full-length or truncated extracellular domain of mouse or human TLR9 was fused to the Fc region of human IgG1 (aa 243 – 473) and GFP. The full-length human and mouse TLR9 ectodomain encompass amino acids 26 – 809 and 26 – 810, while the truncated ectodomains include amino acids 471 – 809 and 471 – 810, respectively. The TLR9 ectodomain is preceded by the SLAM signal peptide (MDPKGSLSWRILLFLSLAFELSYG). As a negative control, amino acids D535 and Y537 were mutated to alanine to reduce the TLR9 – DNA binding interaction (yellow star).

Figure 5-2: TLR9 – phosphorothioate CpG binding at pH 8



293T cells were transfected with HA-tagged human TLR9, the mouse or human TLR9 constructs (full-length extracellular domain only) described in Figure 5-1. Cell lysates were incubated with 400 nM biotinylated phosphorothioate (pt) CpG ODN, ODN-bound TLR9 complexes precipitated with Streptavidin beads and analyzed by immunoblotting.

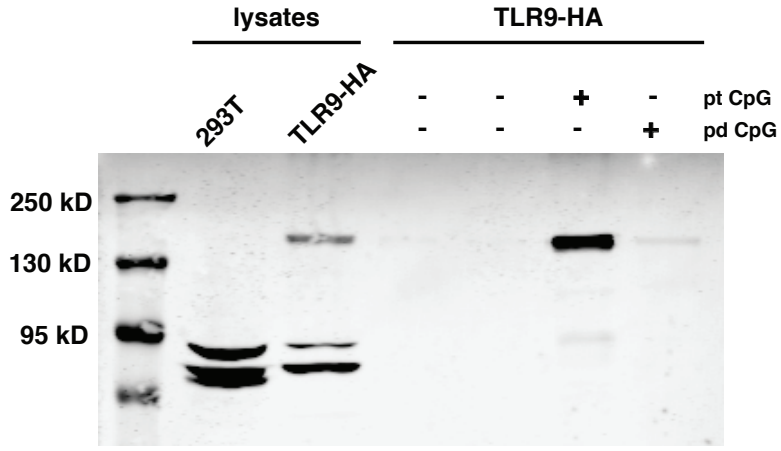
Figure 5-3: TLR9 – phosphorothioate CpG binding *in vitro* is optimal at pH 6



IP: Streptavidin
WB: anti-HA

293T cells transfected with HA-tagged human TLR9 were lysed and incubated with 400 nM biotinylated phosphorothioate (pt) CpG ODN in different pH or buffer conditions. ODN-bound TLR9 complexes were precipitated with Streptavidin beads and analyzed by immunoblotting.

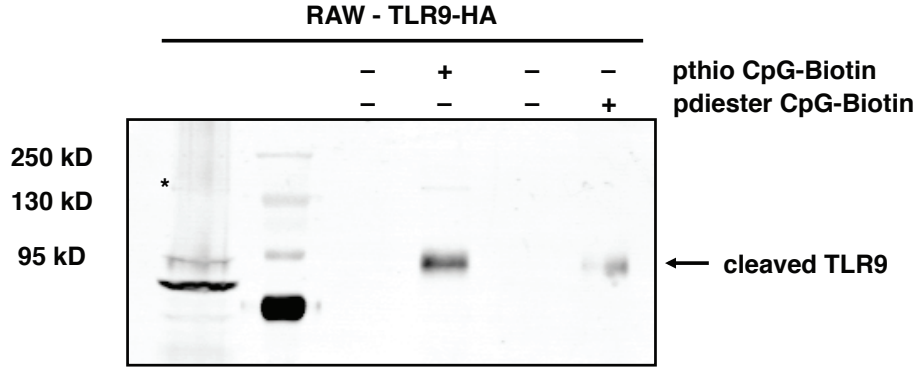
Figure 5-4: Binding of full length TLR9 to CpG ODN with phosphorothioate or phosphodiester-linked backbones



IP: Streptavidin
WB: anti-HA

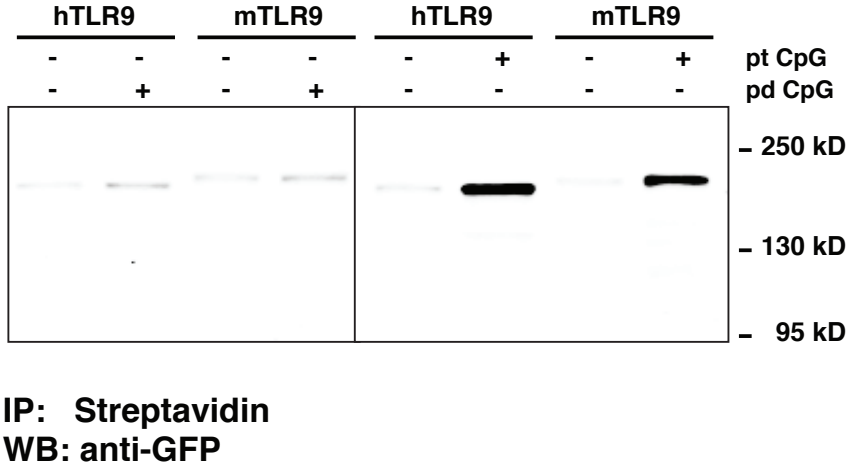
293T cells transfected with HA-tagged human TLR9 were lysed and incubated with 400 nM biotinylated phosphorothioate (pt) or phosphodiester (pd) CpG ODN at pH 6. ODN-bound TLR9 complexes were precipitated with Streptavidin beads and analyzed by immunoblotting.

Figure 5-5: Binding of cleaved TLR9 to CpG ODN with phosphorothioate or phosphodiester-linked backbones



RAW cells stably transfected with HA-tagged TLR9 were lysed and incubated with 400 nM biotinylated phosphorothioate (pthio) or 4 μM phosphodiester (pdiester) CpG ODN at pH 6. ODN-bound TLR9 complexes were precipitated with Streptavidin beads and analyzed by immunoblotting.

Figure 5-6: Binding of full length extracellular domain TLR9 fusion constructs to CpG ODN with phosphorothioate or phosphodiester-linked backbones



293T cells were transfected with the mouse or human full-length extracellular domain TLR9 constructs described in Figure 5-1. Cell lysates were incubated with 400 nM phosphorothioate (pt) or 4 μM phosphodiester (pd) biotinylated CpG ODN. ODN-bound TLR9 complexes were precipitated with Streptavidin beads and analyzed by immunoblotting.

Microfluidic set up to determine all DNA motifs recognized by TLR9

To test whether TLR9 – CpG ODN binding could be observed using MITOMI, I selected ODN that had previously been described to bind TLR9 or not (Table 3). ODN that have low or no affinity for TLR9 are designated neutral. ODN that bind TLR9 are either stimulatory or inhibitory with regard to their effect on TLR9 activation.

Table 3: Names and sequences of stimulatory, inhibitory, and neutral ODN

Stimulatory ODN	
1668-CpG	TCCATGCGTTCCTGATGCT
1826	TCCATGACGTTCCTGACGTT
2084	TCCTGACGTTGAAGT
03	TCCGCAACGTTTTTGATGCT
07	TCCCTGACGTTGGTGATGCT

Inhibitory ODN	
2340	TCCTGAAGGGGAAGT
2088	TCCTGGCGGGGAAGT
2114	TCCTGGAGGGGAAGT
G-ODN	CTCCTATTGGGGGTTTCCTAT

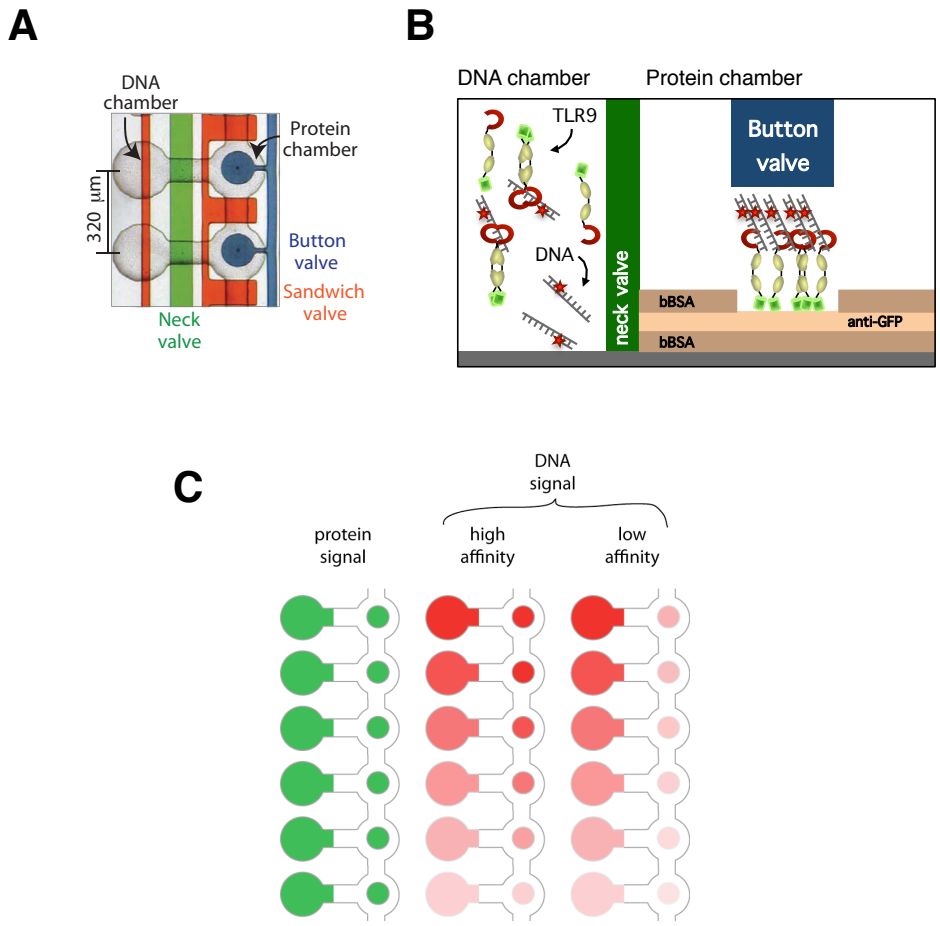
Neutral ODN	
1668 GpC	TCCATGGCTTCCTGATGCT
random-1	AGGATTCCAAGATGGAATAG
All-A	AAAAAAAAAAAAAAAAAAA
1585 GpC	GGGGTCAAGCTTGAGGGGGG
1826 GpC	TCCATGAGCTTCCTGAGCTT
2310	TCCTGCAGGTTAAGT

The selected ODN were labeled with Cy5 and spotted onto DNA microarray slides, which were subsequently overlaid with PDMS creating a 3-dimensional space of DNA and protein chambers. Figure 5-7A shows two such unit cells. Neck valves separate DNA and protein chambers. Sandwich valves isolate unit cells, and depression of the button valves protects DNA – protein interactions. Following alignment of the PDMS mold to DNA slides, protein chambers were derivatized with anti-GFP antibody beneath the button valve and passivated elsewhere. Next, introduction of cellular lysates containing TLR9 fusion proteins solubilized spotted ODN, allowing TLR9 – ODN interactions to occur. Button valves were depressed rapidly to capture interactions at equilibrium concentrations and devices washed to remove unbound material before imaging (Fig 5-7B). Figure 5-7C shows a schematic of a scanned after TLR9 binding to different concentrations of Cy5-labelled ODN contrasting high vs. low affinity

binding. As TLR9 fusion proteins are bound to the surface of the protein chamber regardless of ODN binding, the fluorescent protein signal is constant. The fluorescent intensity of a Cy5-labeled ODN that strongly binds TLR9 should increase as the ODN concentration increases. Conversely, the fluorescent intensity of an ODN with low affinity will be low regardless of ODN concentration. The results of one such experiment are presented in Figure 5-8 with the ratio of fluorescence intensities (DNA fluorescence/protein fluorescence, which is linearly related to fractional occupancy) as a function of DNA chamber intensity (which is linearly related to soluble DNA concentration). Stimulatory ODN presented in red show strong binding behavior to the mouse TLR9 fusion protein. TLR9 – ODN interactions were also strong for three (2340, 2088, 2114) out of the four inhibitory ODN tested. Neutral ODN showed weak binding. Interestingly, two of the neutral ODN (1668-GpC, 1585-GpC), which differ from their stimulatory counterparts only in that the CpG motif was inverted to a GpC motif, showed low but appreciable binding.

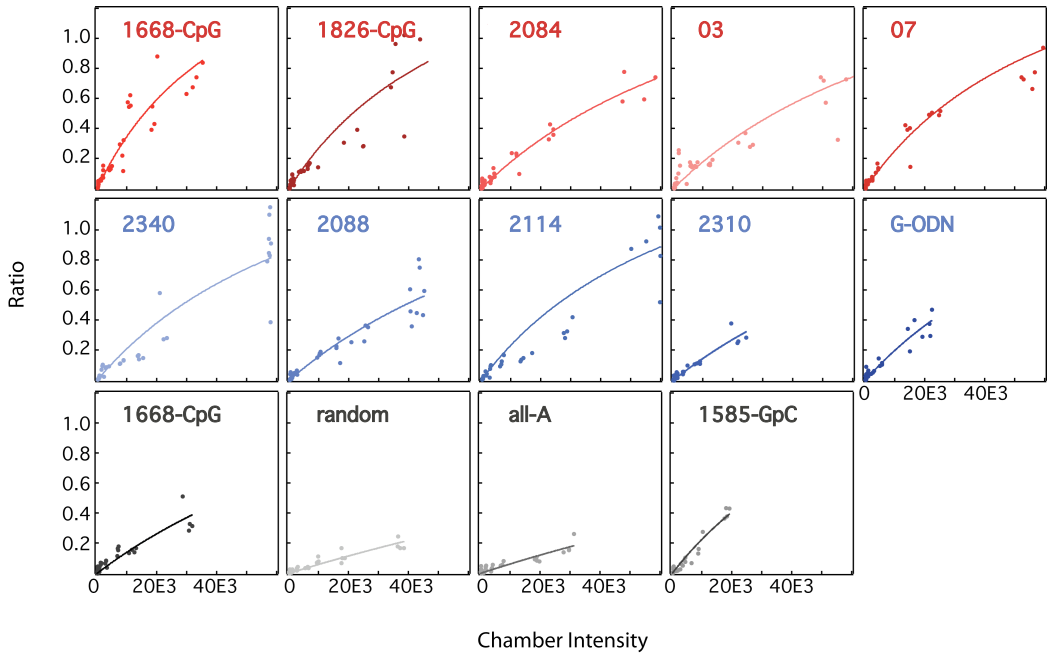
Next, I wanted to analyze how binding behavior measured by MITOMI correlated with TLR9 stimulation. To this end, I stimulated TLR9 reporter cells with increasing concentrations of the ODN presented in Table 3. Despite moderate differences in binding behavior, activation of TLR9 by all stimulatory ODN was very similar (Fig 5-9A). As expected, stimulation with neutral and inhibitory ODN did not lead to TLR9 activation (Fig 5-9B, C). To determine how binding of inhibitory ODN translated into inhibition of TLR9 signaling, TLR9 reporter cells were incubated with increasing concentrations of inhibitory ODN in the presence of 1 or 2 μM stimulatory ODN 03 (Fig 5-10). The inhibitory ODN that had the lowest affinity in our microfluidic analysis also showed no appreciable inhibition (G-ODN). Of the three inhibitory ODN that showed the strongest binding to mouse TLR9, 2114 most strongly inhibited TLR9 activation, followed by 2088. ODN 2340 only showed very modest inhibition of TLR9 signaling. Together, our data show that MITOMI can be used to study sequence-specific binding of ODN to our TLR9 fusion proteins. In addition, I was able to correlate strength of ODN binding to TLR9 with TLR9 activation or inhibition.

Figure 5-7: Microfluidic set up



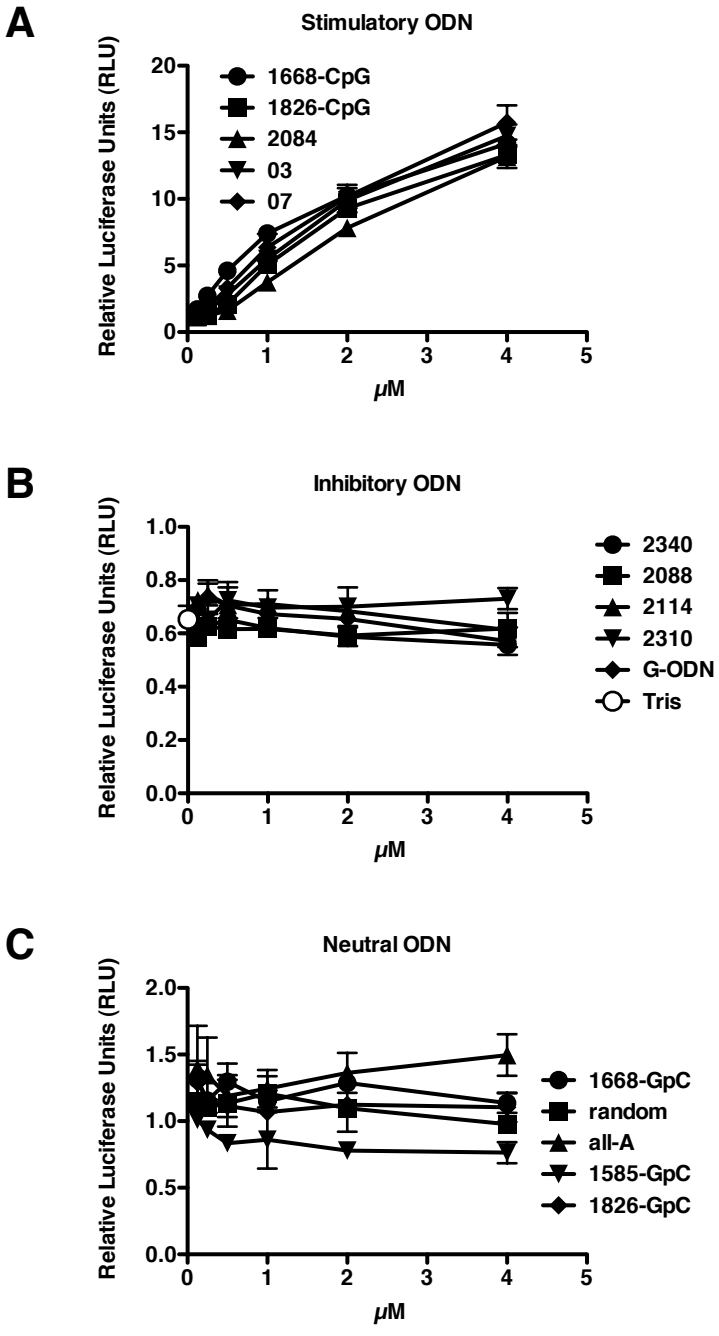
(A) Microfluidic device: Cy5-labelled ODN are spotted on a microarray that is subsequently overlaid with PDMS creating a 3-dimensional space. Unit cells contain a 'DNA chamber' and a 'protein' chamber controlled by three valves: a 'neck' valve (green) separates the two chambers; a 'sandwich' valve (orange) isolates unit cells; and a 'button' valve (blue) protects molecular interactions. (B) ODN are noncovalently spotted onto a microarray. Introduction of lysates containing TLR9 fusion protein solubilized spotted ODN, allowing both to interact. TLR9 – ODN complexes are captured on the surface beneath the button valve. Rapid closure of the button valve traps complexes, and slides are imaged following a final wash to remove unbound material. (C) Schematic of a scanned image of microfluidic device after TLR9 binding to different concentrations of Cy5-labelled ODN contrasting high vs. low affinity binding.

Figure 5-8: TLR9 binding to stimulatory, inhibitory, and neutral ODN



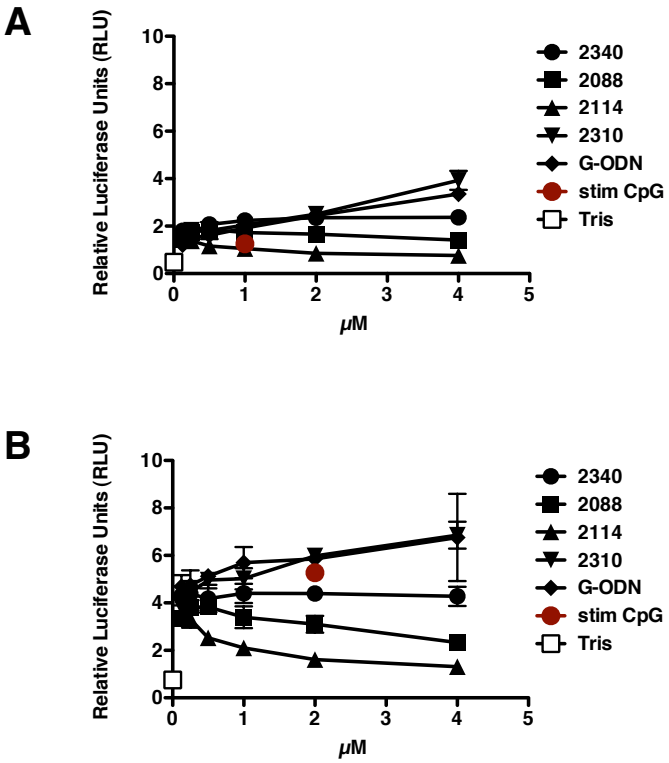
Increasing concentrations of Cy5-labelled stimulatory, inhibitory, or neutral ODN (see Table 3) were spotted onto a DNA microarray and overlaid with PDMS. Lysates containing mouse TLR9 fusion protein were introduced into the microfluidic device. TLR9 – ODN interactions were visualized by scanning the device. Ratio of fluorescence intensities (DNA fluorescence/protein fluorescence, which is linearly related to fractional occupancy) plotted on the y-axis; DNA chamber intensity (which is linearly related to soluble DNA concentration) is shown on the x-axis. Binding curves on each graph are global fits to a single-site binding model (ratio = (A*[D])/([D]+Kd)).

Figure 5-9: Stimulation of TLR9N4C with stimulatory, inhibitory, or neutral ODN



TLR9N4C-HEK293 cells were incubated with stimulatory, inhibitory, or neutral ODN at the indicated concentrations. Luciferase activity was measured 12 hours later.

Figure 5-10: Inhibition of TLR9N4C stimulation by inhibitory ODN



TLR9N4C-HEK293 cells were incubated with 1 (A) or 2 (B) μM of stimulatory, ODN 03 and inhibitory ODN at the indicated concentrations. Luciferase activity was measured 12 hours later.

Discussion

TLR9 interacts with CpG-motif containing ODN, bacterial and viral DNA, yet the precise sequence motifs recognized by TLR9 in the context of a natural infection remain poorly understood. Here, I show that optimal TLR9 – CpG ODN binding *in vitro* occurs at slightly acidic pH. These conditions can be applied in a microfluidic-based approach to measure TLR9 binding to a select number of stimulatory, inhibitory, and neutral ODN. This proof-of-principle experiment suggests that this method can be expanded to identify all DNA motifs within a 6-mer and 8-mer context that interact with TLR9. TLR9 reporter cells can then be incubated with such identified ODN to determine the function outcome of any binding observed.

Previous studies have shown that CpG DNA-mediated activation of leukocytes required endosomal acidification, as activation was blocked upon treatment with chloroquine or bafilomycin A (71, 72). Furthermore, Rutz *et al*. were able to show that TLR9 – CpG ODN binding was markedly improved at pH 6.5 and 5.5. Not surprisingly, precipitation of CpG ODN-associated TLR9 was significantly enhanced at pH 6.0 as well (Fig 5-3). Interestingly, binding of phosphorothioate-modified CpG ODN was always much stronger compared with ODN containing the natural phosphodiester backbone. The differences in TLR9 binding between phosphorothioate-modified and phosphodiester-modified CpG ODN remain unexplained. However, the phosphorothioate backbone is DNA resistant and as precipitations with biotinylated CpG were performed in cell lysates it is likely that phosphodiester-modified ODN were subject to degradation by endogenous DNases.

In order to test whether microfluidic-based MITOMI could be used to measure TLR9 – CpG ODN binding, positive and negative controls comprising stimulatory, inhibitory, and neutral ODN based on commercially available and previously published sequence data were selected. Initial results obtained for murine TLR9 showed that all stimulatory ODN showed strong binding behavior. This was consistent with results obtained in a TLR9 reporter assay, in which strong activation was observed with all stimulatory ODN. Only three out of the four inhibitory ODN tested showed strong binding behavior. Interestingly, those ODN were also able to inhibit CpG ODN-mediated activation of TLR9, albeit to different degrees. G-ODN for which weak binding was observed, did not inhibit CpG ODN-mediated TLR9 activation. This is contrast with a previously published report, which showed that G-ODN was able to inhibit CpG ODN induced cytokine secretion in RAW macrophages (150). The reason for this discrepancy is currently unknown. All five neutral ODN that were tested showed low TLR9 binding. ODN 1668-GpC and ODN 1585-GpC show slightly stronger TLR9 binding compared to the random or all-A ODN. Both former ODN are negative controls of their respective stimulatory ODN with the CpG motive inverted to non-stimulatory GpC motif. These observations suggest that the context surrounding the CpG is important in mediating some binding interactions, but that the

presence of the CpG dramatically enhances the TLR9 – ODN interaction. As the CpG is inverted to a non-stimulatory GpC, binding and consequently stimulation are significantly reduced.

Taken together, these initial studies using MITOMI to measure TLR9 – CpG ODN binding are encouraging and demonstrate that it is feasible to identify all 6-mer or 8-mer DNA motifs that interact with TLR9 using this technique.

REFERENCES

1. O'Neill, L. A., and A. G. Bowie. 2010. Sensing and signaling in antiviral innate immunity. Curr Biol 20:R328-333.
2. Carpenter, S., and L. A. J. O'Neill. 2007. How important are Toll-like receptors for antimicrobial responses? Cellular Microbiology 9:1891.
3. Schnare, M., G. Barton, A. Holt, K. Takeda, S. Akira, and R. Medzhitov. 2001. Toll-like receptors control activation of adaptive immune responses. Nat Immunol 2:947.
4. Pasare, C., and R. Medzhitov. 2004. Toll-like receptors: linking innate and adaptive immunity. Forum in Immunology: Toll-like receptors 6:1382.
5. Takeda, K., and S. Akira. 2005. Toll-like receptors in innate immunity. International Immunology 17:1.
6. Kawai, T., and S. Akira. 2006. Innate immune recognition of viral infection. Nature Immunology 7:131.
7. Barton, G. 2007. Viral recognition by Toll-like receptors. TLR-mediated Innate Immune Recognition 19:33.
8. Koyama, S., K. J. Ishii, C. Coban, and S. Akira. 2008. Innate immune response to viral infection. Cytokine 43:336-341.
9. Takaoka, A., Z. Wang, M. Choi, H. Yanai, H. Negishi, T. Ban, Y. Lu, M. Miyagishi, T. Kodama, K. Honda, Y. Ohba, and T. Taniguchi. 2007. DAI (DLM-1/ZBP1) is a cytosolic DNA sensor and an activator of innate immune response. Nature.
10. Wang, Z., M. Choi, T. Ban, H. Yanai, H. Negishi, Y. Lu, T. Tamura, A. Takaoka, K. Nishikura, and T. Taniguchi. 2008. Regulation of innate immune responses by DAI (DLM-1/ZBP1) and other DNA-sensing molecules. Proceedings of the National Academy of Sciences of the United States of America 105:5477.
11. Hornung, V., A. Ablasser, M. Charrel-Dennis, F. Bauernfeind, G. Horvath, D. R. Caffrey, E. Latz, and K. A. Fitzgerald. 2009. AIM2 recognizes cytosolic dsDNA and forms a caspase-1-activating inflammasome with ASC. Nature 458:514-518.
12. Ablasser, A., F. Bauernfeind, G. Hartmann, E. Latz, K. A. Fitzgerald, and V. Hornung. 2009. RIG-I-dependent sensing of poly(dA:dT) through the induction of an RNA polymerase III-transcribed RNA intermediate. Nat Immunol 10:1065-1072.
13. Chiu, Y. H., J. B. Macmillan, and Z. J. Chen. 2009. RNA polymerase III detects cytosolic DNA and induces type I interferons through the RIG-I pathway. Cell 138:576-591.

14. Kato, H., S. Sato, M. Yoneyama, M. Yamamoto, S. Uematsu, K. Matsui, T. Tsujimura, K. Takeda, T. Fujita, O. Takeuchi, and S. Akira. 2005. Cell type-specific involvement of RIG-I in antiviral response. Immunity 23:19-28.
15. Stetson, D. B., and R. Medzhitov. 2006. Type I interferons in host defense. Immunity 25:373.
16. Yokota, S., T. Okabayashi, and N. Fujii. 2010. The battle between virus and host: modulation of Toll-like receptor signaling pathways by virus infection. Mediators Inflamm 2010:184328.
17. Yoneyama, M., M. Kikuchi, T. Natsukawa, N. Shinobu, T. Imaizumi, M. Miyagishi, K. Taira, S. Akira, and T. Fujita. 2004. The RNA helicase RIG-I has an essential function in double-stranded RNA-induced innate antiviral responses. Nat Immunol 5:730-737.
18. Kawai, T., K. Takahashi, S. Sato, C. Coban, H. Kumar, H. Kato, K. J. Ishii, O. Takeuchi, and S. Akira. 2005. IPS-1, an adaptor triggering RIG-I- and Mda5-mediated type I interferon induction. Nat Immunol 6:981-988.
19. Meylan, E., J. Curran, K. Hofmann, D. Moradpour, M. Binder, R. Bartenschlager, and J. Tschopp. 2005. Cardif is an adaptor protein in the RIG-I antiviral pathway and is targeted by hepatitis C virus. Nature 437:1167-1172.
20. Seth, R. B., L. Sun, C. K. Ea, and Z. J. Chen. 2005. Identification and characterization of MAVS, a mitochondrial antiviral signaling protein that activates NF-kappaB and IRF 3. Cell 122:669-682.
21. Xu, L. G., Y. Y. Wang, K. J. Han, L. Y. Li, Z. Zhai, and H. B. Shu. 2005. VISA is an adapter protein required for virus-triggered IFN-beta signaling. Mol Cell 19:727-740.
22. Hemmi, H., O. Takeuchi, S. Sato, M. Yamamoto, T. Kaisho, H. Sanjo, T. Kawai, K. Hoshino, K. Takeda, and S. Akira. 2004. The roles of two IkappaB kinase-related kinases in lipopolysaccharide and double stranded RNA signaling and viral infection. J Exp Med 199:1641-1650.
23. Satoh, T., H. Kato, Y. Kumagai, M. Yoneyama, S. Sato, K. Matsushita, T. Tsujimura, T. Fujita, S. Akira, and O. Takeuchi. 2010. LGP2 is a positive regulator of RIG-I- and MDA5-mediated antiviral responses. Proc Natl Acad Sci U S A 107:1512-1517.
24. Schlee, M., A. Roth, V. Hornung, C. A. Hagmann, V. Wimmenauer, W. Barchet, C. Coch, M. Janke, A. Mihailovic, G. Wardle, S. Juranek, H. Kato, T. Kawai, H. Poeck, K. A. Fitzgerald, O. Takeuchi, S. Akira, T. Tuschl, E. Latz, J. Ludwig, and G. Hartmann. 2009. Recognition of 5' triphosphate by RIG-I helicase requires short blunt double-stranded RNA as contained in panhandle of negative-strand virus. Immunity 31:25-34.
25. Kato, H., O. Takeuchi, S. Sato, M. Yoneyama, M. Yamamoto, K. Matsui, S. Uematsu, A. Jung, T. Kawai, K. J. Ishii, O. Yamaguchi, K. Otsu, T. Tsujimura, C. S. Koh, C. Reis e Sousa, Y. Matsuura, T. Fujita, and S. Akira. 2006. Differential roles of MDA5 and RIG-I helicases in the recognition of RNA viruses. Nature 441:101-105.

26. Pichlmair, A., O. Schulz, C. P. Tan, J. Rehwinkel, H. Kato, O. Takeuchi, S. Akira, M. Way, G. Schiavo, and C. Reis e Sousa. 2009. Activation of MDA5 requires higher-order RNA structures generated during virus infection. J Virol 83:10761-10769.
27. O'Riordan, M., C. H. Yi, R. Gonzales, K. D. Lee, and D. A. Portnoy. 2002. Innate recognition of bacteria by a macrophage cytosolic surveillance pathway. Proc Natl Acad Sci U S A 99:13861-13866.
28. Ishii, K. J., C. Coban, H. Kato, K. Takahashi, Y. Torii, F. Takeshita, H. Ludwig, G. Sutter, K. Suzuki, H. Hemmi, S. Sato, M. Yamamoto, S. Uematsu, T. Kawai, O. Takeuchi, and S. Akira. 2006. A Toll-like receptor-independent antiviral response induced by double-stranded B-form DNA. Nat Immunol 7:40-48.
29. Stetson, D. B., and R. Medzhitov. 2006. Recognition of cytosolic DNA activates an IRF3-dependent innate immune response. Immunity 24:93-103.
30. DeFilippis, V. R., D. Alvarado, T. Sali, S. Rothenburg, and K. Fruh. 2010. Human cytomegalovirus induces the interferon response via the DNA sensor ZBP1. J Virol 84:585-598.
31. Ishii, K. J., T. Kawagoe, S. Koyama, K. Matsui, H. Kumar, T. Kawai, S. Uematsu, O. Takeuchi, F. Takeshita, C. Coban, and S. Akira. 2008. TANK-binding kinase-1 delineates innate and adaptive immune responses to DNA vaccines. Nature 451:725-729.
32. Burckstummer, T., C. Baumann, S. Bluml, E. Dixit, G. Durnberger, H. Jahn, M. Planyavsky, M. Bilban, J. Colinge, K. L. Bennett, and G. Superti-Furga. 2009. An orthogonal proteomic-genomic screen identifies AIM2 as a cytoplasmic DNA sensor for the inflammasome. Nat Immunol 10:266-272.
33. Roberts, T. L., A. Idris, J. A. Dunn, G. M. Kelly, C. M. Burnton, S. Hodgson, L. L. Hardy, V. Garceau, M. J. Sweet, I. L. Ross, D. A. Hume, and K. J. Stacey. 2009. HIN-200 proteins regulate caspase activation in response to foreign cytoplasmic DNA. Science 323:1057-1060.
34. Iwasaki, A., and R. Medzhitov. 2004. Toll-like receptor control of the adaptive immune responses. Nat Immunol 5:987-995.
35. Wang, T., T. Town, L. Alexopoulou, J. F. Anderson, E. Fikrig, and R. A. Flavell. 2004. Toll-like receptor 3 mediates West Nile virus entry into the brain causing lethal encephalitis. Nat Med 10:1366-1373.
36. Le Goffic, R., V. Balloy, M. Lagranderie, L. Alexopoulou, N. Escriou, R. Flavell, M. Chignard, and M. Si-Tahar. 2006. Detrimental contribution of the Toll-like receptor (TLR)3 to influenza A virus-induced acute pneumonia. PLoS Pathog 2:e53.
37. Yamamoto, M., S. Sato, K. Mori, K. Hoshino, O. Takeuchi, K. Takeda, and S. Akira. 2002. Cutting edge: a novel Toll/IL-1 receptor domain-containing adapter that preferentially activates the IFN-beta promoter in the Toll-like receptor signaling. J Immunol 169:6668-6672.
38. Oshiumi, H., M. Matsumoto, K. Funami, T. Akazawa, and T. Seya. 2003. TICAM-1, an adaptor molecule that participates in Toll-like receptor 3-mediated interferon-beta induction. Nat Immunol 4:161-167.

39. Hemmi, H., O. Takeuchi, T. Kawai, T. Kaisho, S. Sato, H. Sanjo, M. Matsumoto, K. Hoshino, H. Wagner, K. Takeda, and S. Akira. 2000. A Toll-like receptor recognizes bacterial DNA. Nature 408:740-745.
40. Samuelsson, C., J. Hausmann, H. Lauterbach, M. Schmidt, S. Akira, H. Wagner, P. Chaplin, M. Suter, M. O'Keeffe, and H. Hochrein. 2008. Survival of lethal poxvirus infection in mice depends on TLR9, and therapeutic vaccination provides protection. J Clin Invest 118:1776-1784.
41. Zhu, J., X. Huang, and Y. Yang. 2007. Innate immune response to adenoviral vectors is mediated by both Toll-like receptor-dependent and -independent pathways. Journal of virology 81:3170.
42. Lund, J., A. Sato, S. Akira, R. Medzhitov, and A. Iwasaki. 2003. Toll-like Receptor 9-mediated Recognition of Herpes Simplex Virus-2 by Plasmacytoid Dendritic Cells. J. Exp. Med. 198:513.
43. Krug, A., A. French, W. Barchet, J. Fischer, A. Dzionek, J. Pingel, M. Orihuela, S. Akira, W. Yokoyama, and M. Colonna. 2004. TLR9-Dependent Recognition of MCMV by IPC and DC Generates Coordinated Cytokine Responses that Activate Antiviral NK Cell Function. Immunity 21:107.
44. Krug, A., G. Luker, W. Barchet, D. Leib, S. Akira, and M. Colonna. 2004. Herpes simplex virus type 1 activates murine natural interferon-producing cells through toll-like receptor 9. Blood 103:1433.
45. Tabeta, K., P. Georgel, E. Janssen, X. Du, K. Hoebe, K. Crozat, S. Mudd, L. Shamel, S. Sovath, J. Goode, L. Alexopoulou, R. Flavell, and B. Beutler. 2004. Toll-like receptors 9 and 3 as essential components of innate immune defense against mouse cytomegalovirus infection. Proceedings of the National Academy of Sciences of the United States of America 101:3516.
46. Delale, T., A. Paquin, C. Asselin-Paturel, M. Dalod, G. Brizard, E. Bates, P. Kastner, S. Chan, S. Akira, A. Vicari, C. Biron, G. Trinchieri, and F. Briere. 2005. MyD88-Dependent and -Independent Murine Cytomegalovirus Sensing for IFN-{alpha} Release and Initiation of Immune Responses In Vivo. J Immunol 175:6723.
47. Lund, J., M. Linehan, N. Iijima, and A. Iwasaki. 2006. Cutting Edge: Plasmacytoid Dendritic Cells Provide Innate Immune Protection against Mucosal Viral Infection In Situ. J Immunol 177:7510.
48. Zucchini, N., G. Bessou, S. Traub, S. Robbins, S. Uematsu, S. Akira, L. Alexopoulou, and M. Dalod. 2008. Cutting Edge: Overlapping Functions of TLR7 and TLR9 for Innate Defense against a Herpesvirus Infection. J Immunol 180:5799.
49. Fiola, S., D. Gosselin, K. Takada, and J. Gosselin. 2010. TLR9 Contributes to the Recognition of EBV by Primary Monocytes and Plasmacytoid Dendritic Cells. J Immunol.
50. Ito, T., Y. H. Wang, and Y. J. Liu. 2005. Plasmacytoid dendritic cell precursors/type I interferon-producing cells sense viral infection by Toll-like receptor (TLR) 7 and TLR9. Springer Semin Immunopathol 26:221-229.

51. Kurt-Jones, E. A., M. Chan, S. Zhou, J. Wang, G. Reed, R. Bronson, M. M. Arnold, D. M. Knipe, and R. W. Finberg. 2004. Herpes simplex virus 1 interaction with Toll-like receptor 2 contributes to lethal encephalitis. Proc Natl Acad Sci U S A 101:1315-1320.
52. Sato, A., M. M. Linehan, and A. Iwasaki. 2006. Dual recognition of herpes simplex viruses by TLR2 and TLR9 in dendritic cells. Proc Natl Acad Sci U S A 103:17343-17348.
53. Wang, J. P., E. A. Kurt-Jones, O. S. Shin, M. D. Manchak, M. J. Levin, and R. W. Finberg. 2005. Varicella-zoster virus activates inflammatory cytokines in human monocytes and macrophages via Toll-like receptor 2. J Virol 79:12658-12666.
54. Finberg, R. W., J. P. Wang, and E. A. Kurt-Jones. 2007. Toll like receptors and viruses. Rev Med Virol 17:35-43.
55. Compton, T., E. A. Kurt-Jones, K. W. Boehme, J. Belko, E. Latz, D. T. Golenbock, and R. W. Finberg. 2003. Human cytomegalovirus activates inflammatory cytokine responses via CD14 and Toll-like receptor 2. J Virol 77:4588-4596.
56. Boehme, K. W., M. Guerrero, and T. Compton. 2006. Human cytomegalovirus envelope glycoproteins B and H are necessary for TLR2 activation in permissive cells. J Immunol 177:7094-7102.
57. Szomolanyi-Tsuda, E., X. Liang, R. M. Welsh, E. A. Kurt-Jones, and R. W. Finberg. 2006. Role for TLR2 in NK cell-mediated control of murine cytomegalovirus in vivo. J Virol 80:4286-4291.
58. Zhu, J., J. Martinez, X. Huang, and Y. Yang. 2007. Innate immunity against vaccinia virus is mediated by TLR2 and requires TLR-independent production of IFN-beta. Blood 109:619-625.
59. Barbalat, R., L. Lau, R. M. Locksley, and G. M. Barton. 2009. Toll-like receptor 2 on inflammatory monocytes induces type I interferon in response to viral but not bacterial ligands. Nat Immunol 10:1200-1207.
60. Bieback, K., E. Lien, I. M. Klagge, E. Avota, J. Schneider-Schaulies, W. P. Duprex, H. Wagner, C. J. Kirschning, V. Ter Meulen, and S. Schneider-Schaulies. 2002. Hemagglutinin protein of wild-type measles virus activates toll-like receptor 2 signaling. J Virol 76:8729-8736.
61. Chang, S., A. Dolganiuc, and G. Szabo. 2007. Toll-like receptors 1 and 6 are involved in TLR2-mediated macrophage activation by hepatitis C virus core and NS3 proteins. J Leukoc Biol 82:479-487.
62. Zhou, S., E. A. Kurt-Jones, L. Mandell, A. Cerny, M. Chan, D. T. Golenbock, and R. W. Finberg. 2005. MyD88 is critical for the development of innate and adaptive immunity during acute lymphocytic choriomeningitis virus infection. Eur J Immunol 35:822-830.
63. Kurt-Jones, E. A., L. Popova, L. Kwinn, L. M. Haynes, L. P. Jones, R. A. Tripp, E. E. Walsh, M. W. Freeman, D. T. Golenbock, L. J. Anderson, and R. W. Finberg. 2000. Pattern recognition receptors TLR4 and CD14 mediate response to respiratory syncytial virus. Nat Immunol 1:398-401.

64. Rassa, J. C., J. L. Meyers, Y. Zhang, R. Kudaravalli, and S. R. Ross. 2002. Murine retroviruses activate B cells via interaction with toll-like receptor 4. Proc Natl Acad Sci U S A 99:2281-2286.
65. Kumagai, Y., O. Takeuchi, and S. Akira. 2008. TLR9 as a key receptor for the recognition of DNA. Adv Drug Deliv Rev 60:795-804.
66. Tabeta, K., K. Hoebe, E. M. Janssen, X. Du, P. Georgel, K. Crozat, S. Mudd, N. Mann, S. Sovath, J. Goode, L. Shamel, A. A. Herskovits, D. A. Portnoy, M. Cooke, L. M. Tarantino, T. Wiltshire, B. E. Steinberg, S. Grinstein, and B. Beutler. 2006. The Unc93b1 mutation 3d disrupts exogenous antigen presentation and signaling via Toll-like receptors 3, 7 and 9. Nat Immunol 7:156-164.
67. Brinkmann, M. M., E. Spooner, K. Hoebe, B. Beutler, H. L. Ploegh, and Y. M. Kim. 2007. The interaction between the ER membrane protein UNC93B and TLR3, 7, and 9 is crucial for TLR signaling. J Cell Biol 177:265-275.
68. Park, B., M. M. Brinkmann, E. Spooner, C. C. Lee, Y. M. Kim, and H. L. Ploegh. 2008. Proteolytic cleavage in an endolysosomal compartment is required for activation of Toll-like receptor 9. Nat Immunol 9:1407-1414.
69. Kim, Y. M., M. M. Brinkmann, M. E. Paquet, and H. L. Ploegh. 2008. UNC93B1 delivers nucleotide-sensing toll-like receptors to endolysosomes. Nature 452:234-238.
70. Ewald, S. E., B. L. Lee, L. Lau, K. E. Wickliffe, G. P. Shi, H. A. Chapman, and G. M. Barton. 2008. The ectodomain of Toll-like receptor 9 is cleaved to generate a functional receptor. Nature 456:658-662.
71. Yi, A. K., R. Tuetken, T. Redford, M. Waldschmidt, J. Kirsch, and A. M. Krieg. 1998. CpG motifs in bacterial DNA activate leukocytes through the pH-dependent generation of reactive oxygen species. J Immunol 160:4755-4761.
72. Hacker, H., H. Mischak, T. Miethke, S. Liptay, R. Schmid, T. Sparwasser, K. Heeg, G. B. Lipford, and H. Wagner. 1998. CpG-DNA-specific activation of antigen-presenting cells requires stress kinase activity and is preceded by non-specific endocytosis and endosomal maturation. EMBO J 17:6230-6240.
73. Latz, E., A. Verma, A. Visintin, M. Gong, C. M. Sirois, D. C. Klein, B. G. Monks, C. J. McKnight, M. S. Lamphier, W. P. Duprex, T. Espevik, and D. T. Golenbock. 2007. Ligand-induced conformational changes allosterically activate Toll-like receptor 9. Nat Immunol 8:772-779.
74. Barton, G., J. Kagan, and R. Medzhitov. 2005. Intracellular localization of Toll-like receptor 9 prevents recognition of self DNA but facilitates access to viral DNA. Nature Immunology 7:49.
75. Hemmi, H., T. Kaisho, K. Takeda, and S. Akira. 2003. The roles of Toll-like receptor 9, MyD88, and DNA-dependent protein kinase catalytic subunit in the effects of two distinct CpG DNAs on dendritic cell subsets. J Immunol 170:3059-3064.
76. Bafica, A., C. A. Scanga, C. G. Feng, C. Leifer, A. Cheever, and A. Sher. 2005. TLR9 regulates Th1 responses and cooperates with TLR2 in mediating optimal resistance to Mycobacterium tuberculosis. J Exp Med 202:1715-1724.

77. Copin, R., P. De Baetselier, Y. Carlier, J. J. Letesson, and E. Muraille. 2007. MyD88-dependent activation of B220-CD11b+LY-6C+ dendritic cells during Brucella melitensis infection. J Immunol 178:5182-5191.
78. Lee, K. S., C. A. Scanga, E. M. Bachelder, Q. Chen, and C. M. Snapper. 2007. TLR2 synergizes with both TLR4 and TLR9 for induction of the MyD88-dependent splenic cytokine and chemokine response to Streptococcus pneumoniae. Cell Immunol 245:103-110.
79. Rocchi, J., V. Ricci, M. Albani, L. Lanini, E. Andreoli, L. Macera, M. Pistello, L. Ceccherini-Nelli, M. Bendinelli, and F. Maggi. 2009. Torquetenovirus DNA drives proinflammatory cytokines production and secretion by immune cells via toll-like receptor 9. Virology 394:235-242.
80. Haas, T., J. Metzger, F. Schmitz, A. Heit, T. Müller, E. Latz, and H. Wagner. 2008. The DNA Sugar Backbone 2' Deoxyribose Determines Toll-like Receptor 9 Activation. Immunity 28:315.
81. Kandimalla, E. R., L. Bhagat, Y. Li, D. Yu, D. Wang, Y. P. Cong, S. S. Song, J. X. Tang, T. Sullivan, and S. Agrawal. 2005. Immunomodulatory oligonucleotides containing a cytosine-phosphate-2'-deoxy-7-deazaguanosine motif as potent toll-like receptor 9 agonists. Proc Natl Acad Sci U S A 102:6925-6930.
82. Roberts, T. L., M. J. Sweet, D. A. Hume, and K. J. Stacey. 2005. Cutting edge: species-specific TLR9-mediated recognition of CpG and non-CpG phosphorothioate-modified oligonucleotides. J Immunol 174:605-608.
83. Vollmer, J., R. D. Weeratna, M. Jurk, U. Samulowitz, M. J. McCluskie, P. Payette, H. L. Davis, C. Schetter, and A. M. Krieg. 2004. Oligodeoxynucleotides lacking CpG dinucleotides mediate Toll-like receptor 9 dependent T helper type 2 biased immune stimulation. Immunology 113:212-223.
84. Coban, C., Y. Igari, M. Yagi, T. Reimer, S. Koyama, T. Aoshi, K. Ohata, T. Tsukui, F. Takeshita, K. Sakurai, T. Ikegami, A. Nakagawa, T. Horii, G. Nunez, K. J. Ishii, and S. Akira. 2010. Immunogenicity of whole-parasite vaccines against Plasmodium falciparum involves malarial hemozoin and host TLR9. Cell Host Microbe 7:50-61.
85. Coban, C., K. J. Ishii, T. Kawai, H. Hemmi, S. Sato, S. Uematsu, M. Yamamoto, O. Takeuchi, S. Itagaki, N. Kumar, T. Horii, and S. Akira. 2005. Toll-like receptor 9 mediates innate immune activation by the malaria pigment hemozoin. J Exp Med 201:19-25.
86. Wagner, H. 2004. The immunobiology of the TLR9 subfamily. Trends Immunol 25:381-386.
87. Hacker, H., R. M. Vabulas, O. Takeuchi, K. Hoshino, S. Akira, and H. Wagner. 2000. Immune cell activation by bacterial CpG-DNA through myeloid differentiation marker 88 and tumor necrosis factor receptor-associated factor (TRAF)6. J Exp Med 192:595-600.
88. Kawagoe, T., S. Sato, A. Jung, M. Yamamoto, K. Matsui, H. Kato, S. Uematsu, O. Takeuchi, and S. Akira. 2007. Essential role of IRAK-4 protein and

its kinase activity in Toll-like receptor-mediated immune responses but not in TCR signaling. J Exp Med 204:1013-1024.
89. Deng, L., C. Wang, E. Spencer, L. Yang, A. Braun, J. You, C. Slaughter, C. Pickart, and Z. J. Chen. 2000. Activation of the IkappaB kinase complex by TRAF6 requires a dimeric ubiquitin-conjugating enzyme complex and a unique polyubiquitin chain. Cell 103:351-361.
90. Wang, C., L. Deng, M. Hong, G. R. Akkaraju, J. Inoue, and Z. J. Chen. 2001. TAK1 is a ubiquitin-dependent kinase of MKK and IKK. Nature 412:346-351.
91. Sato, S., H. Sanjo, K. Takeda, J. Ninomiya-Tsuji, M. Yamamoto, T. Kawai, K. Matsumoto, O. Takeuchi, and S. Akira. 2005. Essential function for the kinase TAK1 in innate and adaptive immune responses. Nat Immunol 6:1087-1095.
92. Yamamoto, M., T. Okamoto, K. Takeda, S. Sato, H. Sanjo, S. Uematsu, T. Saitoh, N. Yamamoto, H. Sakurai, K. J. Ishii, S. Yamaoka, T. Kawai, Y. Matsuura, O. Takeuchi, and S. Akira. 2006. Key function for the Ubc13 E2 ubiquitin-conjugating enzyme in immune receptor signaling. Nat Immunol 7:962-970.
93. Takaoka, A., H. Yanai, S. Kondo, G. Duncan, H. Negishi, T. Mizutani, S. Kano, K. Honda, Y. Ohba, T. W. Mak, and T. Taniguchi. 2005. Integral role of IRF-5 in the gene induction programme activated by Toll-like receptors. Nature 434:243-249.
94. Schmitz, F., A. Heit, S. Guggemoos, A. Krug, J. Mages, M. Schiemann, H. Adler, I. Drexler, T. Haas, R. Lang, and H. Wagner. 2007. Interferon-regulatory-factor 1 controls Toll-like receptor 9-mediated IFN-beta production in myeloid dendritic cells. Eur J Immunol 37:315-327.
95. Prakash, A., E. Smith, C. K. Lee, and D. E. Levy. 2005. Tissue-specific positive feedback requirements for production of type I interferon following virus infection. J Biol Chem 280:18651-18657.
96. Kawai, T., S. Sato, K. J. Ishii, C. Coban, H. Hemmi, M. Yamamoto, K. Terai, M. Matsuda, J. Inoue, S. Uematsu, O. Takeuchi, and S. Akira. 2004. Interferon-alpha induction through Toll-like receptors involves a direct interaction of IRF7 with MyD88 and TRAF6. Nat Immunol 5:1061-1068.
97. Hoshino, K., T. Sugiyama, M. Matsumoto, T. Tanaka, M. Saito, H. Hemmi, O. Ohara, S. Akira, and T. Kaisho. 2006. IkappaB kinase-alpha is critical for interferon-alpha production induced by Toll-like receptors 7 and 9. Nature 440:949-953.
98. Hochrein, H., B. Schlatter, M. O'Keeffe, C. Wagner, F. Schmitz, M. Schiemann, S. Bauer, M. Suter, and H. Wagner. 2004. Herpes simplex virus type-1 induces IFN-alpha production via Toll-like receptor 9-dependent and -independent pathways. Proc Natl Acad Sci U S A 101:11416-11421.
99. Guggemoos, S., D. Hangel, S. Hamm, A. Heit, S. Bauer, and H. Adler. 2008. TLR9 Contributes to Antiviral Immunity during Gammaherpesvirus Infection. J Immunol 180:438.
100. Gargano, L., J. Moser, and S. Speck. 2008. Role for MyD88 Signaling in Murine Gammaherpesvirus 68 Latency. J. Virol. 82:3853.

101. Hochreiter, R., C. Ptaschinski, S. Kunkel, and R. Rochford. 2007. Murine gammaherpesvirus-68 productively infects immature dendritic cells and blocks maturation. J Gen Virol 88:1896.
102. Smith, C. M., M. B. Gill, J. S. May, and P. G. Stevenson. 2007. Murine gammaherpesvirus-68 inhibits antigen presentation by dendritic cells. PLoS ONE 2.
103. Brawand, P., D. R. Fitzpatrick, B. W. Greenfield, K. Brasel, C. R. Maliszewski, and T. De Smedt. 2002. Murine plasmacytoid pre-dendritic cells generated from Flt3 ligand-supplemented bone marrow cultures are immature APCs. J Immunol 169:6711-6719.
104. Flano, E., B. Kayhan, D. Woodland, and M. Blackman. 2005. Infection of Dendritic Cells by a {gamma}2-Herpesvirus Induces Functional Modulation. J Immunol 175:3225.
105. Weslow-Schmidt, J., N. Jewell, S. Mertz, P. Simas, J. Durbin, and E. Flano. 2007. Type I Interferon Inhibition and Dendritic Cell Activation during Gammaherpesvirus Respiratory Infection. J. Virol. 81:9778.
106. Dutia, B. M., D. J. Allen, H. Dyson, and A. A. Nash. 1999. Type I Interferons and IRF-1 Play a Critical Role in the Control of a Gammaherpesvirus Infection. Virology 261:173.
107. Barton, E., M. Lutzke, R. Rochford, and H. Virgin. 2005. Alpha/Beta Interferons Regulate Murine Gammaherpesvirus Latent Gene Expression and Reactivation from Latency. J. Virol. 79:14149.
108. Wagner, M., S. Jonjic, U. H. Koszinowski, and M. Messerle. 1999. Systematic excision of vector sequences from the BAC-cloned herpesvirus genome during virus reconstitution. J Virol 73:7056-7060.
109. Jiang, Z., P. Georgel, X. Du, L. Shamel, S. Sovath, S. Mudd, M. Huber, C. Kalis, S. Keck, C. Galanos, M. Freudenberg, and B. Beutler. 2005. CD14 is required for MyD88-independent LPS signaling. Nature Immunology 6:565.
110. Andrews, D. M., C. E. Andoniou, F. Granucci, P. Ricciardi-Castagnoli, and M. A. Degli-Esposti. 2001. Infection of dendritic cells by murine cytomegalovirus induces functional paralysis. Nat Immunol 2:1077-1084.
111. Takeuchi, O., and S. Akira. 2007. Recognition of viruses by innate immunity. Immunol Rev 220:214-224.
112. Zhu, F. X., S. M. King, E. J. Smith, D. E. Levy, and Y. Yuan. 2002. A Kaposi's sarcoma-associated herpesviral protein inhibits virus-mediated induction of type I interferon by blocking IRF-7 phosphorylation and nuclear accumulation. Proc Natl Acad Sci U S A 99:5573-5578.
113. Shen, Z., G. Reznikoff, G. Dranoff, and K. L. Rock. 1997. Cloned dendritic cells can present exogenous antigens on both MHC class I and class II molecules. J Immunol 158:2723-2730.
114. Dalod, M., T. Hamilton, R. Salomon, T. P. Salazar-Mather, S. C. Henry, J. D. Hamilton, and C. A. Biron. 2003. Dendritic cell responses to early murine cytomegalovirus infection: subset functional specialization and differential regulation by interferon alpha/beta. J Exp Med 197:885-898.

115. Bozza, S., F. Bistoni, R. Gaziano, L. Pitzurra, T. Zelante, P. Bonifazi, K. Perruccio, S. Bellocchio, M. Neri, A. M. Iorio, G. Salvatori, R. De Santis, M. Calvitti, A. Doni, C. Garlanda, A. Mantovani, and L. Romani. 2006. Pentraxin 3 protects from MCMV infection and reactivation through TLR sensing pathways leading to IRF3 activation. Blood 108:3387-3396.
116. Kawai, T., and S. Akira. 2007. Antiviral signaling through pattern recognition receptors. J Biochem 141:137-145.
117. Sanchez, D., D. Miranda, V. Arumugaswami, S. Hwang, A. Singer, A. Senaati, A. Shahangian, M. Song, R. Sun, and G. Cheng. 2008. A Repetitive Region of Gammaherpesvirus Genomic DNA Is a Ligand for Induction of Type I Interferon. J. Virol. 82:2208.
118. Liang, X., Y. C. Shin, R. E. Means, and J. U. Jung. 2004. Inhibition of interferon-mediated antiviral activity by murine gammaherpesvirus 68 latency-associated M2 protein. J Virol 78:12416-12427.
119. Hwang, S., K. S. Kim, E. Flano, T. T. Wu, L. M. Tong, A. N. Park, M. J. Song, D. J. Sanchez, R. M. O'Connell, G. Cheng, and R. Sun. 2009. Conserved herpesviral kinase promotes viral persistence by inhibiting the IRF-3-mediated type I interferon response. Cell Host Microbe 5:166-178.
120. Huang, E. S., C. H. Huang, S. M. Huong, and M. Selgrade. 1976. Preferential inhibition of herpes-group viruses by phosphonoacetic acid: effect on virus DNA synthesis and virus-induced DNA polymerase activity. Yale J Biol Med 49:93-99.
121. Krieg, A. 2002. CPG MOTIFS IN BACTERIAL DNA AND THEIR IMMUNE EFFECTS. Annual Review of Immunology 20:709.
122. Usherwood, E. J., J. P. Stewart, and A. A. Nash. 1996. Characterization of tumor cell lines derived from murine gammaherpesvirus-68-infected mice. J Virol 70:6516-6518.
123. Chen, J., K. Ueda, S. Sakakibara, T. Okuno, C. Parravicini, M. Corbellino, and K. Yamanishi. 2001. Activation of latent Kaposi's sarcoma-associated herpesvirus by demethylation of the promoter of the lytic transactivator. Proc Natl Acad Sci U S A 98:4119-4124.
124. Tao, Q., and K. D. Robertson. 2003. Stealth technology: how Epstein-Barr virus utilizes DNA methylation to cloak itself from immune detection. Clin Immunol 109:53-63.
125. Krieg, A., A.-K. Yi, S. Matson, T. Waldschmidt, G. Bishop, R. Teasdale, G. Koretzky, and D. Klinman. 1995. CpG motifs in bacterial DNA trigger direct B-cell activation. Nature 374:546.
126. Bauer, S., C. J. Kirschning, H. Hacker, V. Redecke, S. Hausmann, S. Akira, H. Wagner, and G. B. Lipford. 2001. Human TLR9 confers responsiveness to bacterial DNA via species-specific CpG motif recognition. Proc Natl Acad Sci U S A 98:9237-9242.
127. Karlin, S., W. Doerfler, and L. R. Cardon. 1994. Why is CpG suppressed in the genomes of virtually all small eukaryotic viruses but not in those of large eukaryotic viruses? J. Virol. 68:2889.

128. Stevenson, P. G., and S. Efstathiou. 2005. Immune mechanisms in murine gammaherpesvirus-68 infection. Viral Immunol 18:445-456.
129. Chen, L., M. Arora, M. Yarlagadda, T. B. Oriss, N. Krishnamoorthy, A. Ray, and P. Ray. 2006. Distinct responses of lung and spleen dendritic cells to the TLR9 agonist CpG oligodeoxynucleotide. J Immunol 177:2373-2383.
130. Minarovits, J. 2006. Epigenotypes of latent herpesvirus genomes. Curr Top Microbiol Immunol 310:61-80.
131. Tibbetts, S. A., J. Loh, V. Van Berkel, J. S. McClellan, M. A. Jacoby, S. B. Kapadia, S. H. Speck, and H. W. t. Virgin. 2003. Establishment and maintenance of gammaherpesvirus latency are independent of infective dose and route of infection. J Virol 77:7696-7701.
132. Moser, J. M., M. L. Farrell, L. T. Krug, J. W. Upton, and S. H. Speck. 2006. A gammaherpesvirus 68 gene 50 null mutant establishes long-term latency in the lung but fails to vaccinate against a wild-type virus challenge. J Virol 80:1592-1598.
133. Kayhan, B., E. J. Yager, K. Lanzer, T. Cookenham, Q. Jia, T. T. Wu, D. L. Woodland, R. Sun, and M. A. Blackman. 2007. A replication-deficient murine gamma-herpesvirus blocked in late viral gene expression can establish latency and elicit protective cellular immunity. J Immunol 179:8392-8402.
134. Li, H., K. Ikuta, J. W. Sixbey, and S. A. Tibbetts. 2008. A replication-defective gammaherpesvirus efficiently establishes long-term latency in macrophages but not in B cells in vivo. J Virol 82:8500-8508.
135. Stevenson, P. G., J. S. May, X. G. Smith, S. Marques, H. Adler, U. H. Koszinowski, J. P. Simas, and S. Efstathiou. 2002. K3-mediated evasion of CD8(+) T cells aids amplification of a latent gamma-herpesvirus. Nat Immunol 3:733-740.
136. May, J. S., N. J. Bennett, and P. G. Stevenson. 2010. An in vitro system for studying murid herpesvirus-4 latency and reactivation. PLoS One 5:e11080.
137. Miller, S. I., R. K. Ernst, and M. W. Bader. 2005. LPS, TLR4 and infectious disease diversity. Nat Rev Microbiol 3:36-46.
138. Tellam, J., C. Smith, M. Rist, N. Webb, L. Cooper, T. Vuocolo, G. Connolly, D. C. Tscharke, M. P. Devoy, and R. Khanna. 2008. Regulation of protein translation through mRNA structure influences MHC class I loading and T cell recognition. Proc Natl Acad Sci U S A 105:9319-9324.
139. West, J. A., S. M. Gregory, V. Sivaramanan, L. Su, and B. Damania. 2010. Activation of Plasmacytoid Dendritic Cells by KSHV. J Virol.
140. Rajcani, J., and M. Kudelova. 2005. Murine herpesvirus pathogenesis: a model for the analysis of molecular mechanisms of human gamma herpesvirus infections. Acta Microbiol Immunol Hung 52:41-71.
141. Wong, Q. N., V. C. Ng, M. C. Lin, H. F. Kung, D. Chan, and J. D. Huang. 2005. Efficient and seamless DNA recombineering using a thymidylate synthase A selection system in Escherichia coli. Nucleic Acids Res 33:e59.

142. Milho, R., C. M. Smith, S. Marques, M. Alenquer, J. S. May, L. Gillet, M. Gaspar, S. Efstathiou, J. P. Simas, and P. G. Stevenson. 2009. In vivo imaging of murid herpesvirus-4 infection. J Gen Virol 90:21-32.
143. Krieg, A. M., T. Wu, R. Weeratna, S. M. Efler, L. Love-Homan, L. Yang, A. K. Yi, D. Short, and H. L. Davis. 1998. Sequence motifs in adenoviral DNA block immune activation by stimulatory CpG motifs. Proc Natl Acad Sci U S A 95:12631-12636.
144. Adler, H., M. Messerle, M. Wagner, and U. H. Koszinowski. 2000. Cloning and mutagenesis of the murine gammaherpesvirus 68 genome as an infectious bacterial artificial chromosome. J Virol 74:6964-6974.
145. Murphy, K. C. 1998. Use of bacteriophage lambda recombination functions to promote gene replacement in Escherichia coli. J Bacteriol 180:2063-2071.
146. Yu, D., H. M. Ellis, E. C. Lee, N. A. Jenkins, N. G. Copeland, and D. L. Court. 2000. An efficient recombination system for chromosome engineering in Escherichia coli. Proc Natl Acad Sci U S A 97:5978-5983.
147. Fordyce, P. M., D. Gerber, D. Tran, J. Zheng, H. Li, J. L. DeRisi, and S. R. Quake. 2010. De novo identification and biophysical characterization of transcription-factor binding sites with microfluidic affinity analysis. Nat Biotechnol 28:970-975.
148. Maerkl, S. J., and S. R. Quake. 2007. A systems approach to measuring the binding energy landscapes of transcription factors. Science 315:233-237.
149. Rutz, M., J. Metzger, T. Gellert, P. Luppa, G. B. Lipford, H. Wagner, and S. Bauer. 2004. Toll-like receptor 9 binds single-stranded CpG-DNA in a sequence- and pH-dependent manner. Eur J Immunol 34:2541-2550.
150. Peter, M., K. Bode, G. B. Lipford, F. Eberle, K. Heeg, and A. H. Dalpke. 2008. Characterization of suppressive oligodeoxynucleotides that inhibit Toll-like receptor-9-mediated activation of innate immunity. Immunology 123:118-128.